EPRI | ELECTRIC POWER RESEARCH INSTITUTE

Application Guide for Emerging Condition-Monitoring Techniques for Transformers

1024195

Application Guide for Emerging Condition-Monitoring Techniques for Transformers

1024195

Technical Update, December 2012

EPRI Project Manager

L. van der Zel

ELECTRIC POWER RESEARCH INSTITUTE
3420 Hillview Avenue, Palo Alto, California 94304-1338 ▪ PO Box 10412, Palo Alto, California 94303-0813 ▪ USA
800.313.3774 ▪ 650.855.2121 ▪ askepri@epri.com ▪ www.epri.com

DISCLAIMER OF WARRANTIES AND LIMITATION OF LIABILITIES

THE FOLLOWING ORGANIZATIONS PREPARED THIS REPORT:

Electric Power Research Institute (EPRI)

NEETRAC

This is an EPRI Technical Update report. A Technical Update report is intended as an informal report of continuing research, a meeting, or a topical study. It is not a final EPRI technical report.

NOTE

For further information about EPRI, call the EPRI Customer Assistance Center at 800.313.3774 or e-mail askepri@epri.com.

ACKNOWLEDGMENTS

The following organizations prepared this report:

Electric Power Research Institute (EPRI)
1300 West W.T. Harris Blvd.
Charlotte, NC 28262

Principal Investigators
B. Rodriguez
L. van der Zel

NEETRAC
777 Atlantic Drive NW
Atlanta, GA 30332-0250

Principal Investigator
L. Coffeen

This report describes research sponsored by EPRI.

This publication is a corporate document that should be cited in the literature in the following manner:

Application Guide for Emerging Condition-Monitoring Techniques for Transformers. EPRI, Palo Alto, CA: 2012. 1024195.

ABSTRACT

This Technical Update presents the first year of progress in a multi-year effort toward a complete *Application Guide for Emerging Condition-Monitoring Techniques for Transformers*.

The purpose of this guide is to provide practical assistance to members on the selection, application, and interpretation of emerging transformer condition monitoring. To date, the emerging techniques covered in this guide have had limited application in the field. The guide presents the latest application results from the Electric Power Research Institute (EPRI) Charlotte and Lenox laboratories and member field trials. The findings will help inform utility personnel as to how to select and apply the optimal techniques.

The background against which this guide is set is the increasing need for electricity companies to employ assets to the fullest extent possible while maintaining system reliability. In this environment, management of the aging population of power transformers has become the most critical issue facing today's substation managers and engineers. Power transformers are complex, critical components of the power transmission and distribution system. Their reliability not only affects the electric energy availability of the supplied area, but it also affects the economical operation of the utility.

System abnormalities, loading, switching, and ambient conditions normally contribute to transformer accelerated aging and sudden failure. In the absence of critical component monitoring, the failure risk is increased. Therefore, central to transformer management is effective transformer diagnostics and condition assessment. Moreover, effective condition monitoring, proper diagnostics, and accurate interpretation can help reduce the rate of aging and provide a way to assess the overall asset integrity with minimum risk of sudden failure.

Keywords

Condition assessment
Condition monitoring
Diagnostics
Power system monitoring
Power system reliability
Transformer

CONTENTS

LIST OF FIGURES

LIST OF TABLES

1
INTRODUCTION

This Technical Update presents the first year of progress in a multi-year effort towards a full Application Guide for Emerging Condition Monitoring Techniques for Transformers.

The purpose of this application guide is to provide practical assistance to members on the selection, application, and interpretation of emerging transformer condition monitoring. To date, the emerging techniques covered in this guide have had limited application in the field. This guide presents the latest application results from the EPRI Charlotte and Lenox laboratories and member field trials. The findings fully inform utility personnel as to how to select the optimal techniques for early trial or adoption.

Objectives

The objectives of this guide are to provide practical guidance for utility engineers on:

- Basic knowledge of how each emerging technique works
- Guidance on which emerging tool (or combination) to select to solve a specific problem
- Explanations of the various technology approaches available for emerging condition monitoring techniques – and the fundamental benefits and limitations of each approach
- Guidance on interpretation of the results – and when to call in an expert for more detailed analysis
- Application notes from the laboratory – sharing research insights on how the techniques have performed under controlled conditions
- Case studies from the field – providing practical examples of how each emerging technique has performed under real world conditions
- Guidance on factors to consider when writing specifications for purchase of a system or provision of a service by experts

Role of this Report

This report should be used in conjunction with the EPRI Power Transformer Guidebook [1]. The EPRI Power Transformer Guidebook is also referred to as the Copper Book (based on the color of the cover) and serves as the EPRI transformer reference guide. Chapter 9 of the Copper Book covers transformer condition monitoring and diagnosis in detail, including all off- and on-line tests.

This application guide serves to present the latest detailed research progress on emerging condition monitoring technologies. It is thus the source for detailed research findings from the laboratory and the field – and helps with early adoption of these techniques. As these emerging condition monitoring techniques continue to mature, relevant guidance for utility engineers will migrate into the Copper Book. This application guide thus also serves as the "research engine" that feeds new, updated material into the Copper Book.

2
SUMMARY OF CONDITION MONITORING TECHNIQUES

This section provides an overview of the emerging monitoring techniques described in this application guide. Table 2-1 includes a summary of what each technique detects, typical problems the technique is best able to detect, and whether the technique can be applied while the transformer is in service.

Table 2–1
Summary of Condition Monitoring Techniques

Technique	What it Detects	Typical Problems the Technique is Best Suited to Detecting	Applied in Service?
Acoustic Emission	High frequency acoustic pulses emitted by electrical discharges or overheating of oil	Electrical or thermal defects within a transformer, bushing, or load tap changer (LTC) that are not deep within the windings (as that strongly attenuates the signals)	Yes
On-Line Dissolved Gas Analysis (DGA)	Dissolved gases in the oil	Electrical discharges internal to windings or accessories Tracking in or on insulation Poorly bonded stress or flux shields Overheated conductors or core Arcing from poor connections	Yes – but an outage is often needed to fit on-line monitoring system
Bushing Monitoring	Typically relative power factor and capacitance. Some monitors include partial discharges.	Deterioration of the dielectric within the bushing due to discharge activity, overheating, or contamination	Yes – but an outage is needed to fit the sensors
Electrical Partial Discharge Detection	High frequency electrical partial discharge pulses	Electrical discharges internal to windings or accessories Tracking in or on insulation Poorly bonded stress or flux shields	Yes. Some sensors need an outage to be fitted.

Technique	What it Detects	Typical Problems the Technique is Best Suited to Detecting	Applied in Service?
Dielectric Response Measurements	Electrical response of the transformer dielectric over a variety of frequencies	Oil quality and moisture in the solid dielectric	No
High Frequency Transient Monitoring Using Bushing Couplers	Transients at the bushing terminals of a transformer	Characterization of transient peaks and frequency content Breaker re-strike detection LTC anomalies	Yes – but an outage is needed to fit the sensors
Frequency Response Analysis (FRA)	Frequency response of the transformer winding configuration	Winding deformation	Both on-line and off-line approaches
LTC Monitoring	Electrical (vibration, acoustic emission) and chemical (DGA) signals	Contact overheating Contact wear Excessive arcing	Yes. Some sensors need an outage to be fitted.

3
HOW TO CHOOSE THE BEST TECHNIQUES FOR THE SITUATION

This section will guide the reader on the selection of both the best tools and the order of application. This information is important because each technique takes time (which is often at a premium when a transformer needs to return to service) and money. The guidance will help the reader obtain the best answer in the most cost effective manner. This section will be populated when all of the chapters covering each of the emerging techniques have been completed.

The proposed subsections for this chapter are as follows:

When to Apply Each Tool

This subsection will help provide a justification for the implementation of the various emerging condition monitoring techniques.

What Order to Apply Each Tool

This subsection will present or help develop some guidance for the process of deciding the order in which to apply emerging monitoring tools in the most beneficial and cost effective way.

Costs and Benefits

This subsection will explain the typical costs associated with the application of the various technologies and the types of benefits that can be realized from their use.

4
ACOUSTIC EMISSION MONITORING

Basic Principles

Acoustic emission (AE) monitoring is based on the detection of transient elastic waves generated by the rapid release of energy in localized sources inside materials. Piezoelectric sensors strategically located on the tested transformer detect these signals, and high speed instrumentation captures, processes, and stores all data.

AE testing has traditionally been used for the detection and location of partial discharges (PD). However, in recent years the technique has successfully detected the precursors to other types of faults, such as the evolution of gases and micro-turbulence in the oil [2]. In this way, the acoustic emissions technique can also be used to detect thermal faults. The technique can be used either as a spot-check or continuously.

Various Approaches for Applying this Technique

AE analysis of transformers consists of various approaches. Each approach has its advantages and disadvantages, including sensibility of the test, detection of multiple sources, identification of the acoustic emission (electrical or thermal) origin, and correlation with operating parameters. The approaches vary according to the following key factors:

- **Number of transformer faces monitored at a time:** A transformer typically has four faces that are accessible for AE sensor placement (with the top and bottom typically inaccessible). AE techniques either use sensors mounted to all four faces simultaneously or sensors mounted on only one face at a time. Techniques using four faces allow for automatic location of the discharge source with no need to move the sensors during the testing. It is thus well suited for long-term monitoring. Techniques using one face typically deploy a few sensors that are then strategically moved around the tank (a face at a time) to locate the source.
- **Location using static of moveable sensors:** Static sensors require no human intervention to identify the source location. With moveable sensors, a user relocates the sensors on the transformer in response to the signals the instrument produces. The static sensor location is thus well suited for long-term monitoring, while the moveable sensor location is well suited to a quick on-site scan of a transformer. As technologies progress, some of the moveable sensor systems are also being adapted to be left on site for longer-term monitoring so this distinction will have overlaps in future years,
- **Electrical triggering:** AE detection and location techniques can use the AE signals themselves as the trigger. An alternative or complementary technique is to use an electrical PD signal as a trigger. Sources of electrical PD triggers include UHF sensors, clamp-on CTs on a transformer ground, and coupling capacitors. Electrical triggers provide two benefits. The first benefit is that AE signals below the background noise can be extracted using signal averaging. The second benefit is that an electrical confirmation of an AE signal can help determine whether a defect within a transformer is of thermal or electrical origin.

- **Monitoring duration:** Monitoring duration is typically short (a day) or long (months). For short duration tests, the test equipment is typically continually manned by the operator performing the tests – and AE sensors are moved around the transformer in response to the measurements obtained. For long duration tests, the AE sensors are mounted in fixed positions on the transformer tank, typically for a period of months. The monitoring remains unattended, and the data is relayed to experts – usually via a cellular data link. For long duration monitoring, other system parameters are also typically monitored (see the next bullet).
- **System parameter logging:** AE signals are often easier to relate to a specific source if a correlation with system parameters is known. For example, if AE signals increase with top-tank temperature and decrease with pump and fan starts, then the source is more likely to be overheating. Some on-line AE systems thus also trend key system parameters such as load, tank temperature, pump and fan status, and sometimes LTC position.

Table 4-1 presents when each of these approaches is often best applied and provides examples of vendor systems for each approach.

Table 4–1
Technology Application Guide for Acoustic Emission

Faces	Static of moveable sensors	Elec PD	Long-Term	System Log	Example Vendors[1]	EPRI Lab Field Trial	Application
4	Static	Y	Y	Y	e.g. MISTRAS Sensor Highway	L F	A long-term AE application of this nature is typically applicable when gassing in a transformer raises concern and spot measurements did not provide a definitive conclusion. The longer-term application allows for detection of intermittent discharges. The simultaneous logging of system parameters enables correlations between AE and system events and thus improved risk assessment.
			N	N	e.g. Omicron PDL 650		This application is over a short period of time (spot measurement), but during that time provides simultaneous measurements from multiple transformer faces. If the AE signal is intermittent over the test period, this approach maximizes the probability of detection. Since there are multiple fixed sensors, location of the AE source is also possible.
					e.g. Doble Lemke LDA-6		
1	Moveable	Y	N	N	e.g. NDB 150	L	This category application is ideally suited to a first line of defense on a suspect transformer. If the AE signals are active and detectable, then location is typically possible. If the signals are intermittent or system dependent, longer-term AE monitoring is then a possible next step.
					e.g. PowerPD PD TP500A	F	

Results Interpretation

The typical data interpretation process consists of filtering all the information considered unrelated to internal faults. Once the non-relevant data has been filtered, any acoustic activity remaining is considered to be produced by an internal fault. This data is analyzed, and correlations between this data and changes in the operating parameters are typically examined. This correlation can shed valuable information on the type of fault in the transformer.

Finally, the location of the acoustic activity is attempted to be determined and correlated with the location of internal components on the transformer such as bushings, windings, core, leads, de-energize tap changer selector, load tap changer leads, ground connections, etc. This can be achieved by comparing the location of the fault to drawings or photographs of the internal structure of the transformer.

[1] The vendor list is under continual review and is updated with each revision of the guide

A grading system has been developed by EPRI [2] to consider different factors such as total dissolved combustible gases (TDCG), combustible gas generating trend, location of the fault, timing of the activity during the monitoring period, and acoustic energy.

If multiple faults are detected, the intensity of each fault is determined to help prioritize inspection and/or repair work on the transformer. The transformer can receive four different grades:

A – Normal operation.

B – Acoustic activity detected is minor or negligible; continue normal operation.

C – Fault of medium intensity is detected; follow-up is recommended.

D – High intensity fault is detected; internal inspection is recommended.

By 2008, 277 cases had been analyzed by the grading system [3]. The breakdown of grading results is shown in Figure 4-1. The grading system has proven to be a helpful assessment tool, and two areas of future research are planned. The first is to enhance the existing grading system for AE systems fitted to the four faces of a transformer. The second is to extend the grading tool to other approaches of AE, such as four-sensor portable systems or AE systems used together with electrical PD detection.

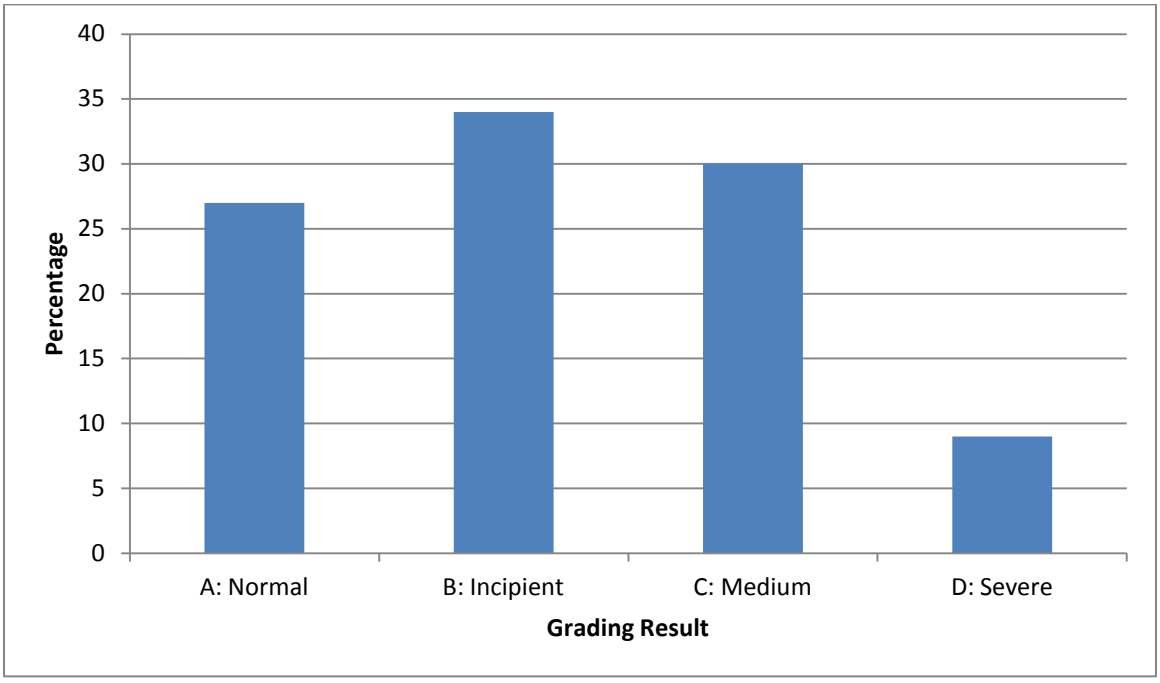

Figure 4–1
Grading Results for 277 AE Cases. The Grading System and the Results Used to Produce this Plot are Presented in [3].

Specifications Guidelines

As the guide is expanded, this subsection will present the proposed approach for specifying the monitoring system such that it meets the most important performance requirements. These specifications include any additional testing that should be performed to validate these performance requirements.

Laboratory Application Notes

Technologies Applied	AE, Single Sensor	Laboratory	Rensselaer Polytechnic Institute	Date	2002
Laboratory Test Objective	The test objective was to prove that the acoustic emission technique could be used for detection of hot-spots in a transformer (in addition to the already-known ability to detect electrical discharges).				
Approach	The experiments were design to generate gassing by locally heating oil without introducing any type of noise source that could be electrical in nature (e.g., PD, arcing). AE data was collected using a similar test set-up as the one typically used in the field for transformer testing. Temperature was recorded on the AE instrument along with AE signals and hit features. At various times during the experiments, samples of oil and head space gas were taken for analysis. Only responses to low temperature excitation (below 200˚C) were studied.				
Results	AE activity started to pick up between 100 to 120˚C. AE activity became pronounced as the temperature reached 200˚C and gas bubbles were observed in the oil on a regular basis.				
Lessons Learned	Rapid changes in temperature seem to cause turbulence in the oil, which manifest as an AE source. AE activity seems to increase steadily as temperature rises from 100 to 200˚C. AE could be used for detection of hot-spots in a transformer.				

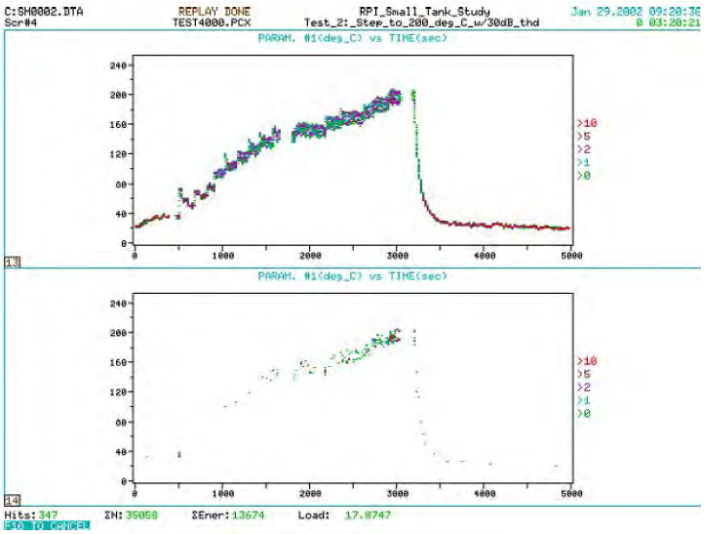

Figure 4–2
Temperature versus Time Plot; Lower Plot Shows Only Temperatures Where AE Was Detected

Field Case Studies

Hundreds of case studies have been performed, but not all of the case studies provide learning that is of benefit to others. A subset of a dozen highly educational case studies has been identified. Each of these case studies is presented in this subsection. For the first edition of this update, the first case study has been completed and is presented in Table 4-2 and Figure 4-3. As this application guide is expanded, further case studies will be added.

Table 4–2
Case Study: Acoustic Emission Applied to Confirm Flux Shield Heating

Technologies Applied	AE, On-Line, 4 Sides	**Transformer Details**	GSU, 482MVA, 22.5/500kV, Single-Phase, Core-Form	**Utility and Date**	TVA 2012
Objective	DGA results indicated a hot-spot. The objective of applying AE was to determine the source of the hot-spot and decide whether to take a forced outage or run until the next planned outage.				
Approach	An on-line AE system was installed on four faces of the transformer. Load, tank temperature and fun/pump status, and rain were also logged.				
Results	AE successfully located two clusters of activity. The locations predicted the source to be flux shield heating. Logging of load and tank temperature allowed the AE signals to be correlated with these parameters and further confirm the prediction. The transformer was run until the planned outage, and an internal inspection confirmed the prediction – thus validating the decision to keep operating.				
Lessons Learned	The case study confirmed again that AE is sensitive to hot-spots (in addition to electrical discharges). It was again confirmed that AE is sensitive when there is minimal paper between the source and the tank wall. The on-line AE allowed for the capture of intermittent signals. (There were days with little or no signal, which would have been missed if a spot-check been performed on that day).				

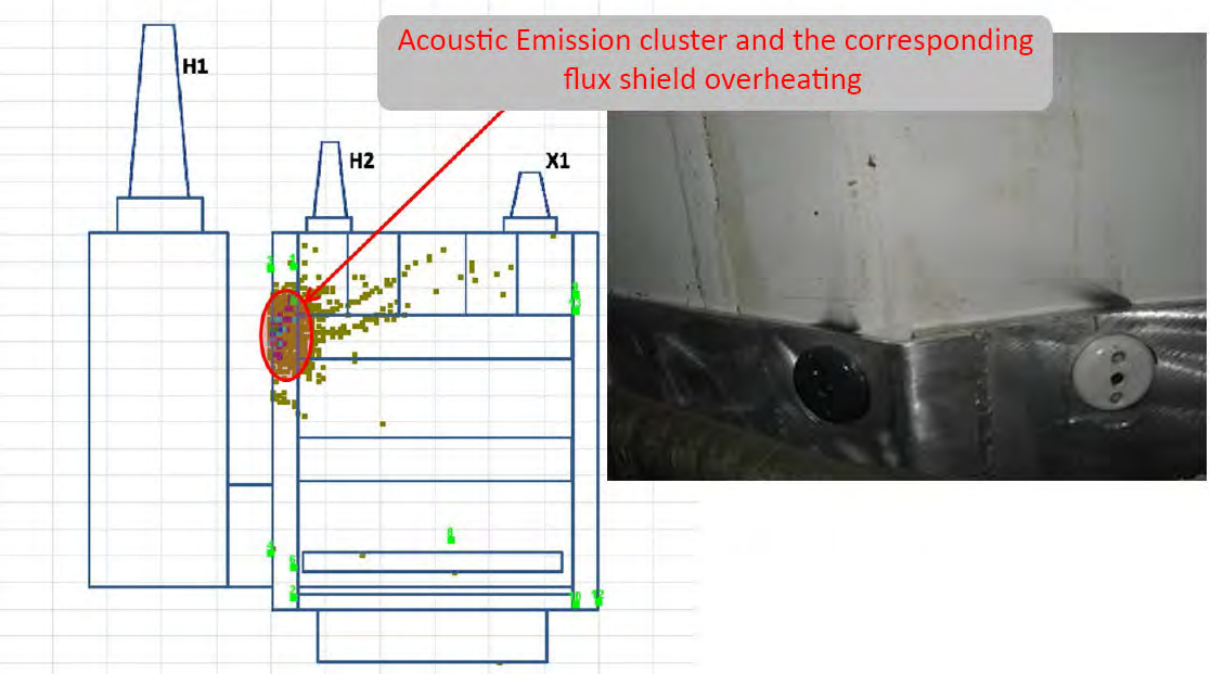

Figure 4–3
The AE Cluster Location Corresponded Very Well with Location of the Defect – in This Case, Overheating in the Flux Shields

5
ON-LINE DISSOLVED GAS ANALYSIS

Dissolved Gas Analysis (DGA) represents a powerful diagnostic tool for transformers. Of all the technologies presented in this guide, DGA is the most widely applied - but the on-line application is still covered in this guide as it is not as widely used as the periodic off-line laboratory analysis. This section is scheduled for publication in the 2013 version of this application guide. The section will cover the following key aspects:

- Basic principles
- Various approaches in application of the technique
- Results interpretation
- Specification guidelines
- Laboratory application notes
- Field case studies

Basic Principles

This subsection will present the underlying theory of DGA production and detection. An understanding of these basics will help in the selection of optimal technologies.

Various Approaches in Application of the Technique

There are numerous technical approaches to detecting the dissolved gases in oil. This subsection will discuss each approach in detail. The understanding of these approaches will allow for assessment of the benefits and limitations of each.

Results Interpretations

Worldwide (including EPRI), significant effort has been dedicated to the interpretation of DGA patterns. A utility engineer is faced with the difficult choice of determining which interpretation approaches to use under which circumstances. This subsection will provide this guidance.

Specifications Guidelines

This subsection will present the proposed approach for specifying the monitoring system such that it meets the most important performance requirements. These specifications will include any additional testing that should be performed to validate these performance requirements.

Laboratory Application Notes

Laboratory test results that guide in the application of the technology will be presented here.

Field Case Studies

Case studies from the field provide valuable examples for applications and will be shared here.

6
BUSHING MONITORING

Basic Principles

This first version of the guide presents the start of this chapter on bushing monitoring. Future years will expand this work.

A variety of on-line bushing monitoring technologies exists. Most use a sensor inserted into the bushing tap port. The main purpose of bushing sensors is to provide a reliable external diagnostic signal to the measurement equipment and to keep the tap voltage at a safe level to protect the bushing and test personnel.

There are two main types of commercially available sensors for bushing monitoring applications, depending on the type of impedance used to limit the open-circuit tap voltage:

- Capacitive-type
- Resistive-type

The capacitive-type design inserts a capacitor between the bushing tap and the grounded bushing flange, which reduces the output voltage to a safe level. The resistive-type design uses a resistor of similar impedance value. For both types of sensor, a varistor is connected in parallel with the sensor impedance to provide a second line of defense against transient overvoltages in the event of switching or lightning impulses.

Various Approaches in Application of the Technique

A bushing can be represented by several small capacitance values in series and parallel, as shown in Figure 6-4. As a fault develops in the bushing, the insulation in some of these very small capacitors tracks or punctures and becomes more resistive (as indicated in the figure) by the single capacitor with the line struck through it. The leakage current from deep inside the bushing is miniscule and is difficult to measure in the ground connection. However, by utilizing a capacitive voltage divider, the voltage drops due to a change in the value of these capacitive/resistive components can be sensed and measured by the bushing monitor connected to the bushing capacitance tap.

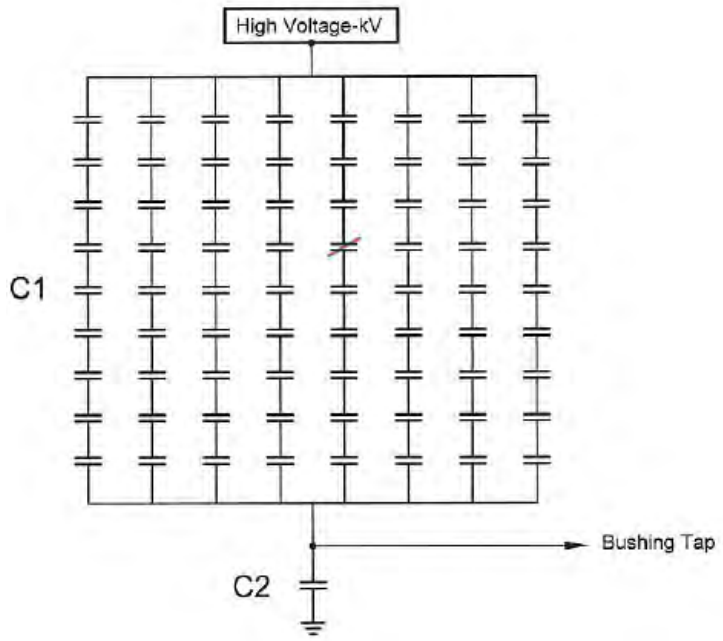

Figure 6–1
Schematic Representation of a Bushing [1]

On-line monitoring systems are available for monitoring the insulation quality of transformer-mounted bushings by continuously monitoring the leakage current, insulation power factor, and capacitance. There are two main methods used for on-line monitoring of bushings (however, there are new monitors that aim at monitoring absolute power factor):

- Relative power factor
- Sum of current

Each requires the fitting of bushing tap couplers to the bushings capacitance test tap (see Figure 6-2).

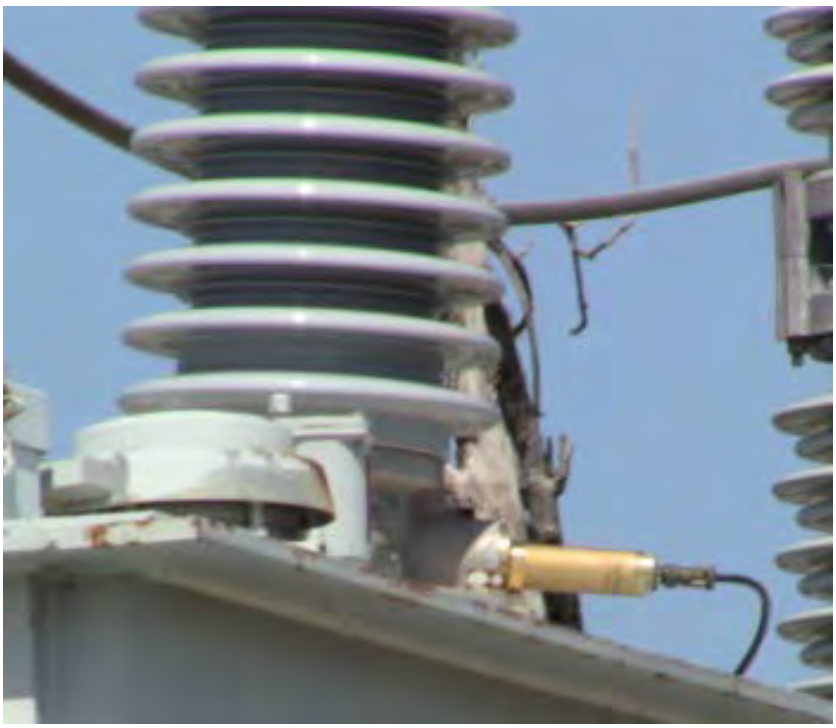

Figure 6–2
Bushing Tap Coupler in a Bushing Capacitance Test Tap

Relative Power Factor Monitors

One method of analyzing the health of bushings is by use of the relative power factor technique. This technique uses the concept of a "virtual schering bridge." The power factor of a bushing as a relative value is determined by comparing the bushing tap voltage with a reference voltage from another bushing in service. This eliminates the need for a precision standard capacitor as is used in a standard schering bridge circuit.

Virtual Schering Bridge Measurements

In the virtual schering bridge, the reference device does not have to be associated with the same phase, because the virtual schering bridge algorithm can automatically perform the proper phase angle adjustments. Relative measurements and evaluation can reduce the influence of parameters such as ambient temperature, operating voltages, loading conditions, different aging characteristics, different designs, operating conditions, etc.

The power factor or tan-δ calculation is based on the fundamental schering bridge calculation. Data is acquired under software control from the bushing sensor represented as C_X in series with R_X in Figure 6-3. The data is compared to data from another bushing used as a reference shown as C_1. The amount of difference between the two measurements is calculated as the relative change in power factor and capacitance between the two bushings under test. One of the advantages of this technique is that each bushing can be compared to all other bushings in the substation, which removes any ambiguity with regard to which bushing is changing when only two bushings are compared.

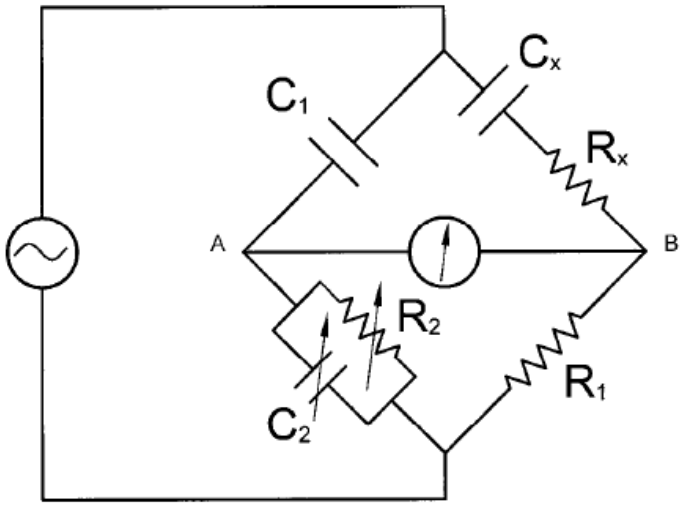

Figure 6–3
Schering Bridge Circuit [1]

Sum Current Monitors

Sum current monitors analyze the condition of the bushing by looking at the vector sum of the currents from the capacitance or power factor taps of the bushings of a three-phase system as shown in Figure 6-4. The principle of the sum current method is based on the fact that the sum of the current vectors is zero in a symmetrical three-phase system with all bushings identical. Any non-zero value of the sum current indicates a difference in the capacitance and/or power factor of the three bushings. Any future change in the sum current from the initial value indicates a deterioration of the insulation of one or more of the bushings. Therefore, the condition of the bushings can be determined by evaluating the change of the sum current vector over time.

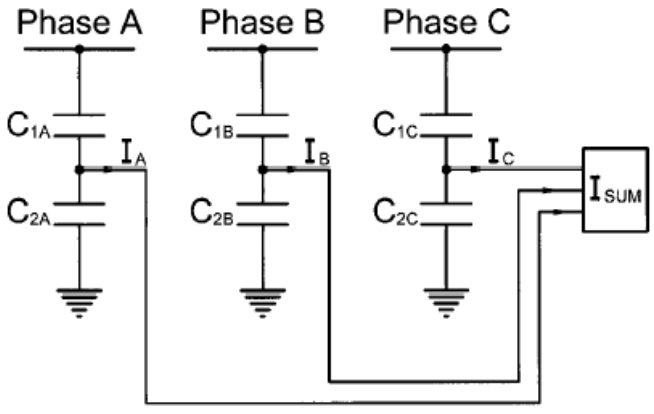

Figure 6–4
Schematic for the Sum Current Method [1]

Monitors with PD Detection

On-line PD offers another option, generally in parallel with one of the methods mentioned above, but tends to be seldom used due to challenging technical issues in high noise substation environments.

Summary of Technologies

Table 6-1 summarizes these techniques.

Table 6–1
Technologies for Bushing Monitoring

Technique	[2]Example Vendors	Long-Term	Electrical or Acoustic PD Detection?
Relative PF	e.g. BPL Global	X	No PD detection
	e.g. GE	X	Electrical PD detection
	e.g. GridSense	X	No PD detection
Sum of Current	e.g. Doble	X	No PD detection
	e.g. Dynamic Ratings	X	Electrical and Acoustic PD detection
	e.g. Eaton	X	Electrical PD detection
	e.g. TreeTech	X	No PD detection
Absolute PF Relative PF Sum of Current	e.g. TechImp	X	Electrical PD detection
Relative PF Sum of Current	e.g ZTZ Service	X	Electrical PD detection

Results Interpretation

Absolute Power Factor Monitors

An increase of bushing capacitance is an important indicator that something is wrong inside the bushing. An excessive change, on the order of 2-5% (depending on the voltage class of the bushing) over its initial reading, probably indicates that insulation between two or more grading elements has shorted out. Such a change in capacitance is an indication that the bushing should be removed from service as soon as possible.

[2] The sample vendor list is under continual expansion in future versions

Relative Power Factor Monitors

Virtual Schering Bridge Measurements

In order to interpret the results, the power factor or tan-δ calculation is compared to data from the bushing(s) used as a reference. The amount of difference between the two measurements is calculated as the relative change in power factor and capacitance between the two tested bushings.

If trended, when the PF values on any bushing change, it will be visible in the graphs. Relative condition shows changes in pairs of data samples based on the "butterfly phenomena". For example, if the data from phase-A referenced to phase-B shows a power factor trend and the data from phase-B referenced to phase-C shows a mirror image power factor trend, the phase-B bushing is experiencing problems.

Moreover, the power factor value of the last off-line test or nameplate power factor values for each bushing monitored can be used to normalize and provide an actual power factor comparable to an off-line test value.

Sum Current Monitors

The principle of the sum current method is based on the fact that the sum of the current vectors is zero in a symmetrical three-phase system with all bushings identical. Any non-zero value of the sum current indicates a difference in the capacitance and/or power factor of the three bushings. In reality, the initial sum current is usually non-zero due to dissimilarities in the three bushings, and the power factor and capacitance of each of the three bushings change over time. This results in changes to the sum current, requiring a more complex mathematical analysis to determine the condition of the individual bushings.

The magnitude of the change of the sum current is the indicator of the problem's severity, and the vector change indicates which bushing is deteriorating and whether the power factor or capacitance is changing. For example, if there is a change in tan-δ in one of the phases, an additional active current passes through that phase bushing insulation and causes the system to be out of balance. The vector created by the imbalance is equal to the change in tan-δ and directed along the affected phase voltage vector. Moreover, a change in capacitance causes the additional current to be perpendicular to the phase voltage and causes the imbalance to be directed along the affected phase current vector.

Therefore, the key diagnostic factor is the sum current and the phase angle of the sum. Only estimates of the power factor and capacitance can be made with this method, because all the data required to calculate the absolute PF and capacitance is not available. When the sum current shows unbalance, the change of PF and/or capacitance is estimated. These values are then added/subtracted to baseline values (nameplate or recent off-line test values). As the sum current increases, the accuracy of the PF and capacitance calculations improve.

Laboratory Application Notes

Over the past year, utilities have provided several intact bushings to EPRI for research. The bushings ranged from 34.5 kV to 230 kV. Power factor testing and oil sampling was performed on all bushings. Additionally, some of the bushings have been disassembled and forensically investigated. The forensic investigation of the intact bushings consisted of the following (see Table 6-2):

- Power factor testing to confirm field measurements (all intact bushings)
- Oil sampling to perform DGA and extensive oil quality testing (all intact bushings)
- Teardown of two bushings

Table 6–2
Summary of Results from Bushings sent to EPRI for research in 2012

Rated (kV)	BIL (kV)	Year Manufactured	Power Factor	DGA	Oil Quality	Particle Count	Visible Inspection	DP
138	650	1999	X	X	X	X	X	X
138	650	1999	X	X	X	X		
138	650	1999	X	X	X	X	X	X
138	650	1999	X	X	X	X		
138	650	1999	X	X	X	X	X	X
115	550	2002	X	X	X	X		
115	550	2002	X	X	X	X		
115	550	2002	X	X	X	X		
138	650	1999	X	X	X	X	X	X
161	750	2004	X	X	X	X		
69	350	2004	X	X	X	X	X	X
230	900		X	X	X	X		
34.5	200	2002	X	X				
34.5	200	2002	X	X			X	
34.5	200	2002	X	X			X	
34.5	200	2002	X	X				

Power Factor Testing

Power factor testing measurements were obtained using a test fixture fabricated by EPRI that allowed the bushing to be mounted vertically in air (see Figure 6-5). This arrangement should have little to no effect on C_1 power factor measurements. Bushings were situated vertically for at least 48 hours prior to testing.

The general rule of thumb for bushing C_1 power factor is that the measured value should not deviate from the nameplate C_1 power factor by more than 100%. In addition, the C_1 capacitance should not vary by more than 5%. Note that power factor values are generally corrected for temperature to 20˚C (see Table 6-3).

Figure 6–5
Power Factor Testing Set-Up at EPRI's Lenox Facility

Table 6–3
Example of Power Factor Test Results from Intact Bushings

Rated (kV)	BIL (kV)	Nameplate		EPRI	
		%PF C_1	Capacitance C_1	%PF C_1	Capacitance C_1
115	550	0.28	508	0.31	499.95
115	550	0.28	508	0.28	500.48
115	550	0.26	499	0.25	491.50
138	650	0.31	550	0.33	544.36
161	750	0.30	495	0.32	487.44
69	350	0.23	417	0.26	437.97
230	900	0.34	622	0.37	614.06

Note: Air temperature at test was approximately 18˚C

Oil Sampling and Testing

In order to gain some insight into what was happening inside the bushings, as well as to assess the dielectric integrity of the insulating oil, a thorough array of oil tests were conducted on samples drawn from each of the bushings received (see Figure 6-6). These tests included:

- DGA
- Particle counts
- Furan measurements
- Interfacial tension (IFT)
- Neutralization number (NN)
- Dielectric breakdown voltage, D1816
- Moisture
- Oil power factor at 25˚C and 100˚C

Figure 6–6
Taking Oil Samples from Bushings

DGA Results

There is no broad consensus on the interpretation of bushing DGA results, because this test is rarely performed, given the technical risks inherent in drawing samples from a sealed system with little oil volume. The practice of sampling bushing oil for DGA is more prevalent outside of North America. International standards [4] provide some guidance on the interpretation of the DGA levels (see Table 6-4).

Table 6–4
DGA Thresholds for Concern in Bushings [4]

Type of Gas	Threshold for Concern (ppm)
Hydrogen (H_2)	140
Methane (CH_4)	40
Ethylene (C_2H_4)	30
Ethane (C_2H_6)	70
Acetylene (C_2H_2)	2
Carbon Monoxide (CO)	1000
Carbon Dioxide (CO_2)	3400

None of the measured gas concentrations in the seven intact bushings shown in Table 6-5 approached levels of concern. All gas levels were low.

Table 6–5
Example of DGA Results from Intact Bushings

Rated (kV)	BIL (kV)	H_2	CH_4	C_2H_6	C_2H_4	C_2H_2	CO	CO_2	O_2	N_2
115	550	16	6.7	1.5	0	0	121	917	11,800	57,300
115	550	6.7	5.7	0.8	0	0	129	764	11,100	59,100
115	550	6.6	6.0	1.0	0	0	188	785	6560	59,000
138	650	7.4	6.8	1.1	0	0	188	665	10,700	59,000
161	750	13	11	0	0	0	200	872	1070	31,200
69	350	15	7.5	2.2	0	0	184	641	1000	40,200
230	900	38	4.7	0.6	0	0	73	307	1670	40,800

Oil Quality

A battery of general oil quality tests was performed on each sample to assess the suitability of the oil for reliable service given the electrical stresses in a bushing. Again, no standards exist to provide clear guidance on the acceptability of various quantities. However, standards guidance [5] for the acceptance of oils in power equipment can provide some insight. In general, the oil quality for the tested bushings is marginal, but acceptable.

Teardown of Intact Bushings

The bushing core was removed from each bushing by removing the upper collar to release the clamping pressure, unthreading the lower resin cone, and then lifting the core out (see Figure 6-7).

Figure 6–7
Removing a Bushing Core

The core was then placed horizontally on a set of rollers to allow for easy and controlled unrolling of the paper core (see Figure 6-8).

Figure 6–8
Unrolling the Paper

As each core was unrolled, detailed measurements were taken of foil locations and general dimensions, both to verify proper construction and to allow for any subsequent analysis that may be needed (see Figure 6-9). The paper and foils were visibly examined as carefully as possible to identify any foreign contaminants or areas where partial discharge or breakdown between foil layers may have occurred.

Figure 6–9
Measuring the Foil Locations and General Dimensions

In addition, paper samples were obtained at regular intervals for analysis of the degree of polymerization (DP). This is a measure of the paper's thermal degradation. Squares, approximately 2 cm x 2 cm (0.79 in. x 0.79 in.), were taken roughly after every 50 layers of paper (e.g., six radial locations for the 69 kV bushings, or nine locations radially for the 138 kV bushings). At each layer where samples were taken, seven samples were taken axially along the length of the core at regular intervals (see Figure 6-10). A select subset of these samples were sent for testing to assess the overall condition of the paper, as well as the distribution of DP spatially throughout the core.

Figure 6–10
Samples were Obtained Axially along the Length of the Core at Regular Intervals

Degree of Polymerization

Some of the DP results obtained so far have indicated that a significant amount of thermal degradation has taken place throughout the bushings. While there is no established DP end-of-life value for bushings, values were lower than expected (more degradation).

In the example results shown in Figure 6-11, there is a drop-off in DP toward the air (outboard) end of the bushings. This is generally expected, as the air provides a less efficient cooling medium than the oil in which the lower end is immersed. Moreover, there is also a decrease radially, with outer layers being significantly lower. This decreasing trend is consistent between all the bushings tested so far (see Figure 6-12).

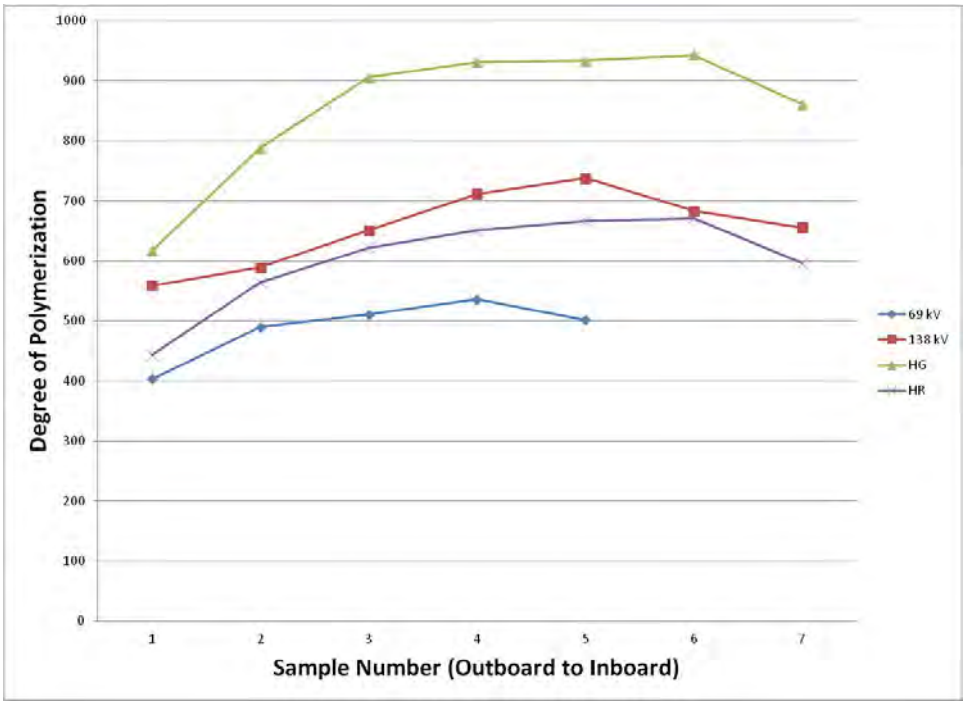

Figure 6–11
Comparison of Bushings Axial DP Distribution against Others Tested

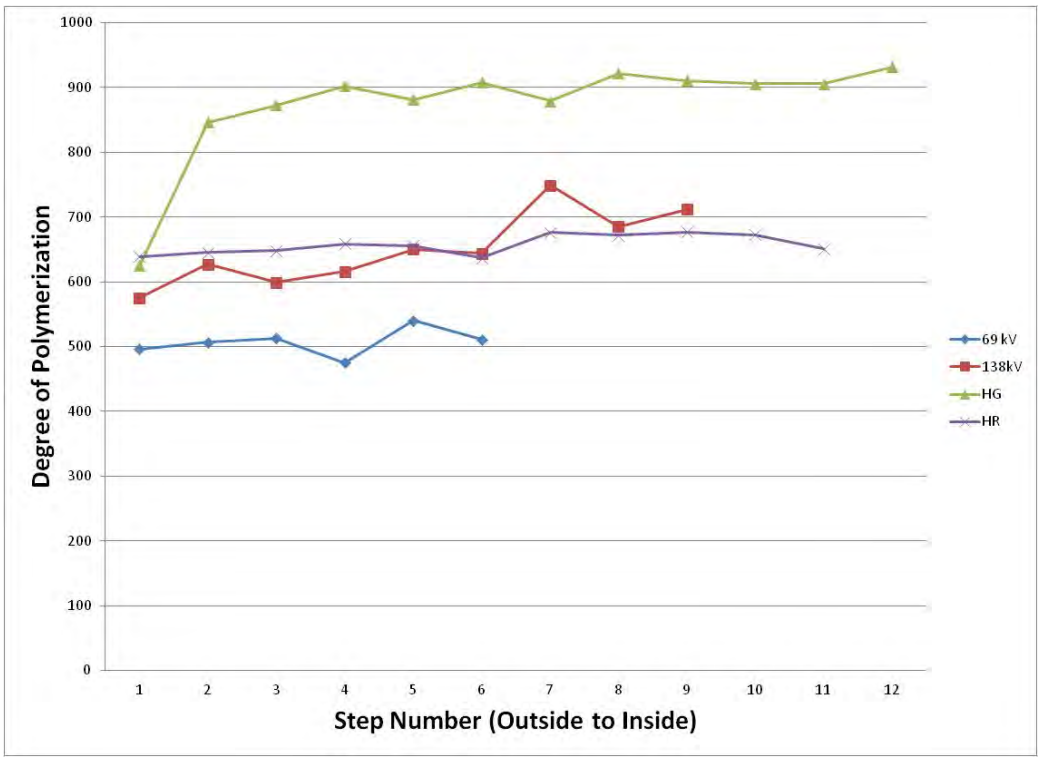

Figure 6–12
Comparison of Bushings Radial DP Distribution against Others Tested

The laboratory research will slowly guide us on which emerging technologies are ideal for bushing monitoring. In this first year of work we have gathered some data but a far larger set of laboratory tests is needed to draw conclusions. These laboratory tests will continue with this goal in mind. EPRI is presently expanding the laboratory testing to allow bushings to be energized at rated voltage. This will allow for laboratory assessment of field monitoring approaches prior to forensic analysis of the bushings.

Field Case Studies

Through the EPRI research underway, four sites are being monitored with on-line bushing monitoring. In subsequent updates of this application guide, lessons learned from these four case studies will be presented.

Specifications Guidelines

This subsection will present the proposed approach for specifying the monitoring system such that it meets the most important performance requirements. These specifications will include any additional testing that should be performed to validate these performance requirements.

7
ELECTRICAL PARTIAL DISCHARGE DETECTION

Basic Principles

Electrical partial discharge (PD) detection in transformers is an emerging application for on-line field monitoring. PD detection is commonly used in transformer factory testing, but on-line monitoring in the field is less common due to the challenges of how to couple the PD signals from the transformer and how to reject the high levels of background noise typically present on an in-service transformer. The research in this section examines emerging techniques both in the field and in the laboratory.

Research has begun in the laboratory and is reported below. Further revisions of the application guide will expand the work and present case studies from the field.

Various Approaches in Application of the Technique

This subsection will present the various options for coupling PD from an in-service transformer. These include, among others, UHF sensors, high frequency current transformers around a transformer ground, and bushing capacitive taps.

Results Interpretation

Interpretation of electrical PD signals is made challenging by the high levels of background noise in the field. In addition, a PD magnitude alone cannot be easily related to the risk of failure of a transformer. The risk depends on numerous other factors, including the location of the discharge. This subsection will highlight these challenges and guide the engineer on complementary tests to help reduce the risk of failure.

Laboratory Application Notes

UHF Sensor Signal-to-Noise Ratio Tests in the EPRI Charlotte Test Transformer

An experiment was designed and conducted to explore the difference in the signal-to-noise gathered from permanently mounted UHF sensors and temporarily mounted drain valve UHF sensors.

Description of the Experimental Set-Up:

- UHF calibration pulses were produced by a UHF Calibrator (Omicron Model UPG620)
- UHF calibration pulses were inserted into the permanently mounted UHF sensor on the top lid of the test transformer (designated U04). (See Figure 7-1.)
- UHF signals were measured from the remaining three permanently mounted UHF sensors on the transformer (designated U01, U02, and U03).
- UHF signals were also measured from two UHF probes temporarily inserted into the bottom drain valve.

- The first UHF probe used in the drain valve was manufactured by NDB Technologies and supplied as an option to NDB's AE-150 system. (See Figure 7-2.)
- The second UHF probe used in the drain valve was an Omicron UVS 610, supplied as an option to the MPD 600 measurement system. (See Figure 7-3.)
- Each drain valve UHF sensor was inserted into the valve such that the tip of the sensor was flush with the inside wall of the transformer – i.e., the sensor was at the threshold of protruding into the transformer tank.

Figure 7–1
UHF Calibrator Injecting Signals into the UHF Sensor Mounted to the Lid of the Test Transformer (Sensor Designated U04)

Figure 7–2
Drain Valve UHF Probe Manufactured by NDB Technologies (Supplied as Part of Their AE-150 System)

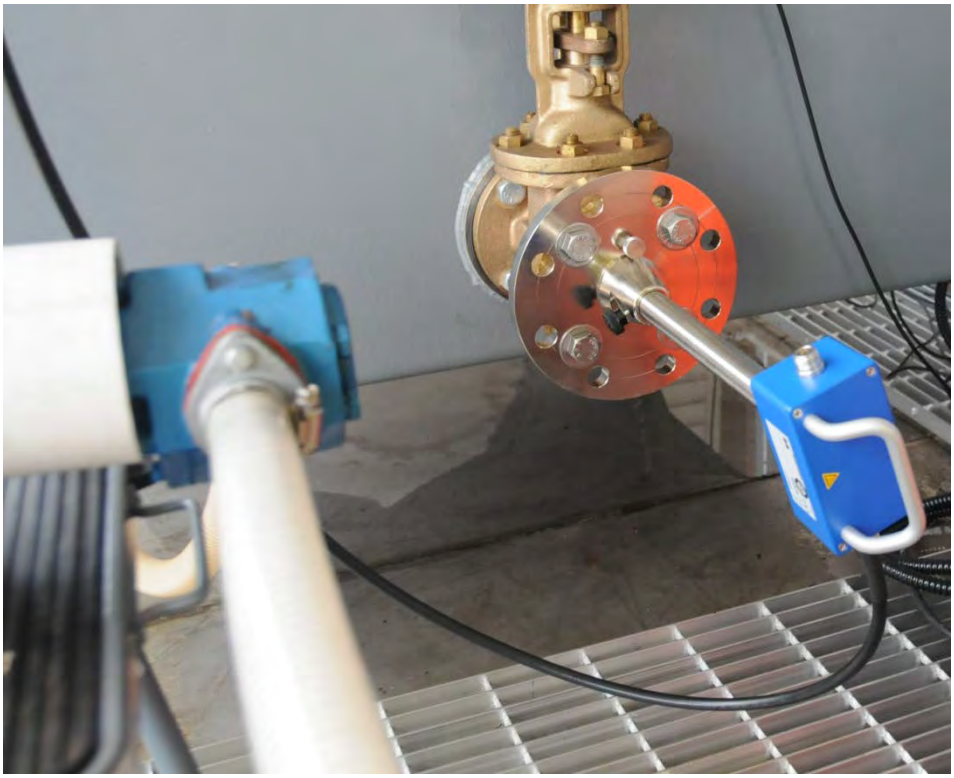

Figure 7–3
Omicron Drain Valve UHF Probe UVS610 Supplied as an Option to the MPD600 Measurement System

Description of the Measurement Set-Up:

- Measurements were made using a Tektronix oscilloscope, model DPO 7104.
- All signals were captured with the analog bandwidth set to the maximum of 1 GHz.
- The permanently mounted UHF sensors were terminated into 50 Ω For the permanently mounted UHF sensors the oscilloscope gain was fixed at 10mV/div for all the measurements. This gain was fixed because the oscilloscope lowers the analog bandwidth as the gain increases. At higher gains the bandwidth was too low to capture the peaks of the high frequency UHF pulses.
- The NDB Technologies drain valve sensor has a built-in amplifier and the signal was analyzed at the output of this amplifier. The oscilloscope gain was fixed at 60 mV/div for all of the measurements. The oscilloscope input was terminated into 50 Ωas this produced improved signal-to-noise ratios compared to terminating into 1 M Ω
- The Omicron UVS-610 UHF probe was fed into an Omicron UHF-608 UHF Converter. The oscilloscope input was terminated into 1 M Ωas this gave improved signal-to-noise ratios compared to terminating into 50 Ω The oscilloscope gain was fixed at 60 mV/div for all of the measurements.

Description of the Test Protocol:

- For each voltage level of the calibrator input, the following measurements were made from each of the four sensors: background noise (peak-peak) and measured pulse magnitude (peak-peak).
- For each voltage level of the calibrator input, the signal-to-noise ratio was then calculated by dividing the measured pulse magnitude by the measured noise.
- The resulting signal-to-noise ratio as a function of calibrator input is shown in Figure 7-4.

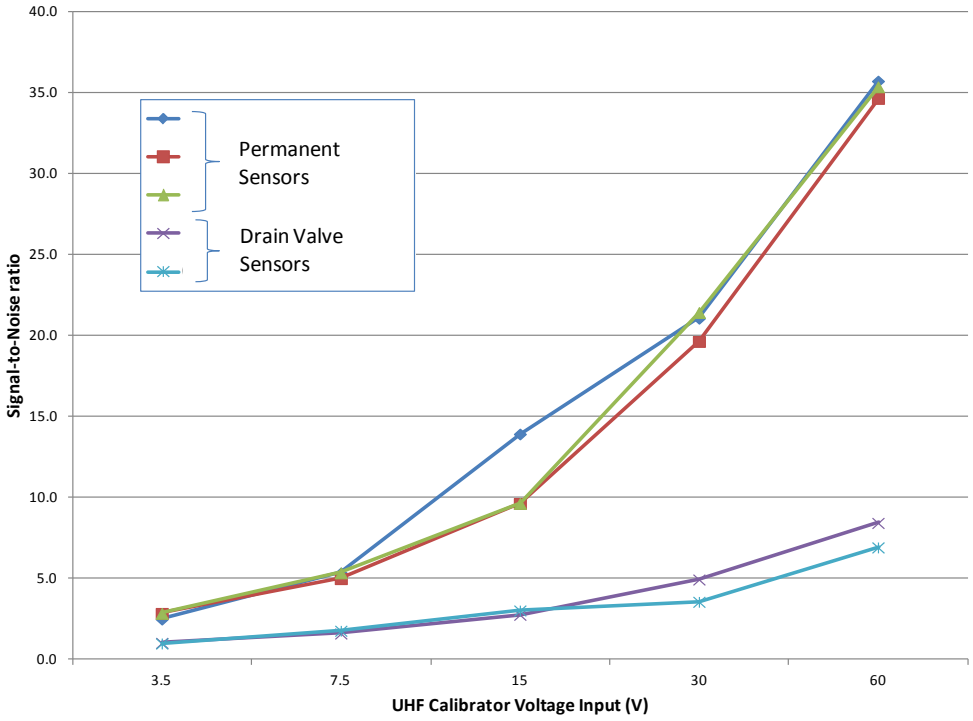

Figure 7–4
Signal-to-Noise Ratio of the Three Permanently Mounted UHF Sensors and Two Drain Valve Sensors

These earlier results indicate that permanently mounted UHF sensors are likely to offer an improved signal-to-noise ratio compared to drain-valve sensors. Retrofitting permanent UHF sensors to existing transformers is often costly and difficult, so drain valve sensors have a valuable role to play in gathering signals from existing installations. For utilities considering long-term monitoring of UHF signals from transformers, these preliminary results indicate the signal improvements that could be gained from specifying permanently mounted UHF sensors at the time of manufacture. These early experimental results are from a small transformer with no internal windings. A next step is to further validate the findings in a field transformer.

Field Case Studies

Case studies in this area are relatively rare, but in this subsection past case studies will be summarized and field deployments will be performed to create informative field studies.

Specifications Guidelines

This subsection will present the proposed approach for specifying the monitoring system such that it meets the most important performance requirements. These specifications will include any additional testing that should be performed to validate these performance requirements.

From the published literature, a proposed approach for selection of UHF sensors has been reported from National Grid Company Technical Guidance Note (Number 121). The selection approach involves testing the UHF sensor in a transient calibration system. The UHF sensor is attached to the calibration system in the geometry that represents its final deployment onto a transformer. The calibration system calculates two key parameters: minimum and mean

effective height over the frequency band of interest. The minimum and mean effective heights are then compared against the requirements to determine whether the proposed UHF sensor is sensitive enough for the proposed application [6].

The following limits are quoted for a 420 kV GIS UHF sensor [7] and the limits have been reported to also apply well for selection of transformer UHF sensors [8]:

- Mean effective height: 6 mm (0.24 in.)
- Minimum effective height: 2 mm (0.079 in.)
- Frequency range: 500 MHz to 1500 MHz

These premilinary studies will be extended in future versions of the application guide.

8
ELECTRICAL PARTIAL DISCHARGE DETECTION IN COMBINATION WITH ACOUSTIC EMISSION

Electrical and acoustic PD detection are commonly used independently in transformers. However, an electrical signal synchronized with the signal from acoustic sensors can be used to detect, and in some cases locate, the PD source. This section is intended to cover the electrical PD detection in combination with acoustic emission, and is scheduled for publication in the 2013 update of this application guide. The section will cover the following key aspects:

- Basic principles
- Various approaches in application of the technique
- Results interpretation
- Specification guidelines
- Laboratory application notes
- Field case studies

Basic Principles

This subsection will present the underlying theory for detection. An understanding of these basics will help in the selection between technologies.

Various Approaches in Application of the Technique

There are various technical approaches for combining electrical and acoustic emission PD detection. This subsection will discuss each approach in detail. Understanding these approaches will allow for assessment of the benefits and limitations of each.

Results Interpretation

A utility engineer is faced with the difficult choice of determining which interpretation approaches to use under which circumstances. This subsection will provide this guidance.

Specifications Guidelines

This subsection will present the proposed approach for specifying the monitoring system such that it meets the most important performance requirements. These specifications will include any additional testing that should be performed to validate these performance requirements.

Laboratory Application Notes

Laboratory test results that provide guidance in the application of the technology will be presented here.

Field Case Studies

Case studies from the field provide valuable examples for applications and will be shared here.

9
DIELECTRIC RESPONSE MEASUREMENTS

Diagnostic measurement techniques that analyze the response of the transformer dielectric system across multiple frequencies are collectively known as dielectric response measurements. This section is intended to cover the different dielectric response methods and is scheduled for publication in the 2013 version of this application guide. The section will cover the following key aspects:

- Basic principles
- Various approaches in application of the technique
- Results interpretation
- Specification guidelines
- Laboratory application notes
- Field case studies

Basic Principles

This subsection will present the underlying theory of the use of different stimuli to measure the dielectric response. An understanding of these basics will be useful in the selection between technologies.

Various Approaches in Application of the Technique

There are now three available methods that use different stimuli and measure the dielectric response to provide diagnostics of the insulation: return voltage measurements (RVM), polarization/depolarization current, and dielectric frequency response. This subsection will discuss each approach in detail. The understanding of these approaches will allow for assessment of the benefits and limitations of each.

Results Interpretation

A utility engineer is faced with the difficult choice of determining which interpretation approaches to use under which circumstances. This subsection will provide this guidance.

Specifications Guidelines

This subsection will present the proposed approach for specifying the monitoring system such that it meets the most important performance requirements. These specifications will include any additional testing that should be performed to validate these performance requirements.

Laboratory Application Notes

Laboratory test results that guide in the application of the technology will be presented here.

Field Case Studies

Case studies from the field provide valuable examples for applications and will be shared here.

10
HIGH FREQUENCY TRANSIENT MONITORING USING BUSHING COUPLERS

This version of the application guide populates an extensive case study. Future versions will extend the work to include details on the following topics:

- Basic principles
- Various approaches in application of the technique
- Results interpretation
- Specification guidelines
- Laboratory application notes
- Field case studies

Basic Principles

Measurements from the capacitive tap of bushings have typically been used to diagnosis the condition of the bushing. Emerging technologies now also allow for wideband measurement of the voltages impinging on the bushings. These measurements could potentially provide insight into the magnitude and frequency content of overvoltages that the bushings and transformer are subject to – and thus are of value for both forensics after a failure or for validation of insulation coordination approaches.

Various Approaches in Application of the Technique

There are presently few examples of this measurement approach, but as different approaches emerge they will be described here.

Results Interpretation

This subsection will be used to detail how an engineer could use measurement results for forensic studies, insulation coordination studies, or potential diagnosis of re-striking breakers or poor contacts in load tap changers.

Specification Guidelines

This subsection will present the proposed approach for specifying the monitoring system such that it meets the most important performance requirements. These specifications will include any additional testing that should be performed to validate these performance requirements.

Laboratory Application Notes

In this subsection, details of laboratory testing will be presented. The first laboratory test that will be a published is a calibration of a bushing monitoring system against a reference high voltage divider.

Field Case Studies

Case Study 1: Transient Monitoring on Three Single-Phase 765/345kV 750MVA Transformers at AEP

The case study for transient monitoring made use of the on-line frequency response analysis (OLFRA) installation on these transformers. (The OLFRA case study is presented in this report as "

Case Study 4: Three Single-Phase 765/345 KV Auto-Transformers" in Section 11).

There is increased interest in the interaction between substation transients and transformers in HV and EHV applications. This is due to the number of transformer bushing and winding failures that cannot be explained by the traditional low frequency methods. The raw data for OLFRA is a time stamped database of the high voltage and high frequency transients in the area of and at the location of the transformer with the OLFRA equipment installation. At present, the 60 Hz power frequency component is filtered out to increase the dynamic range of the high frequency transients recorded. A future OLFRA development is to locate the high frequency transients on the 60 Hz waveform.

The remainder of this case study presents examples of different types of transients gathered from the OLFRA system at the AEP substation.

Example: Energization of a 765kV Transformer

The AEP transformer is unique in energization, in that the 765 kV line and the attached 765 kV transformer are energized by closing a breaker about 90 miles (144.8 km) away. The phase 1 transients are shown in Figure 10-1 and Figure 10-2.

The voltage scale for the H1 and X1 voltage is the left vertical scale. The multiplier for the 50 kHz dominant H1 frequency peak is 133, which gives a peak of about 39 kV at the H1 bushing input. The multiplier for the X1 6.7 kHz frequency is 1250, which gives a peak of about 114 kV at the X1 bushing input. Note that the normal 60 Hz to ground voltage is 199 kV, and a worst case could be when the 114 kV pulse peak occurs at the 60 Hz voltage peak of 282 kV.

The voltage scale for the neutral voltage of the phase 1 transformer is the right vertical scale. The multiplier for the 50 kHz dominant neutral peak is 1.1, which gives a peak of about 96 volts at the top of the neutral bushing when the phase 1 transformer is energized.

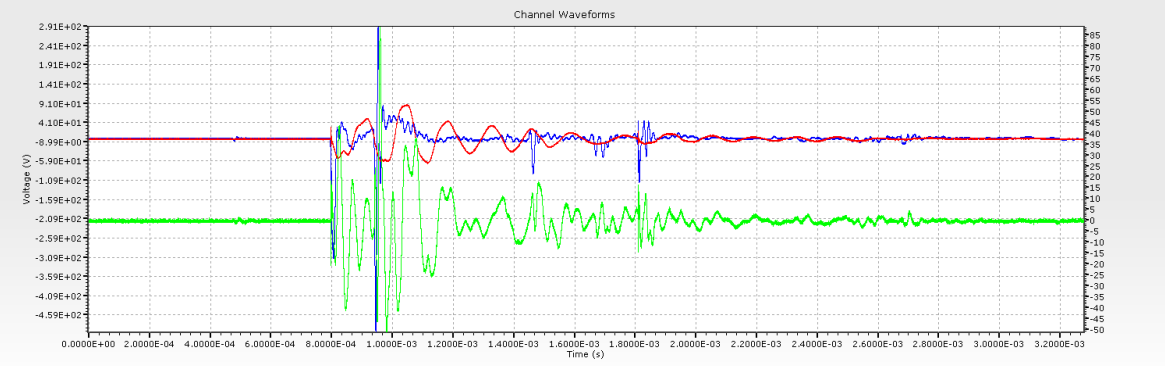

Figure 10–1
Energization of the 765 kV Auto-Transformer from 90 Miles (144.8 km) Away (Recorded on Phase 1). H1 Voltage (Blue), X1 Voltage (Red), Neutral Voltage (Green).

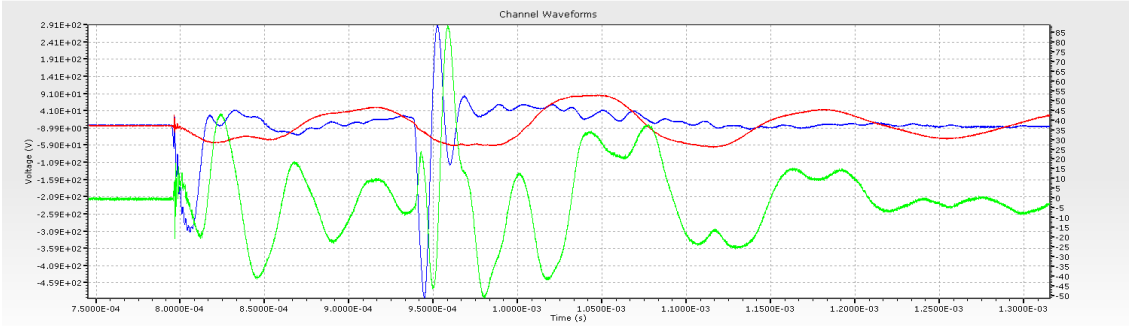

Figure 10–2
Zoom In of Energization of the 765 kV Auto-Transformer from 90 Miles (144.8 km) Away (Recorded on Phase 1). H1 Voltage (Blue), X1 Voltage (Red), Neutral Voltage (Green).

Example: Induced Lightning Strike on the 765 kV Line

A transient waveform set representing induced lightning on the 765 kV line for phase 3 is shown in Figure 10-3 and Figure 10-4.

Using the same multiplier (133) as above for the 5 kHz H3 input voltage, the blue trace voltage peak is about 37 kV. The X3 input voltage is less than 20 volts, and the neutral voltage is about 108 volts with a multiplier of 1.2 for 25 kHz.

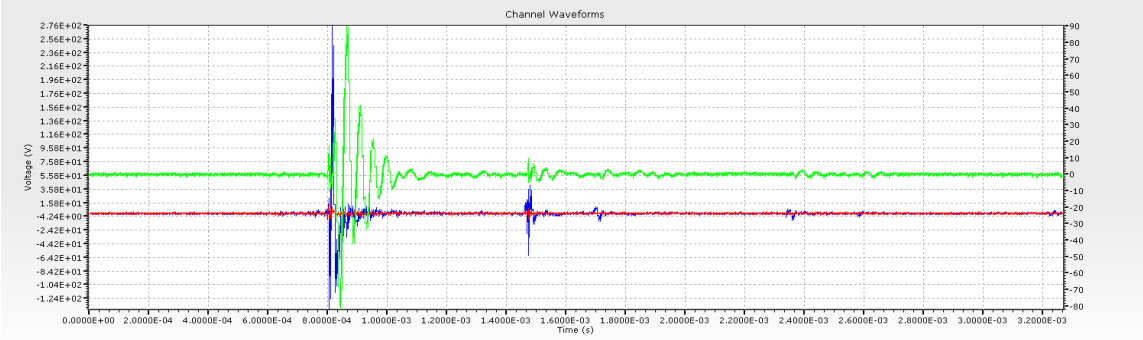

Figure 10–3
Induced Lightning on 765kV Line (Recorded on Phase 3). H3 Voltage (Blue), X3 Voltage (Red), Neutral Voltage (Green).

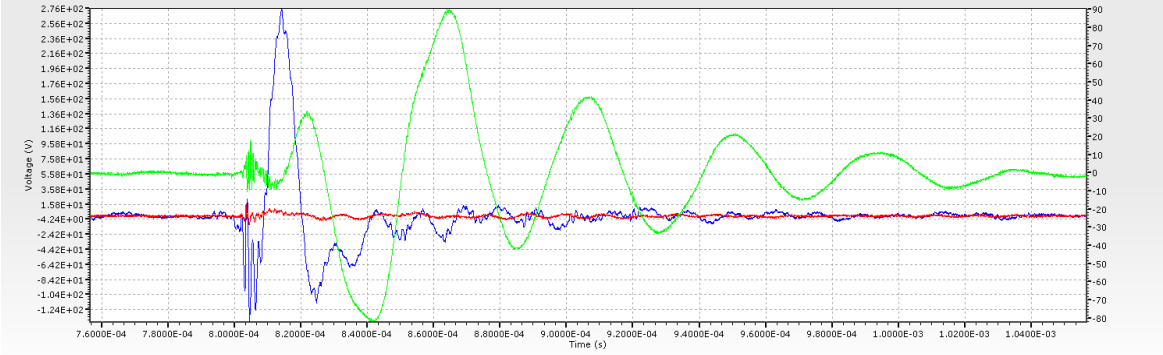

Figure 10–4
Zoom of Induced Lightning on 765kV Line (Recorded on Phase 3). H3 Voltage (Blue), X3 Voltage (Red), Neutral Voltage (Green).

Example: Induced Lightning Strike on the 345kV Line

Figure 10-5 and Figure 10-6 represent induced lightning on the 345 kV line side of the transformer. This lightning pulse happens to be broadband up to 2 MHz as indicated by the lower FFT graph.

The multiplier for the 900 kHz dominant peak is 3.6, which gives 1.3 kV for the 900 kHz for input to the phase 2 low side bushing. The dominant frequency for the high side bushing is also about 900 kHz, which uses the same multiplier to give 371 volts at the input of the X2 bushing. The dominant frequency for the phase 2 neutral bushing is about 20 kHz, and the peak voltage for this frequency is 182 volts with a multiplier of 1.2.

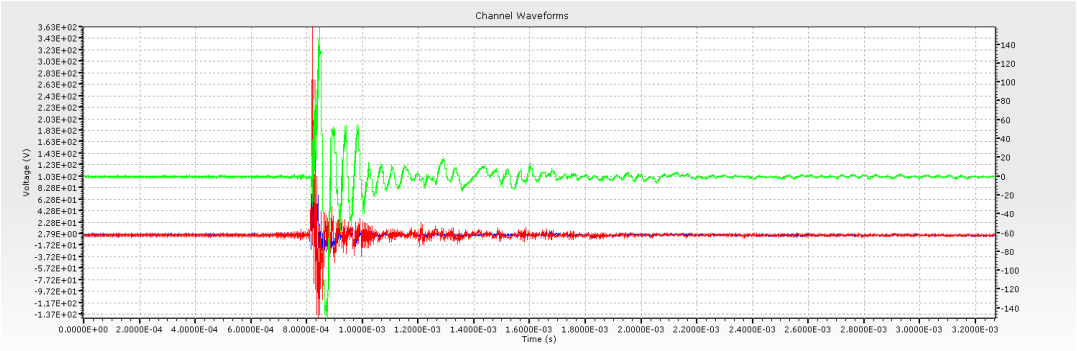

Figure 10–5
Induced Lightning on 345kV line (Recorded on Phase 2). H2 Voltage (Blue), X2 Voltage (Red), Neutral Voltage (Green).

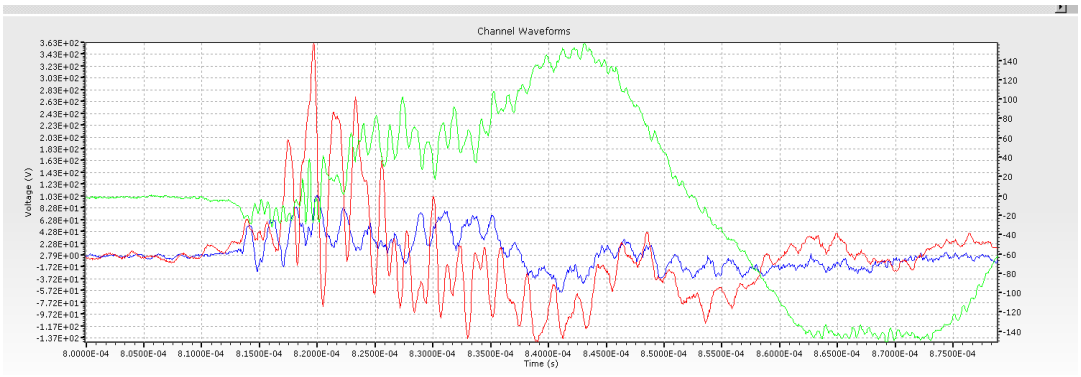

Figure 10–6
Zoom In of Induced Lightning on 345kV Line (Recorded on Phase 2). H2 Voltage (Blue), X2 Voltage (Red), Neutral Voltage (Green).

Example: Disconnect Switch Closing

Figure 10-7 and Figure 10-8 represent the first triggers of the digitizer for the closing of a 345 kV disconnect switch.

The X2 500 kHz dominant peak voltage is about 7.2 kV with a multiplier of 12.5. The H2 500 kHz dominant peak voltage is about 1 kV with a multiplier of 13.9. The phase 2 neutral bushing voltage is about 348 volts peak with a multiplier of 2.9.

Note that the disconnect switch closing has the highest frequency content of the transients recorded. All multipliers for the waveforms are derived from the transfer functions of the total measurement system.

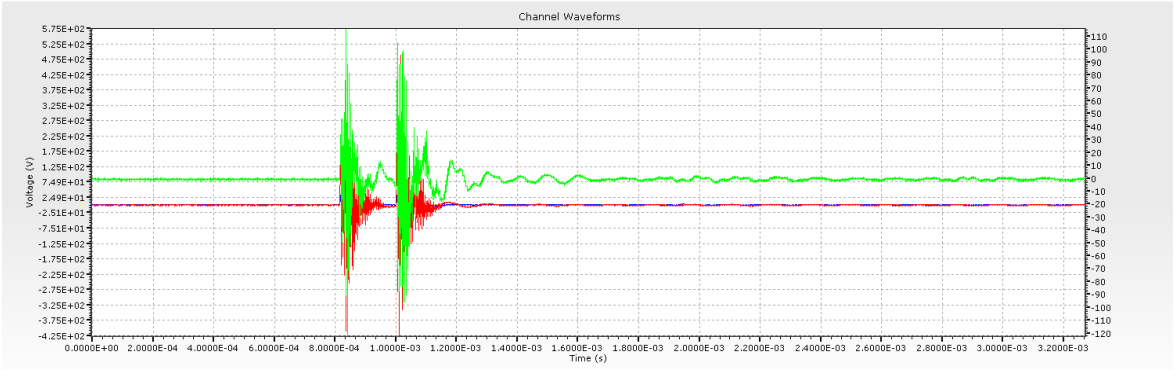

Figure 10–7
Closing of a 345 kV Disconnect Switch (Recorded on Phase 2). H2 Voltage (Blue), X2 Voltage (Red), Neutral Voltage (Green).

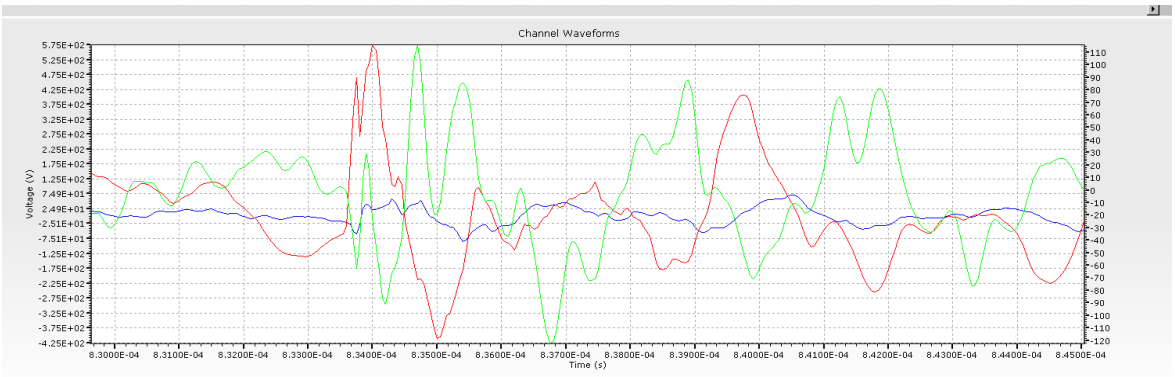

Figure 10–8
Zoom In of Closing of a 345 kV Disconnect Switch (Recorded on Phase 2). H2 Voltage (Blue), X2 Voltage (Red), Neutral Voltage (Green).

11
FREQUENCY RESPONSE ANALYSIS

This section focusses on results obtained using on-line frequency response analysis (OLFRA). To-date there is one case study on off-line FRA and three case studies on on-line FRA. In future updates the section will be expanded to include additional field and laboratory case studies.

Basic Principles

Transformer windings require strong clamping forces to resist mechanical deformation during system faults. For this reason, these transformer windings are braced mechanically to prevent movement. However, clamping pressure can be compromised in various ways, such as shipping damage, cumulative stress from an excessive number of through-faults, or insulation shrinkage as the transformer ages. In any case, as winding materials age, the clamping forces tend to relax. With inadequate clamping pressure, windings can move when subjected to forces caused by external short-circuit faults. Resonant vibration associated with load current can also lead to mechanical abrasion of the insulation. When this occurs, the transformer has an increased probability of failure during a subsequent through-fault.

Various Approaches in Application of the Technique

On-Line Frequency Response Analysis

Off-line frequency response analysis (FRA) testing is an effective method to identify partially damaged or loose transformer windings. The method calls for examination of frequency-dependent parameters, such as magnitude and phase of impedance or admittance, as well as comparison with a previous measurement. The frequency response analysis test is performed by applying a low voltage impulse or a swept frequency to one winding, then recording the applied signal and the coupled current or coupled voltage on another winding. Changes in capacitance between windings, as well as changes in the inter-turn winding capacitances (caused by winding movement) are reflected in the change of the wave shape of the measured current or voltage. A Fourier transform is performed on the recorded data. The Fourier transform of the measured output current or voltage is divided by the transform of the input voltage. By comparing the results (signature) recorded initially with the results recorded later or with results recorded on an identical transformer, movements of windings may be detected. By using the admittance or transfer function, any variation caused by changes in the applied voltage waveform is eliminated. This makes the test repeatable over time. Correlations between curve comparisons and potential internal defects can then be made. This replaces earlier techniques based on low voltage impulse (LVI), due to the availability of high performance network analyzers with greater sensitivity to subtle winding resonances. The off-line FRA test requires the transformer to be de-energized and disconnected, and instrumentation must be used to determine the transfer functions.

In general, off-line FRA is performed in at least two different LTC tap positions, one in the neutral position and another in the position with the maximum range, so as to consider all possible windings.

Two connection methods to the transformer have been reported. The first measures the voltage response between ends of a winding. The second measures the driving point admittance or impedance at one terminal, or the transfer impedance between pairs of terminals. The latter method requires a current transducer, but offers the advantage of less sensitivity to artifacts introduced by lead connections.

The experience to-date with FRA testing indicates that major fault-induced winding deflections can be detected at the terminals. However, the method does not presently assign any risk of failure associated with this.

An Off-Line Frequency Response Analysis Example

When a winding insulation is damaged, differences in the frequency response analysis of the system can be observed. Below, Figure 11-1 shows an example of an off-line test performed on a transformer taken out of service after 120 ppm of acetylene was found on a routine dissolved gas analysis (DGA). The power factor and transformer turn-ratio tests (TTR) did not indicate any cause for concern, but the off-line FRA test indicated an abnormal phase in the high side delta, as shown below. As can be seen in Figure 11-1, the H1H2 winding is significantly different in frequency peak location, and is missing a frequency peak at 2 MHz, as compared to the other two phases. The asymmetry value was calculated to be 495.4%. This is a cross-phase comparison test, since there was no previous history on this transformer for a historical same-winding comparison. The cross-phase test works well here, since in normal condition this transformer did not have extreme differences between phases, as evidenced by the similarity of the other two phases.

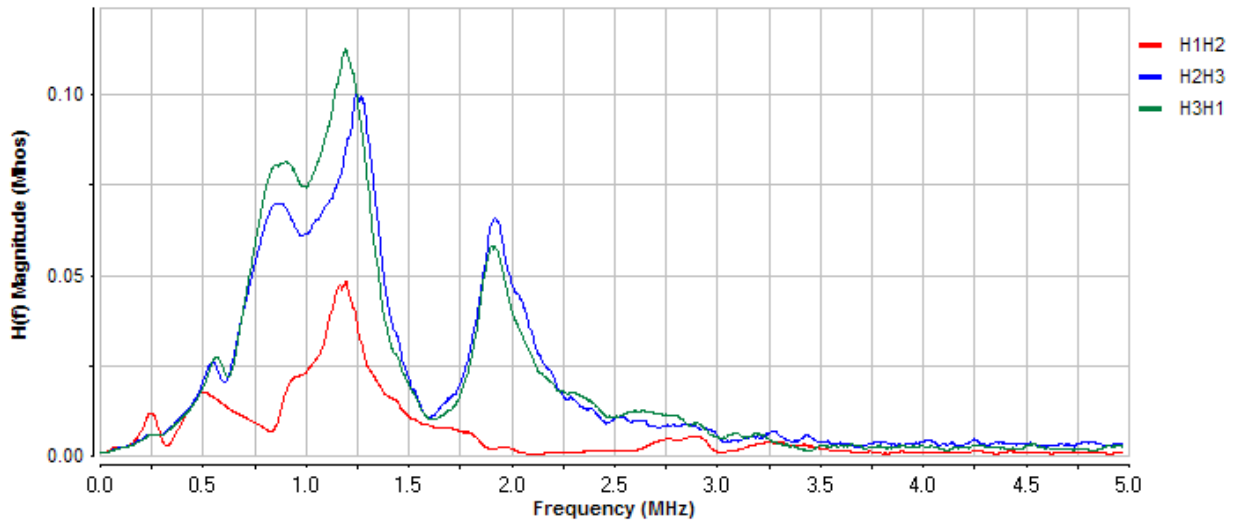

Figure 11–1
Off-Line FRA Test Result Indicating Winding Damage

The transformer was subsequently un-tanked and visually inspected for signs of arcing on the surface, but none were found. The coil assembly, indicated by FRA to be significantly different, was taken to the local manufacturer and unwound. The results are shown in Figure 11-2 below. The bond between the copper ribbon and the inner static shield on the H1H2 winding had lost good contact and had begun to produce small arcs and carbon deposits.

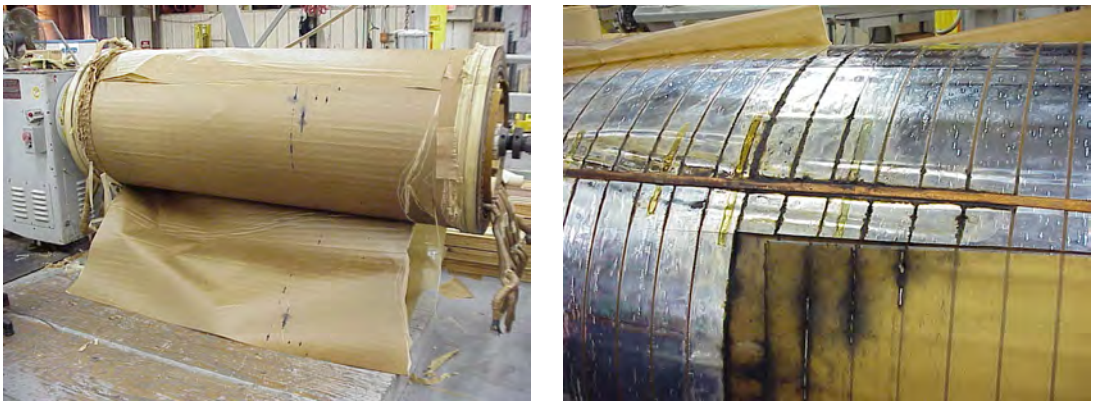

Figure 11–2
Insulation Damage Found by Unwinding Coil Assembly

On-Line Frequency Response Analysis

On-line frequency response analysis (OLFRA) is a new type of early condition assessment for power transformer windings. The method described below has been developed by NEETRAC with support from EPRI in field demonstrations and hardware improvements. The FRA method is an on-line (transformer energized) technique designed to perform winding movement diagnostics while the transformer remains in service. The technique can provide a periodic condition assessment of transformer winding deformation and therefore provide a new input for on-line end-of-life assessment.

New and re-conditioned transformer windings are assembled with symmetrical dimensions to evenly distribute the magnetic force. This minimizes winding deformations that cause fault conditions. Once normal winding deformation starts, due to normal aging, through-faults, design deficiencies, etc., the unsymmetrical areas produce greater local magnetic forces and deformation until conditions to bridge insulation become imminent. After winding deformation occurs, the associated insulation and shielding are disturbed and the conditions are set for partial discharge (PD) and gassing.

This unique OLFRA method uses induced lightning and routine substation maintenance switching as the test source for winding FRA determination. Winding test results are usually obtained in a time period of three months to a maximum of one year. Off-line baseline tests with the on-line equipment can also be performed when the equipment is installed and again during any planned or unplanned outages for comparisons to install baseline tests.

The results to date suggest that OLFRA equipment would respond to significant winding deformation after damaging through-faults and significant winding aging changes as a precursor to a transformer fault or as an indicator for end-of-life conditions. In addition, the OLFRA equipment could be used as a high voltage wide band bus transient recorder.

To carry out the OLFRA test, on-line system transient voltages are recorded. During normal switching operations, such as capacitor bank and reactor operations, lightning from thunderstorms or other high bandwidth transients are created and flow through the system. These are used as the input signal to the transformer. Commercially available bushing couplers connected to the transformer bushings serve as the voltage dividers.

On average, ten usable pulse sets per winding are required to create a useable winding transfer function for the designated winding.

An on-line test would have the following advantages:

- Lower cost to test
- No transformer outage required
- Disconnection of the transformer from the system not required

There are also some challenges to an on-line test:

- Requires installation of bushing taps and couplers
- Results are obtained throughout an undetermined period; it takes around 3-6 months to obtain an OLFRA trace, due to the limited frequency content of the transients recorded

Field Case Studies

Off-Line Frequency Response Analysis:

Case Study 1: 41-Year-Old Westinghouse Shell Form Transformer

The case study presented was performed by NEETRAC on a 41-year-old Westinghouse shell form transformer that was taken out of service for the installation of OLFRA. The off-line FRA measurements indicated a significant change in the H1 winding since the last FRA test over eight months prior. The transformer is located in a high fault current location where the frequency of through-faults is also high. The on-line DGA was good and the water content was low. The only reason the transformer was taken out of service was to install OLFRA equipment. However, an in-tank inspection revealed some very loose blocking between the phase windings. The upper blocks were available for manual inspection. The inspector noted that the very loose blocks indicated both horizontal and vertical movement by hand. The high frequency difference in the H1 winding off-line FRA is shown in Figure 11-3.

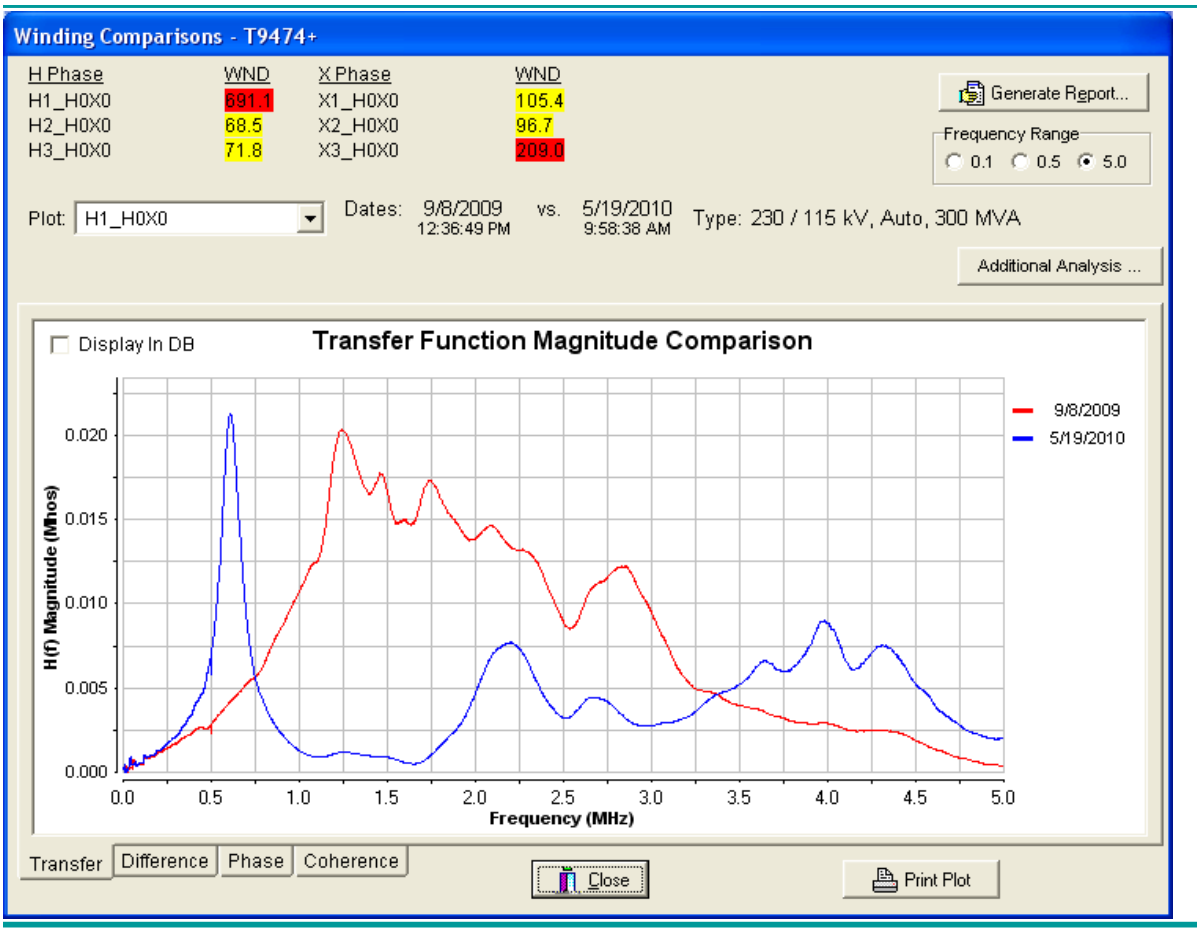

Figure 11–3
41-Year-Old Westinghouse Shell Form after Through-Fault Damage. High Frequency Changes from Off-Line Testing.

Differences in frequencies above 500 kHz have traditionally been indicators of damaged lead blocking on entrance to winding, high resistance connection to winding static shield, and winding overall looseness. In this case, extreme winding looseness is indicated by inspection.

Figure 11-4 shows the low frequency changes below 100 kHz over the eight month period. These low frequency changes usually indicate bulk winding or disk movement. The larger the bulk that moves, the lower the indicating frequency. The lowest frequencies – up to 10 to 20 kHz – are usually affected by the difference in residual magnetism in the core between tests, but can also indicate core structural problems. The sound and vibration of the energized transformer were considered normal, so no core or lamination problems were indicated.

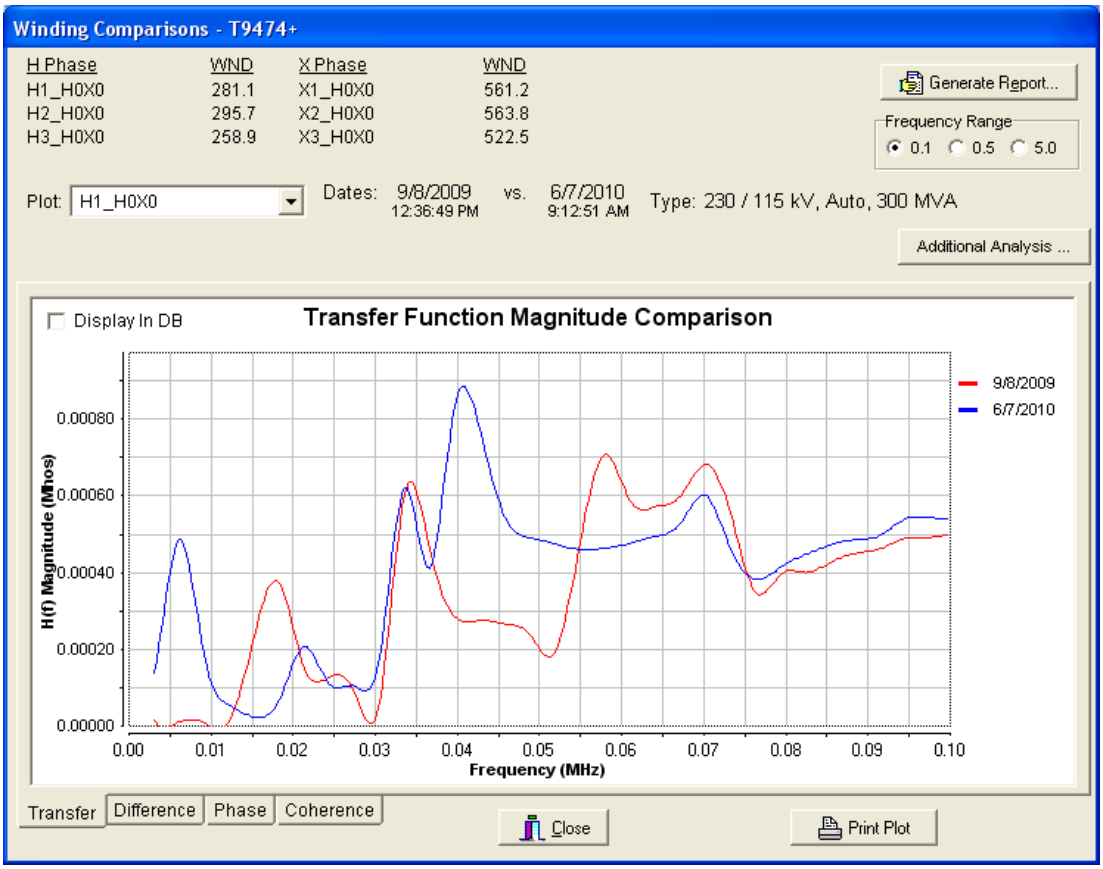

Figure 11–4
41-Year-Old Westinghouse Shell Form after Through-Fault Damage. Low Frequency Changes From Off-Line Testing.

Figure 11-5 shows the upper blocks that were available for manual inspection.

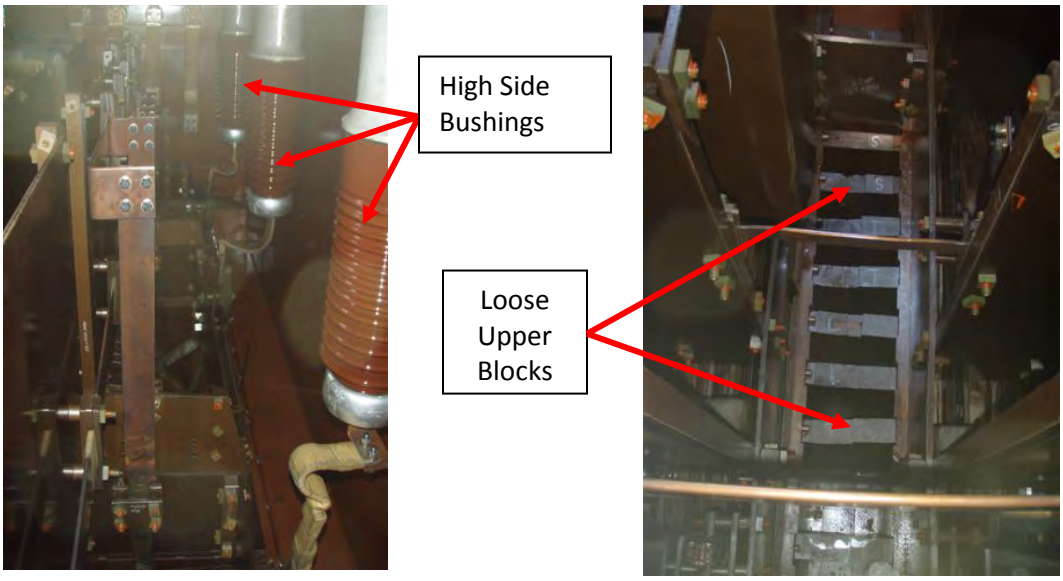

Figure 11–5
Left Shows Top of All Three Phases with High Side Bushings on Right. Right Shows Loose Upper

Blocking between A and B Phases

Three of the upper blocks were considered by the inspector to be tight (could not move vertically or horizontally by hand). Two of the blocks were considered loose (could wiggle vertically but not horizontally). Two of the blocks were considered very loose (could wiggle blocks both vertically and horizontally). Each block was labeled accordingly for future reference. This type of shell form winding does not lend itself to normal methods of block tightening and the process was not attempted.

It is likely that this transformer withstood through-faults at this substation location between 9/8/2009 and 6/7/2010 to cause FRA (and winding) change. The off-line power factor tests revealed oil contamination, so the oil was processed.

The transformer was re-energized because no replacement was immediately available. The unit was scheduled for replacement at this high fault location in 2011 due to extreme winding looseness, but was replaced over a year later due to manufacturing lag time for a new replacement unit.

As can be seen in Figure 11-3 and Figure 11-4, the winding deformation is indicated by a significant change in the higher and lower frequencies, as seen in the significant differences between the blue trace and the red trace on the respective figures.

On-Line Frequency Response Analysis:

Case Study 1: Three-Phase Auto-Transformers and External Neutral Bushing

This case study summarizes the first attempt to perform OLFRA on a three-phase auto-transformer with all three phases in one tank, and with one external neutral bushing. In order to be successful, this system must be able to separate the three phase influences from one composite neutral waveform and determine which phase is the source of the input pulse, as well as determine whether the input source is the H or X winding. The installation is shown in Figure 11-6.

Installation

Figure 11–6
First OLFRA Installation on a Three-Phase Auto-Transformer with All Three Phases in One Tank

In order to demonstrate repeatability, the FRA signature should remain constant unless the winding conditions change. Figure 11-7 shows the transfer function results from the X2-H0X0 winding taken at two periods in time, one and a half months apart. Although the magnitude and phase graphs do not show a complete overlay, they are sufficiently similar to demonstrate repeatability.

The coherence graph is a measure indicating degree of linearity including how well the impulse data has been digitized. The larger the impulse signal recorded and the higher the bandwidth of the signal (the more frequencies the impulse contains), the higher the level of coherence. A level of 1 indicates perfectly linear data from input to output, while a 0 indicates non-linear and unusable data. Any data above approximately 0.3 is usable, with the best data having a coherence greater than approximately 0.5. The similarities of the transfer functions before and after indicate that there was no significant X2-H0X0 winding or insulation damage during the season. In addition to indicating no significant damage, the results also indicate good repetitive data from before to after the hurricane season.

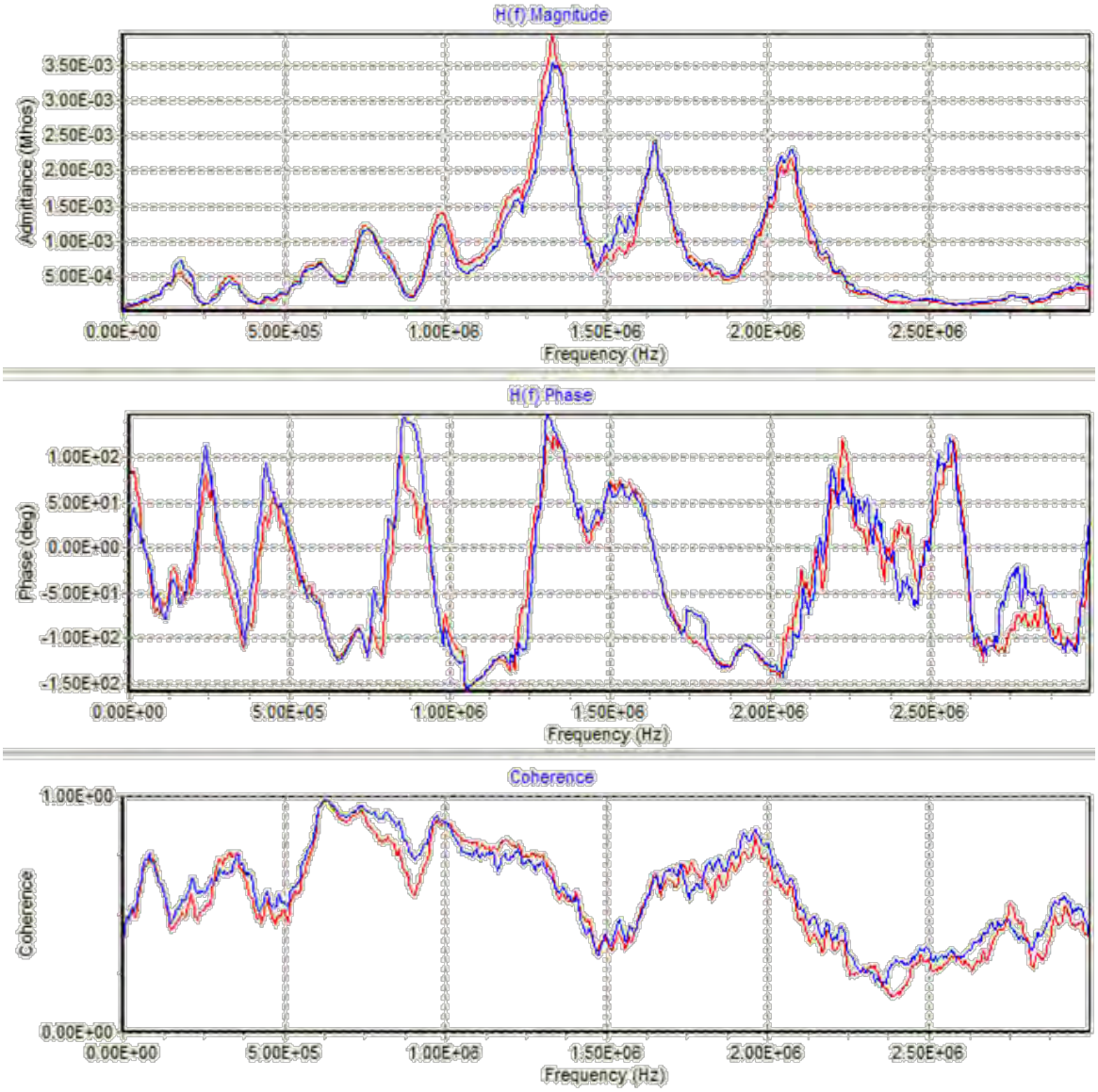

Figure 11–7
X2-H0X0 (Blue Trace Taken Spring 2005 and Red Trace Winter 2006)

An example of the results taken using the OLFRA technology on a high-side winding, in this case H2-H0X0, are shown in Figure 11-8 to corroborate the repeatability of the technology.

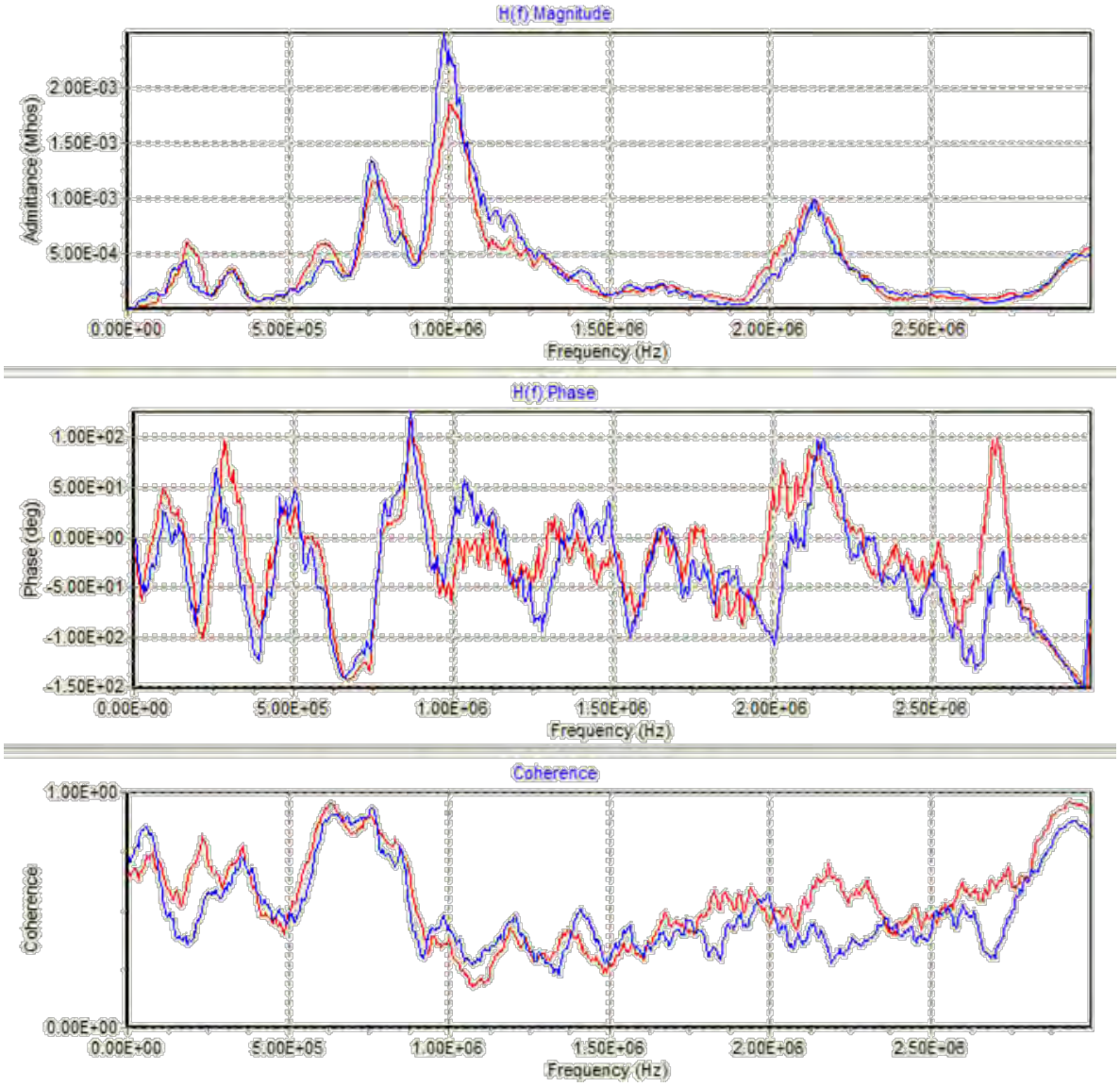

Figure 11–8
H2-H0X0, Before versus After Hurricane Season

The auto-transformer has a plus 8 to neutral to minus 8 tap position tap changer under load (TCUL), which ranged from 2L to 2R during the last year of OLFRA monitoring. A TCUL position monitor was installed in order to record the tap position in the database along with the rest of the information.

Throughout the monitoring period, 2000 pulses were recorded on tap L1, approximately 900 on tap 2L, and approximately 100 on 2R. Figure 11-9 shows a comparison between the OLFRA traces obtained from various pulses on tap 1L and 2L. The most significant differences for tap 1L compared with 2L are the frequency shifts in the resonance peaks in the magnitude plot, as well as the absence of a peak at about 1.65 MHz on tap 2L compared to the transfer function for tap 1L. There are accompanying differences in the phase (time delay) plot (center traces), most notably at the same frequency region as the resonance peak shifts in the magnitude plot above.

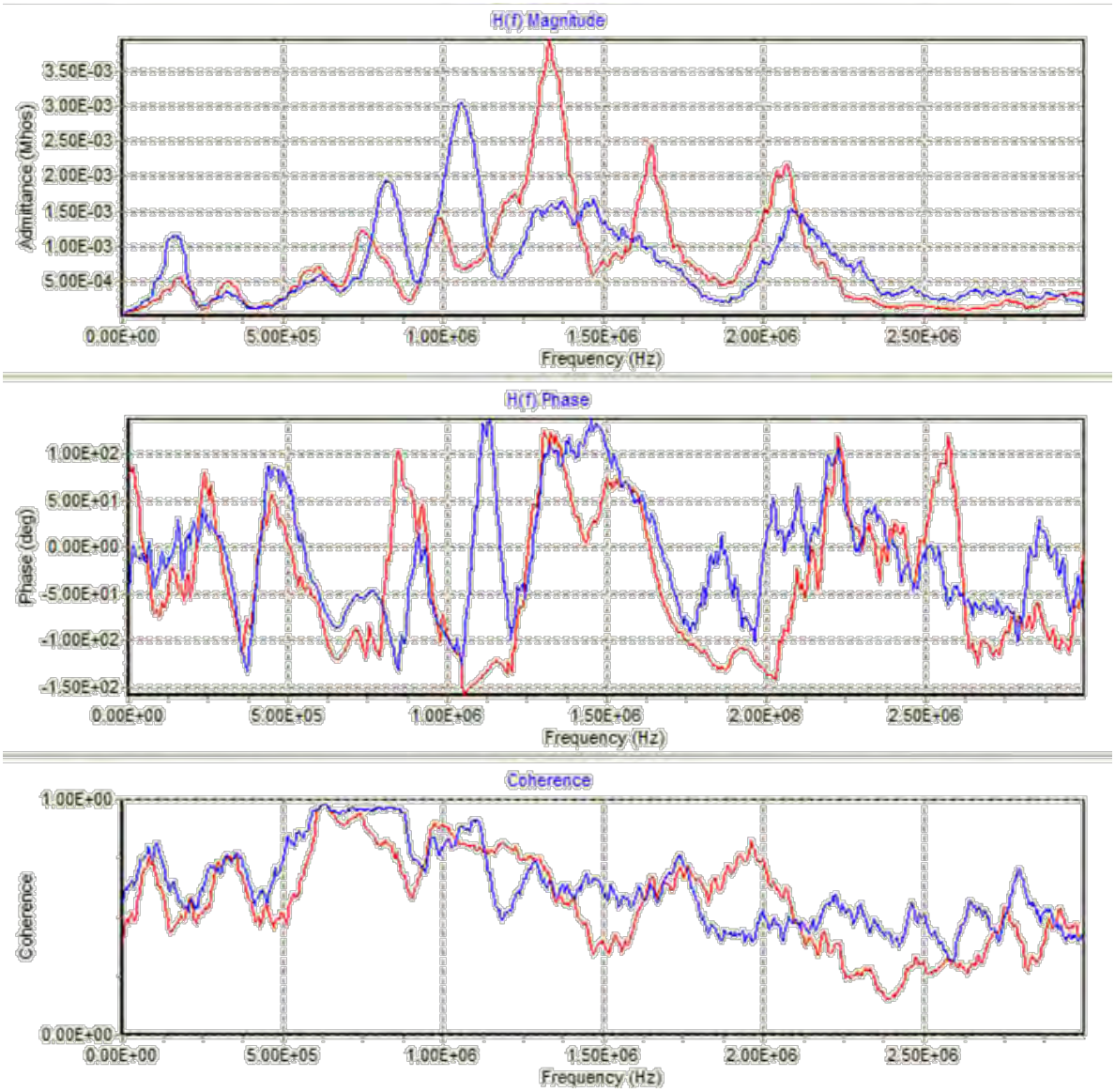

Figure 11–9
X2-H0X0, Tap 1L (Blue Trace) Compared to Tap 2L (Red Trace)

The difference in a one tap change from 1L to 2L can also be seen in the H winding on-line transfer function, even though the TCUL tap windings are physically part of the X windings. The H2-H0X0 Tap 1L versus Tap 2L transfer functions are shown in Figure 11-10. The difference in transfer function magnitude is displayed in the top graphs by a shift in the resonance peaks. These results demonstrate the sensitivity of the OLFRA technique to these changes within a transformer.

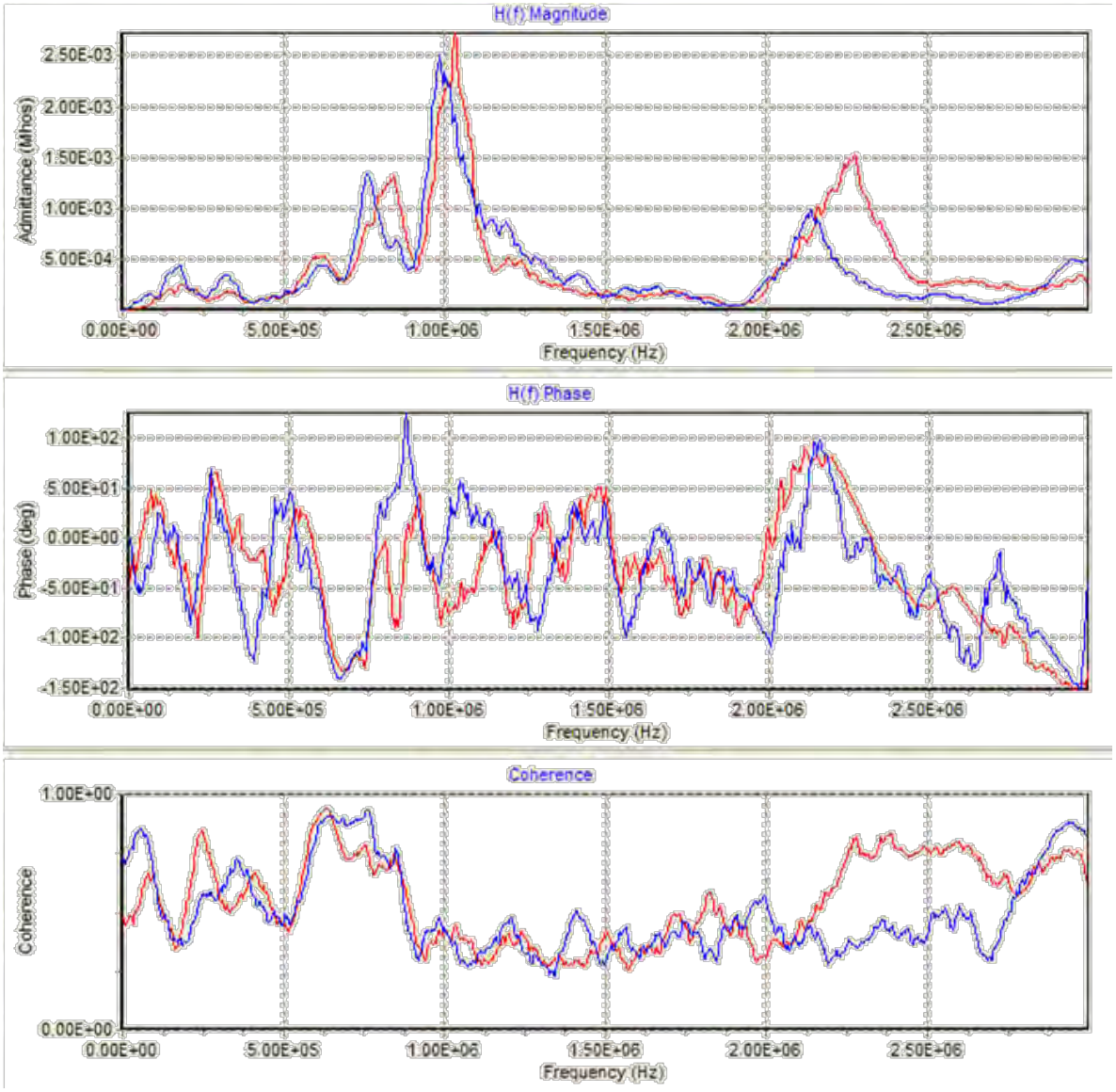

Figure 11–10
H2-H0X0, Tap 1L (Blue Trace) Compared to Tap 2L (Red Trace)

Case Study 2: Delta-Delta Winding Configuration

This case study summarizes the results gained from the installation of an OLFRA system on a delta-delta transformer. The transformer is owned by FirstEnergy and is a 345/138 kV, 448 MVA auto-transformer, manufactured in 2000.

During the period of installation, an average of over 100 pulse data sets was recorded per month. These are distributed over the three H and three X windings.

Installation

This installation of the OLFRA system took place in May 2009. Figure 11-11 shows the final installation set-up. The capacitive bushing taps are coupled with purpose-designed high pass filters to enable extraction of both transient data for FRA and 60 Hz data for the bushing relative

power factor monitor. Since the bushings are used as the means to record the transients, a change in the bushing condition would affect the transfer function of the system and hence the FRA signature. Therefore it is vital to also track the condition of the bushings. The on-line bushing monitor used is a commercially-available PF Live Plus system from Gridsense.

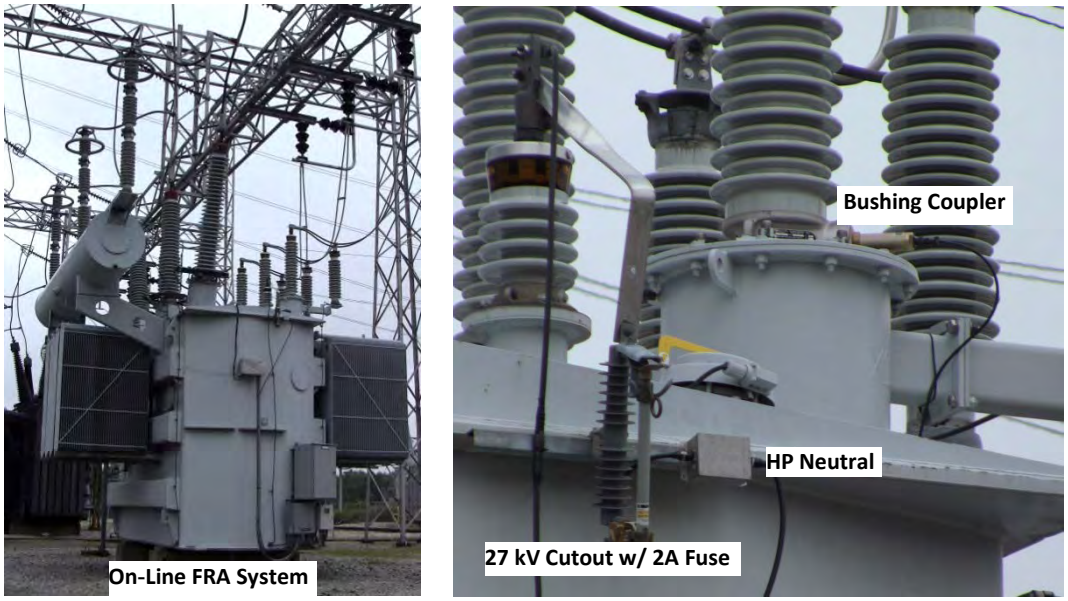

Figure 11–11
On-Line FRA Installation on a Delta-Delta Transformer

Results

Off-Line Tests Compared to On-Line Tests

An off-line test was performed with separate equipment (Phenix FRA-100) at the time of the OLFRA equipment installation. The X1-H0X0, X2-H0X0, and X3-H0X0 traces for the Phenix FRA-100 off-line test set are shown in Figure 11-12. The OLFRA results for the first year are shown in Figure 11-13. The peaks and valleys are the same for frequencies of 400 kHz to 2 MHz. Note that the valleys in the traces at about 1.5 MHz are both at about -45 db, so the high frequency amplitudes are also similar. The frequencies below 400 kHz indicate some differences because of the impedances of the in-service bus connections to the H and Y windings, which are not present for the off-line tests.

Since this case study in 2009, technology has progressed and the supplier (NEETRAC) has developed a compact high voltage pulse source so that off-line and on-line tests can be performed with the OLFRA equipment. Once on-line equipment is installed, there will be no need for a separate off-line FRA test. If the transformer experiences a through-fault, a FRA can be performed more easily using the in-place OLFRA equipment with the addition of a single high voltage pulse source. The pulses can be applied to the bushing tops with a hot stick from the pulse box, and the testing is planned to be guided and automated by the existing software in the computer on the side of the transformer. In this manner, an immediate condition assessment is made of each winding. If a baseline test is made with the OLFRA equipment, with grounds and the jumpers attached, then the windings can be condition-assessed when the bank is de-energized without removing jumpers from the transformer bushings.

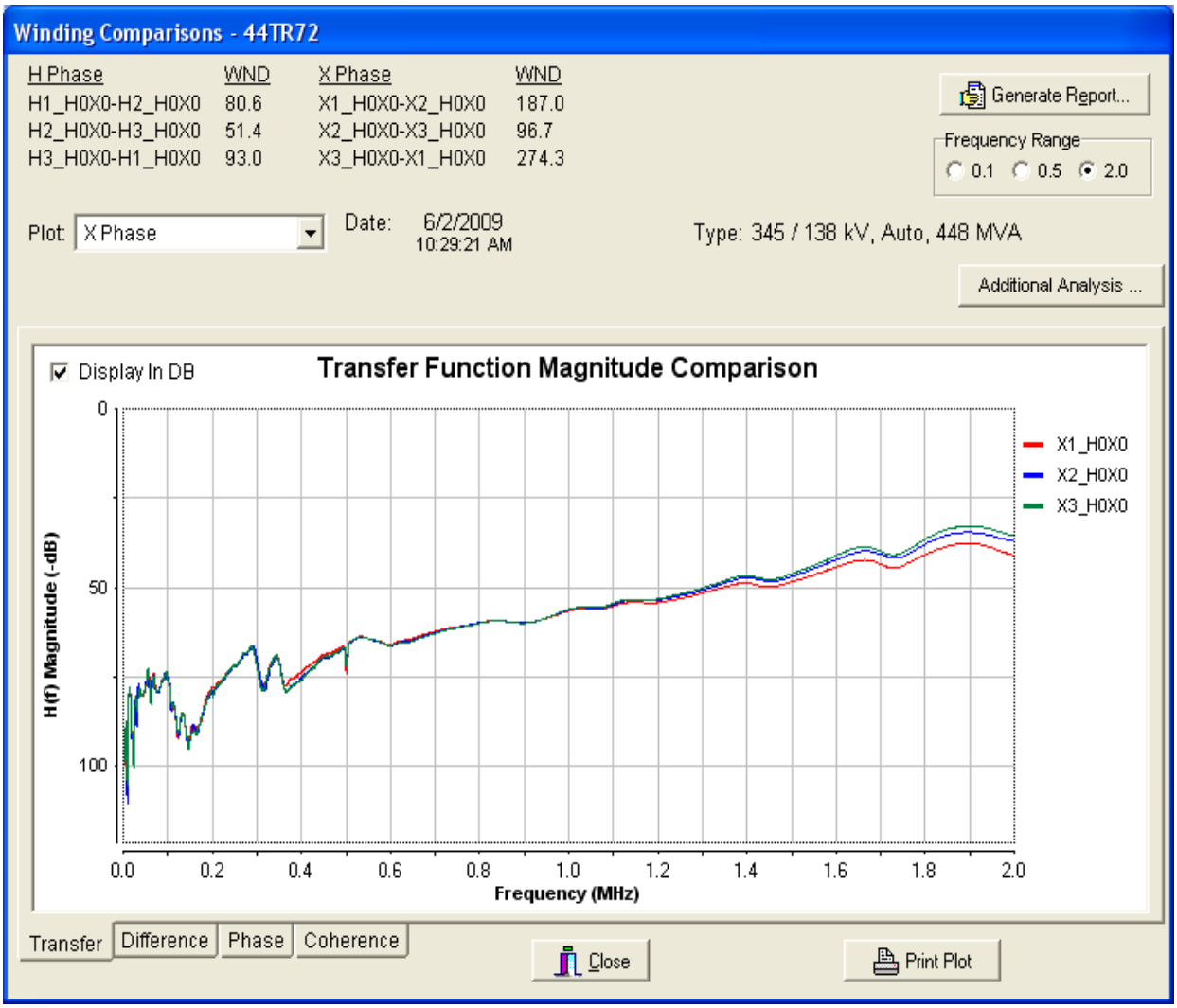

Figure 11–12
Off-Line Test with Phenix FRA-100 Test Set at 2 MHz Bandwidth

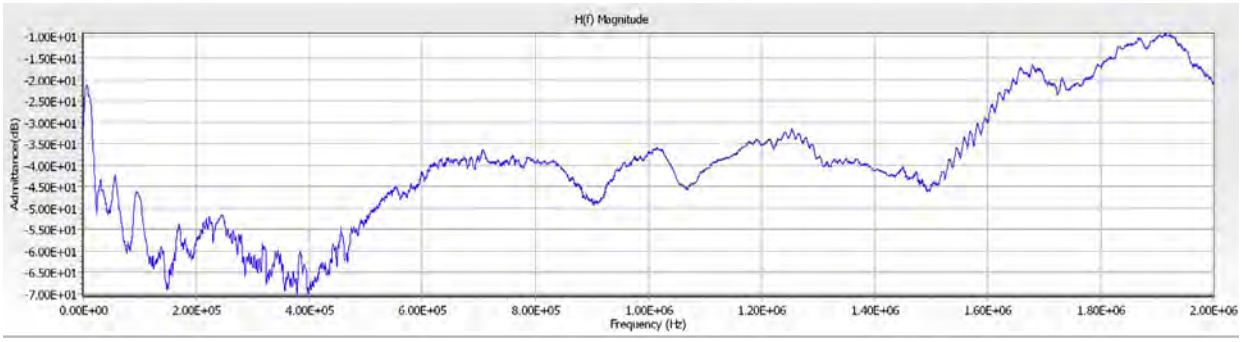

Figure 11–13
OLFRA Results for the First Year: X1-H0X0 at 2MHz Bandwidth

Subsequent OLFRA Test Comparisons

To date, this 345/138 kV auto-transformer has the longest history for OLFRA data. The first year compared to the third year transfer functions for H1, H2, and H3 windings are shown in Figure 11-14, Figure 11-15, and Figure 11-16, respectively. As can be seen, the curves are the same general shape and magnitude for each plot. An example of curve difference for winding deformation is shown in the first case study for off-line FRA. By comparison to changes seen in that case study, it can be concluded that there is no significant change in each H winding in the 345/138 kV auto-transformer over the three-year test period.

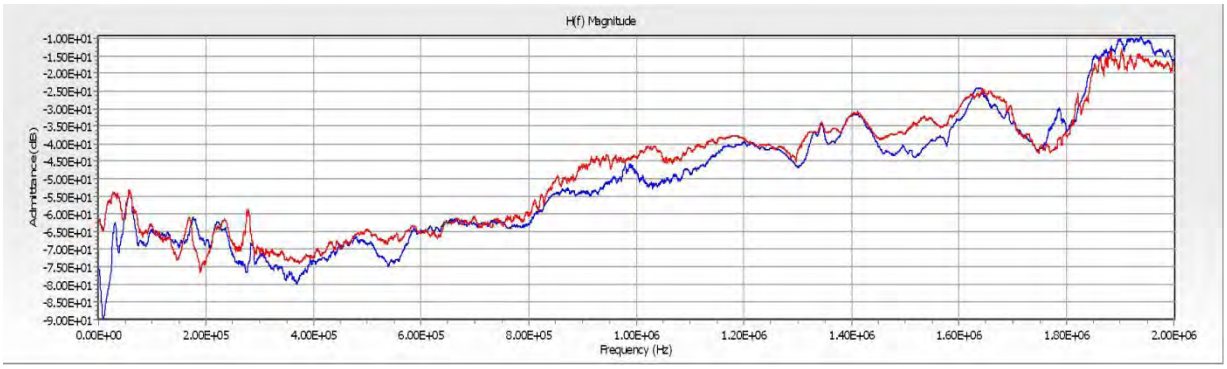

Figure 11–14
H1-H0X0 Data: Red Trace = 1st Year, Blue Trace = 3rd Year

Figure 11–15
H2-H0X0 Data: Blue Trace = 1st Year, Red Trace = 3rd Year

Figure 11–16
H3-H0X0 Data: Blue Trace = 1st Year, Red Trace = 3rd Year

Similarly, the first year compared to the third year transfer functions for X1, X2, and X3 windings are shown in Figure 11-17, Figure 11-18, and Figure 11-19, respectively. Again, the curves are the same general shape and magnitude for each plot. Therefore, there is no significant change in each X winding condition over the three-year test period. The mid frequency differences in the red, third year, curve for X2-H0X0 (Figure 11-18) may reflect the instability in the X2 bushing power factor during 2011 and 2012. It is expected that the area of frequencies around 1 MHz represents the most sensitivity to bushing parameter change. The X2 bushing condition value trend in Figure 11-24 indicates an alarm level around 70 for about a three month period during the winter months of December 2011 through February 2012.

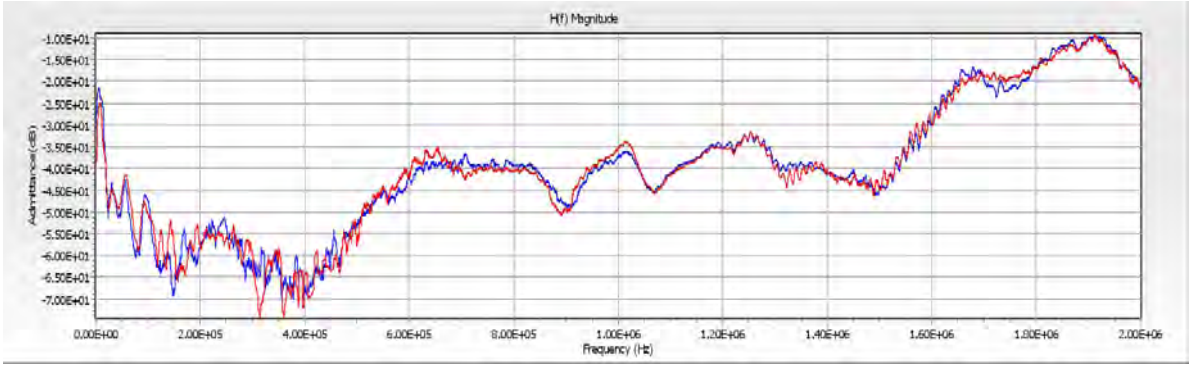

Figure 11–17
X1-H0X0 Data: Blue Trace = 1st Year, Red Trace = 3rd Year

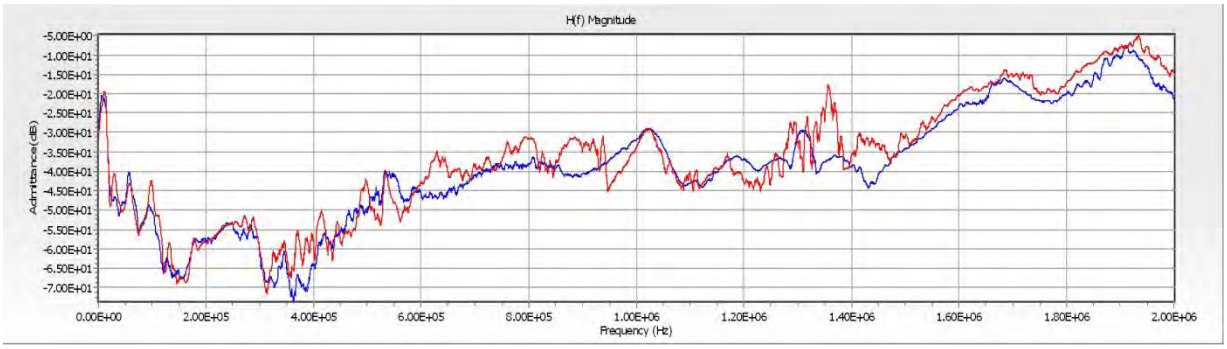

Figure 11–18
X2-H0X0 Data: Blue Trace = 1st Year, Red Trace = 3rd Year

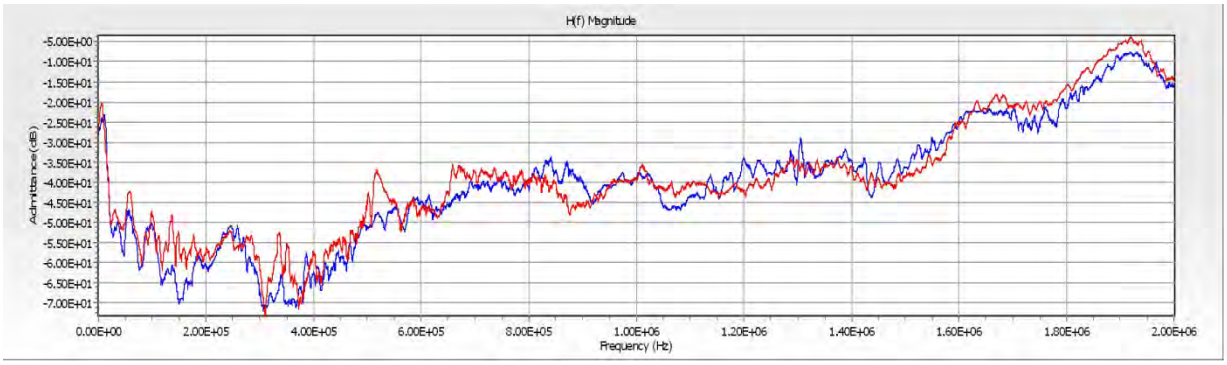

Figure 11–19
X3-H0X0 Data: Blue Trace = 1st Year, Red Trace = 3rd Year

Bushing OLRPF (On-Line Relative Power Factor) Results

The GridSense OLRPF works simultaneously with the NEETRAC OLFRA using the same bushing taps for signal inputs to both units. The OLRPF results for the H and X bushings for the time period of 9/1/2011 to 10/23/2012 are presented in Figures 11-20 through 11-25.

The plots are expressed in condition value versus time. A condition value ranges from zero to 100, where zero is the best state and a condition value of 100 is a full-alarm state. A yellow alarm state starts at a condition value of 1 and increases in severity to a condition value of 70. Seventy-one starts a red alarm state and can increase in severity to 100 for the most significant alarm state to indicate immediate action needed. The time intervals for a condition value calculation depend on the rate of change of the condition value. The intervals vary from about eight hours before rapid condition value change to about every two hours at rapid change, and the rate of calculation also increases for absolute condition values above 40. The raw data from the bushing sensors is recorded continually in about 30 minute intervals. As with other monitoring technologies, the trend of the output is usually the most important criteria for evaluation of the device under test.

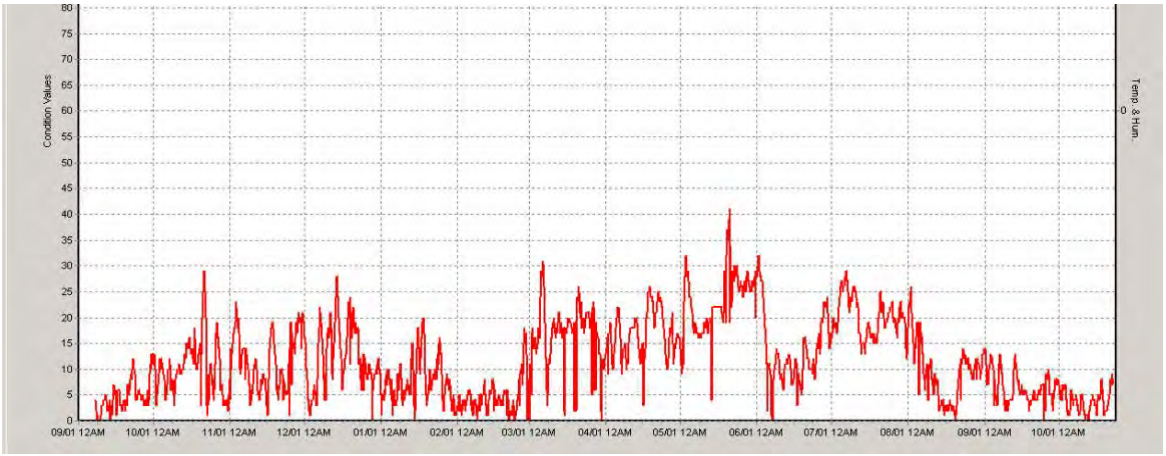

Figure 11–20
Condition Value Trend for the H1 Bushing

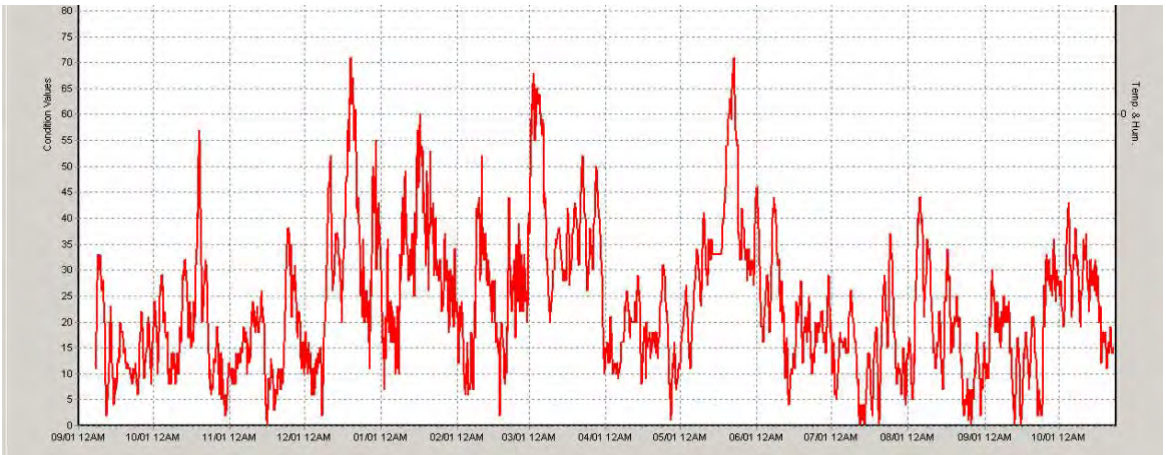

Figure 11–21
Condition Value Trend for the H2 Bushing

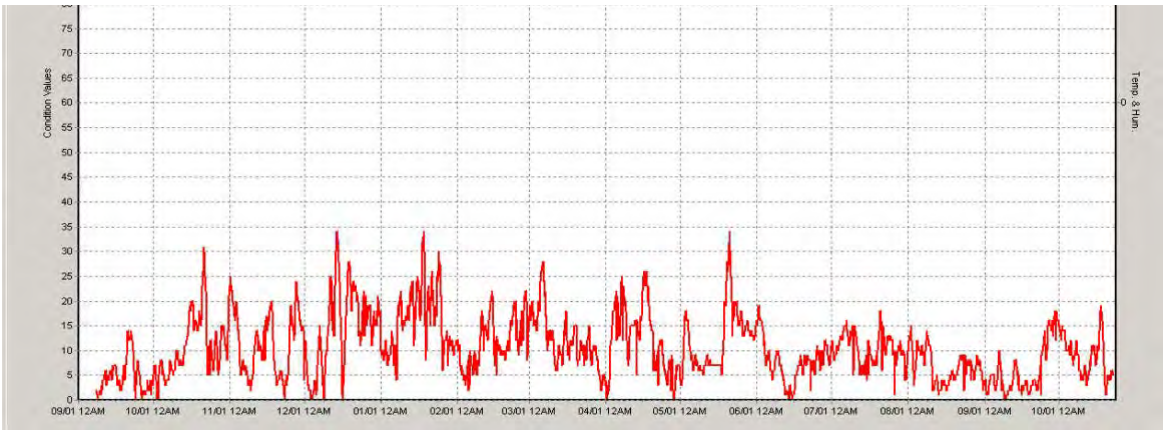

Figure 11–22
Condition Value Trend for the H3 Bushing

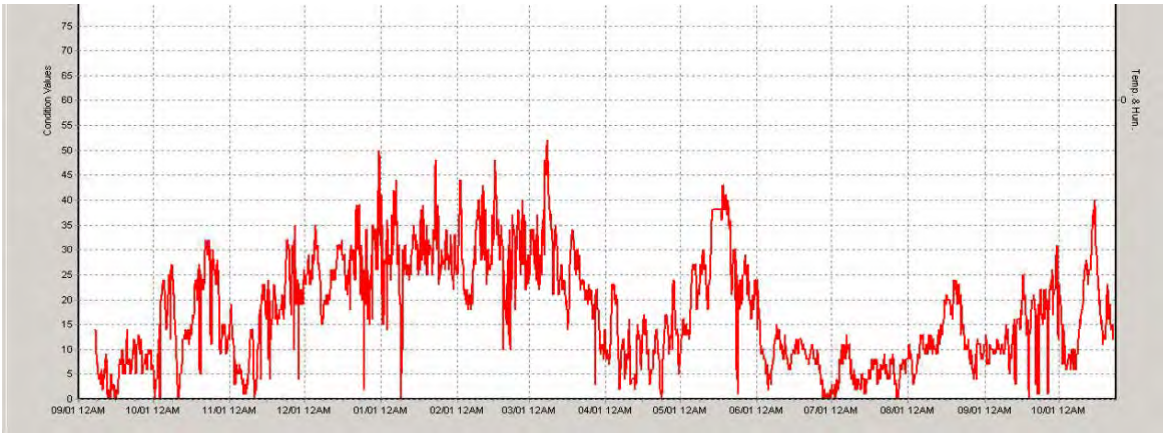

Figure 11–23
Condition Value Trend for the X1 Bushing

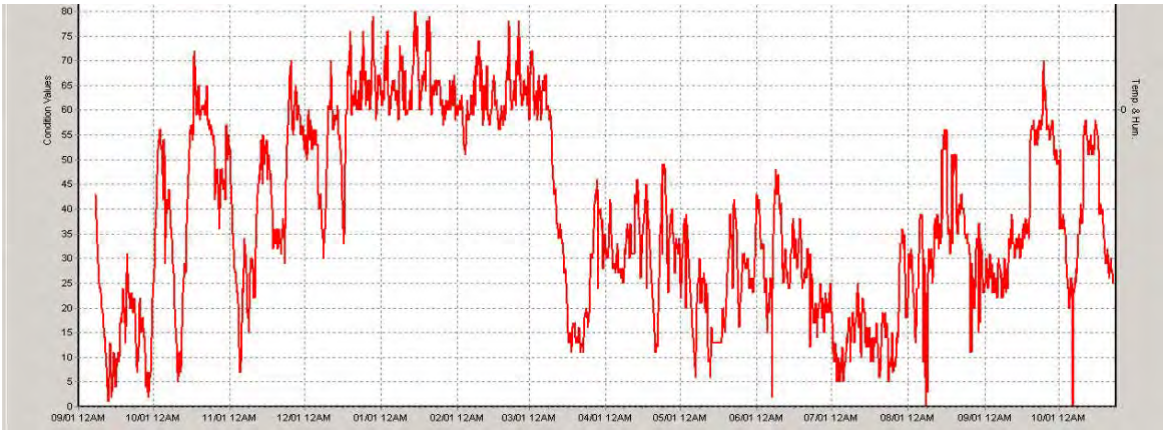

Figure 11–24
Condition Value Trend for the X2 Bushing

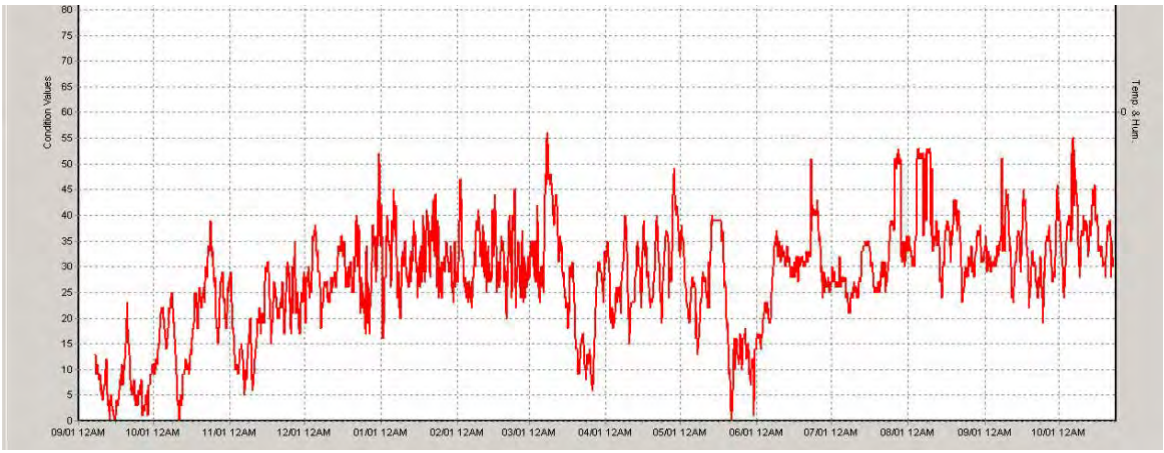

Figure 11–25
Condition Value Trend for the X3 Bushing

The OLRPF was set up at installation to have bushing comparisons which included high side and low side voltages in the same group. However, the relative power factor (RPF) trend plots that include high and low side voltage comparisons show, most likely, a loading thermal effect of the winding to cause a phase shift between high and low side windings. For example, the RPF plots cycle up and down with the daily load. A 30 day example for H1-X3 (blue) is shown in Figure 11-26. This indicates that, for this installation, the RPF plots are not as useful as the condition value trend plots. The bushing groupings can be changed in the OLRPF software to be only same-voltage, but the existing OLRPF history could not be used for comparison to future results.

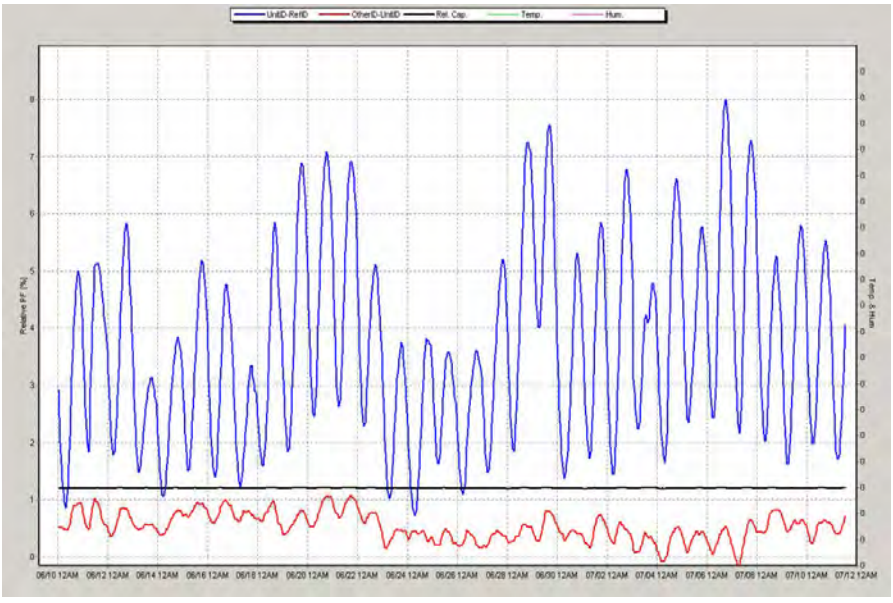

Figure 11–26
H1-X3. Blue Trace: RPF for 30 Days with Thermal Effects Indicated. Red Trace: H2-H1 RFP for 30 Days with Much Reduced Thermal Effects through Using the Same Voltage Group.

Case Study 3: OLFRA on a Delta-Wye Winding Configuration

Installation

This case study represented the first installation on a transformer with delta windings and insulated windings, which presented new challenges to determine OLFRA for the H windings. For example, the bushing taps for signal inputs represent a phase-to-ground measurement at each corner of the high side delta and does not represent a measurement directly across the winding as with the previous auto-transformers. The OLFRA equipment was installed in 2011 on Oncor's 138/26kV, 47 MVA, delta-wye transformer with a UZDRT LTC. The transformer was manufactured in 1989. Installation required an outage of one week. In order to speed up the installation, the high pass filter box was installed beside the on-line FRA cabinet, at the foot of the transformer. The on-line bushing monitor used was a commercially-available PF Live Plus system from Gridsense. In this installation, an LTC encoder was installed to allow the recording and monitoring of the LTC operations and position. The installation is shown in Figure 11-27.

Figure 11–27
OLFRA Installation on a Delta-Wye Transformer with an LTC

Results

Off-Line SFRA Tests Compared to On-Line Tests

The off-line tests for the Oncor transformer were performed with two different technologies for comparison. The first was a sweep frequency response analysis (SFRA) off-line method with all jumpers removed from the transformer (normal off-line conventional test) and the second off-line method used the OLFRA equipment with all jumpers removed but with the neutral still

attached. In addition, an off-line test was performed with the OLFRA equipment while all the transformer jumpers and neutral were attached *and* the safety grounds were applied at the normal maintenance location near the transformer. The off-line SFRA test is described first.

The OLFRA equipment is compared to the off-line SFRA on the low side windings of the 138/26kV, 47 MVA, transformer. This is an off-line test comparison with the H and X transformer bushing jumpers removed for both tests. The neutral conductor is removed from the neutral bushing for the SFRA test but, the neutral conductor is attached for the OLFRA equipment test. Short circuiting the winding neutral output with a copper conductor of about 15 feet (4.6 m) long will significantly affect winding frequency response up to about 100 kHz. This is the normal in-service neutral connection. The neutral conductor has less effect as the frequency is increased. Note that an additional OLFRA off-line response could have been made without the neutral attached, but for future on-line comparisons, the neutral remained attached for off-line testing.

The X to neutral (X-N) responses with 2.5 MHz bandwidth for the OLFRA equipment is shown in Figure 11-28. The scale is log amplitude versus linear frequency so that the response from 300 kHz to 3 MHz can be examined closely. Experience with end-of-life winding/insulation indicates that the greatest changes are in this frequency band. The off-line SFRA (X-N) results with 2 MHz bandwidth are shown in Figure 11-29. The SFRA indicates the same peaks and valleys from 130 kHz to 1.7 MHz as the OLFRA equipment test. The results below 130 kHz are different because the in-service neutral tie to ground significantly alters the test circuit for low frequencies, and, for the high frequencies, the SFRA is limited to 2 MHz maximum bandwidth. The phase plots are also similar, but represent two different formats. The OLFRA is presented in an un-wrapped form and the SFRA phase is presented in a plus to minus 180 degree format. (The SFRA test was performed independently by separate test personnel).

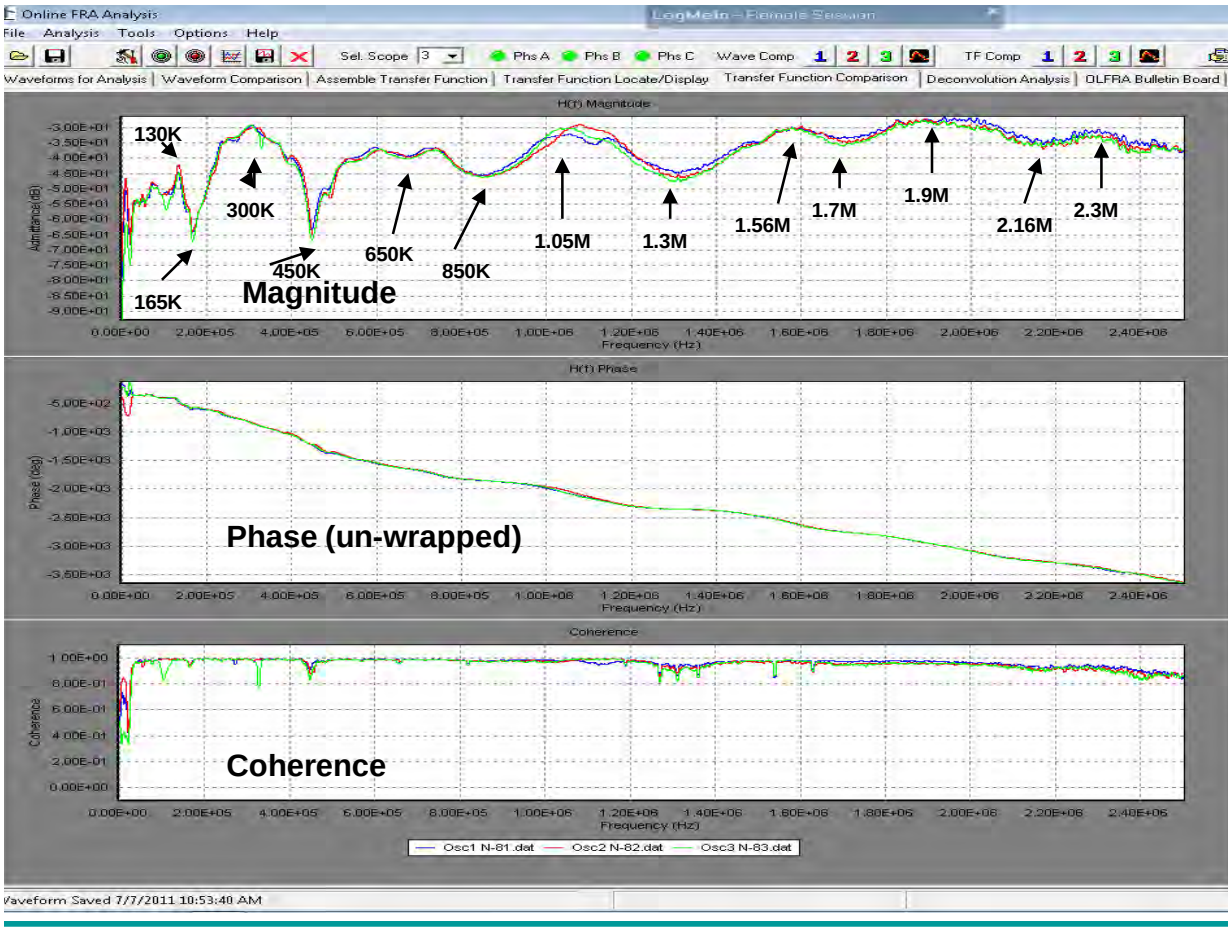

Figure 11–28
OLFRA Off-Line Response with NEUTRAL ATTACHED

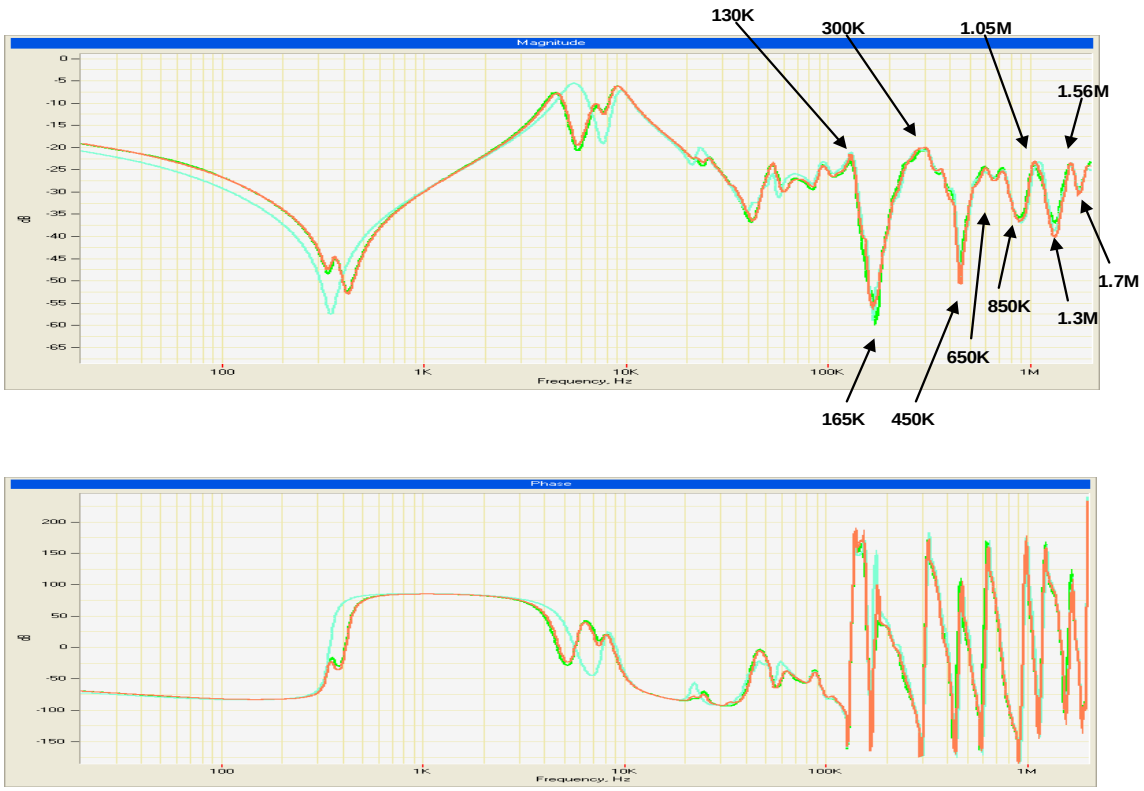

Figure 11–29
SFRA Off-Line Response without NEUTRAL ATTACHED

Off-Line Tests Compared to On-Line Tests Using OLFRA Equipment

A compact high voltage pulse source has been developed by NEETRAC so that off-line and on-line tests could be performed with the same equipment, namely the on-line equipment. Once on-line equipment is installed, there is no need for additional off-line FRA test equipment for future diagnostics. A FRA can thus be more easily performed using the in-place OLFRA equipment with the addition of a single high voltage pulse source. The pulses can be applied to the bushing tops with a hot stick from the pulse source.

The baseline off-line FRA tests are performed with the OLFRA equipment at installation. This baseline test is made using the OLFRA equipment, with grounds attached and the jumpers still attached. The windings can then be condition-assessed when the bank is de-energized without removing jumpers from the transformer bushings and with the safety grounds in place.

This is the first test case with grounds attached and with a delta winding, and the decision was made to ground the other end of the delta winding that is under test for this procedure. Other configurations of grounds may be investigated in the future. The X3-N off-line test results for jumpers and grounds attached are shown in Figure 11-30**.**

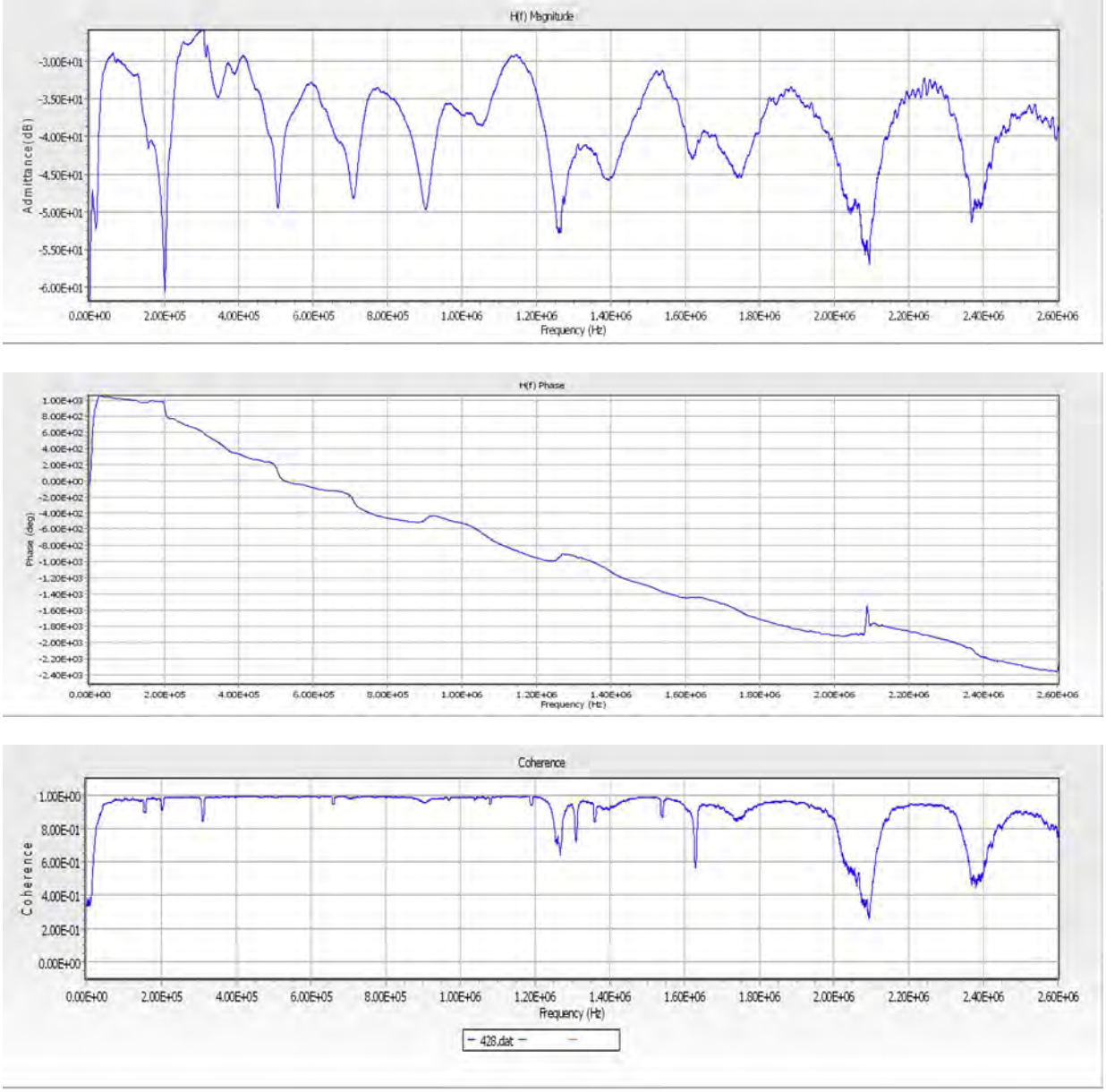

Figure 11–30
X3-N Off-Line Test Results for Jumpers and Neutral Attached AND Grounds Attached

The top magnitude plot and the middle phase plots are accurate and repeatable for the frequencies where the coherence is ≥0.9 in the bottom plot of Figure 11-30. If the same or equivalent grounds are placed in approximately the same locations for a future transformer outage, then the future X3-N off-line test should be similar to the original X3-N test at equipment installation and a winding condition comparison can be made to the past baseline test. X1-N and X2-N can also be evaluated in the same manner.

The case study also compared the on-line test results to the off-line test results to verify the on-line technique and to gain empirical knowledge and improve the on-line technology. The comparisons of the on-line test results to the off-line tests for X3-N are shown in Figure 11-31 from 305 Hz to 2.0 MHz.

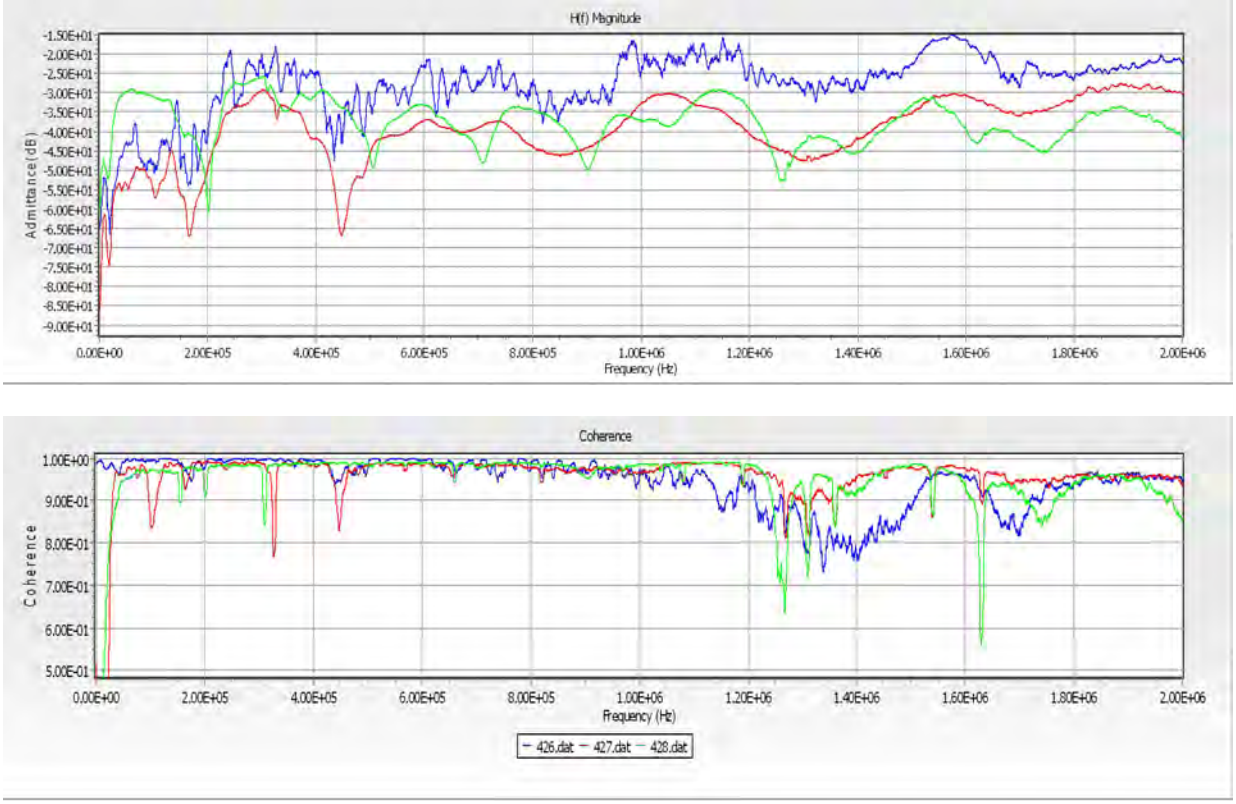

Figure 11–31
X3-N OLFRA TF426 (Blue Trace), Calculated from 14 On-Line Data Sets. X3-N Off-Line TF427 (Red Trace), Neutral Attached, Jumpers Removed. X3-N Off-Line TF428 (Green Trace), Neutral Attached, Jumpers in Place, Safety Grounds On.

The OLFRA (from in-service transient sources) transfer function, TF426, is the blue trace. The off-line transfer function, TF427, with the neutral attached and jumpers off is the red trace. The off-line transfer function, TF428, with jumpers on, neutral attached, and safety grounds attached is the green trace. The on-line TF426 is similar to the off-line TF427 from about 200 kHz to 2 MHz. The high frequencies are similar because the impedance of the jumper/lightning arrester combination is much higher than the transformer winding characteristic for the higher frequencies. The low frequencies (less than 200 kHz) produce different characteristics because the jumper-arrester-bus connections produce parallel connected impedances that affect the winding measurements at low frequencies, but their effects are generally constant from one test result to the next. TF428 with grounds attached begins to acquire a more similar characteristic to the other two traces as the frequency is increased. So the on-line data will have different terminal impedance characteristics on other windings compared to the off-line test made with the transformer bushing jumpers removed and with the un-tested windings open. But the differences diminish as the frequency of test increases. X1-N and X2-N can also be evaluated in the same manner.

The results of the challenge posed by the first case study on a transformer with delta high side windings are presented next. For example, the bushing taps for signal inputs represent a phase-to-ground measurement at each corner of the high side delta and do not represent a measurement directly across the winding as with previous auto-transformers. The sensitivity and repeatability of bushing tap to bushing tap data for an insulated winding is empirically determined.

The best initial scenario to determine the winding condition of the high side delta windings is selected to be a high side to low side winding voltage ratio calculation. This test configuration was selected, in part, due to the limitation of four input channels for the digitizers and the fact that a current output for each delta winding is not cost-effective to acquire.

The H2-X2 off-line test results for neutral attached, jumpers in place, and grounds attached are shown in Figure 11-32.

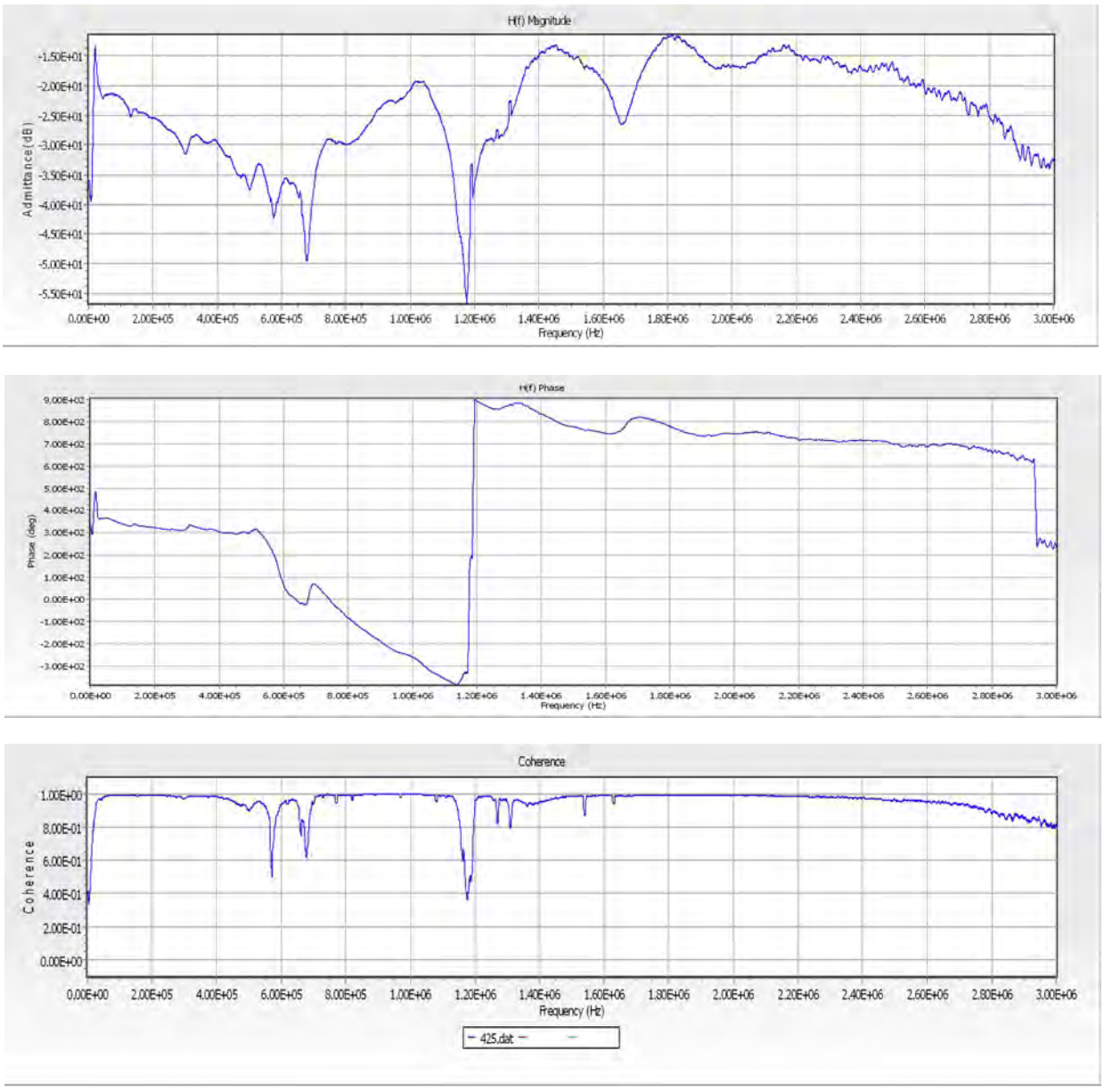

Figure 11–32
H2-X2 Off-Line Test Results for Jumpers and Neutral Attached AND Grounds Attached

The top magnitude plot and the middle phase plots are accurate and repeatable for the frequencies where the coherence is ≥0.9 in the bottom plot of Figure 11-32. The data for coherences <0.9 are not used. For example, a dramatic dip in coherence, such as at about 1.15 MHz, caused a dramatic dip in the magnitude and a dramatic discontinuity in the otherwise continuous phase plot, and the data around these low coherences are not used.

If the same or equivalent grounds are placed in approximately the same locations for a future transformer outage, then the future H2-X2 off-line test should be similar to the original H2-X2 test at equipment installation, and the data can make a valuable diagnostic winding condition comparison to the past baseline test for H2 and X2 windings. H1-X1 and H3-X3 can also be evaluated in the same manner.

The case study also compares the on-line H-X test results to the off-line H-X test results to verify the on-line technique and to gain empirical knowledge and improve the on-line technology. The comparisons of the on-line test results to the off-line tests for H2-X2 are shown in Figure 11-33 from 305 Hz to 2.0 MHz.

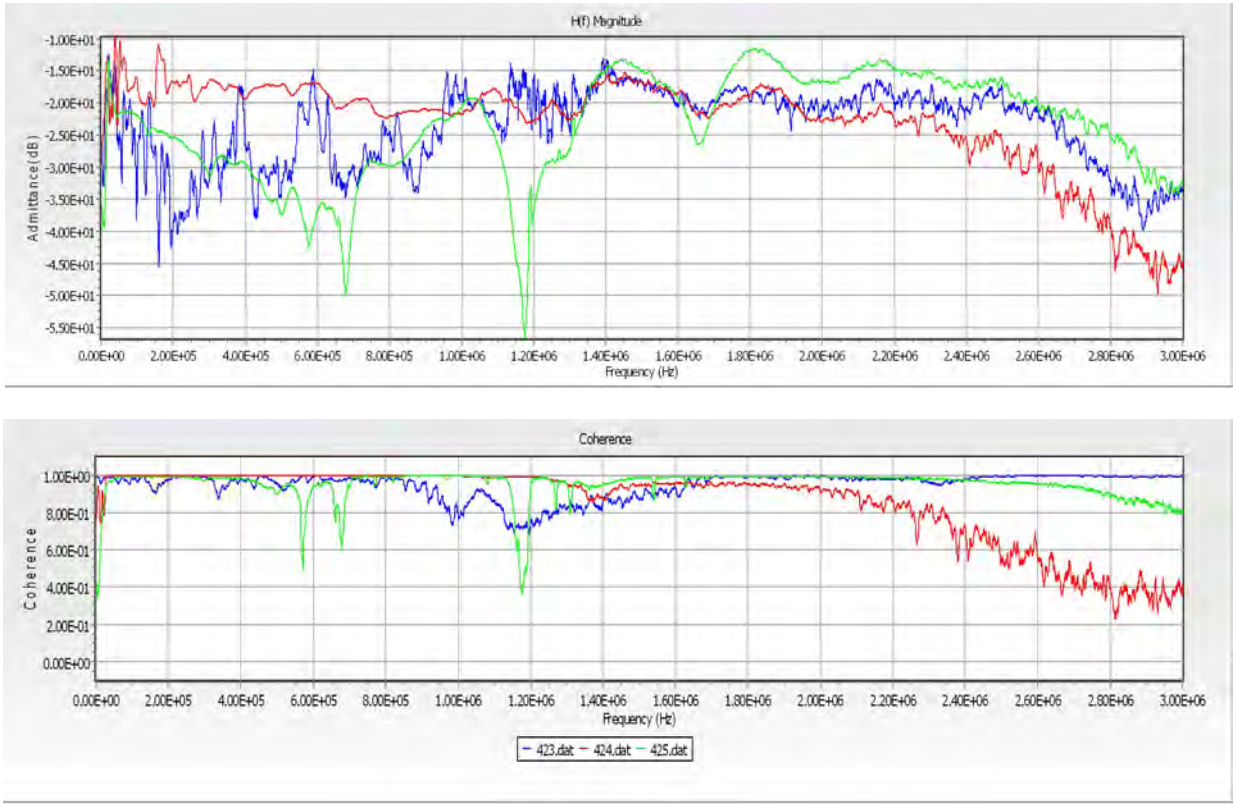

Figure 11–33
H2-X2 On-Line TF423 (Blue Trace), Calculated from 14 On-Line Data Sets. H2-X2 Off-Line TF424 (Red Trace), Neutral Attached, Jumpers Removed. H2-X2 Off-Line TF425 (Green Trace), Neutral Attached, Jumpers in Place, Safety Grounds On.

The on-line (from in-service transient sources) transfer function, TF423, is the blue trace. The off-line transfer function, TF424, with the neutral attached and jumpers off is the red trace. The off-line transfer function, TF425, with jumpers on, neutral attached, and safety grounds attached is the green trace. The on-line TF423 is similar to the off-line TF424 from about 1.3 MHz to 3 MHz. The high frequencies are similar because the impedance of the jumper/lightning arrester combination is much higher than the transformer winding characteristic for the higher frequencies.

The frequencies less than 1.3 MHz produce different characteristics because the jumper-arrester-bus connections produce parallel connected impedances that affect the winding measurements at low frequencies, but their effects are generally constant from one test result to the next. In addition, for the off-line tests, the other end of the delta winding under test is directly grounded across the respective bushing. This ground has a greater overall effect on the FRA measurement that the remotely-located work safety grounds. Therefore, the frequency where the curves become similar is at a higher frequency as opposed to the X-N tests.

TF425 with grounds attached begins to acquire a more similar characteristic to the others as the frequency is increased to about 1.3 MHz as shown in Figure 11-33. Therefore, the on-line data will have different terminal impedance characteristics on other windings compared to the off-line test made with the transformer bushing jumpers removed and with the un-tested windings open; however, the differences diminish as the frequency of test increases. H1-X1 and H3-X3 can also be evaluated in the same manner.

Subsequent OLFRA Test Comparisons

This transformer is the first attempt to perform OLFRA on an insulated winding. In addition to characterizing a delta winding, there are other mitigating circumstances in this test application. The on-line transient data was scarce. There are two main circumstances contributing to the reduction in usable data.

First, it was expected that the OLFRA result would change for each tap change of the load tap changer (LTC), but there was not enough data available in the one-year test period to perform a transfer function on each individual tap of the LTC. It became necessary to evaluate the results from combining data from several neighboring taps of the LTC to obtain sufficient data for test results. It was determined from the data available that taps 4L, 5L, and 6L positions produced the most transient data and could be combined to produce a viable and repeatable OLFRA result within a one-year maximum period. In addition, the off-line testing at installation shows that tap changes affect the frequencies mostly below 500 kHz, and additionally, that these changes to the transfer functions are minimal.

Secondly, the low side loads are composed of underground cable circuits that begin with potheads on the station bus and are naturally well protected from normal lightning transients. So the number of transients available for low side winding condition assessment is significantly reduced from lightning sources. However, the normal breaker maintenance switching produced enough transient data to characterize the low side windings over the one-year period.

To date there is not enough data for subsequent comparisons over the one year period, but we do have enough data to produce good and repeatable transfer functions on all windings at the end of the one-year test period. These results can be used for comparisons to results for future one-year periods to assess winding condition change. The low side over high side (voltage ratio) test

results for the first year are given in Figure 11-34, Figure 11-35, and Figure 11-36 below. Since the vast majority of the magnitude results produce coherences of >0.9, it is expected that these curves represent a viable and repeatable comparison for future year curves for a broadband of frequencies from 305 Hz to 2.0 MHz with magnitude calculations at 305 Hz intervals.

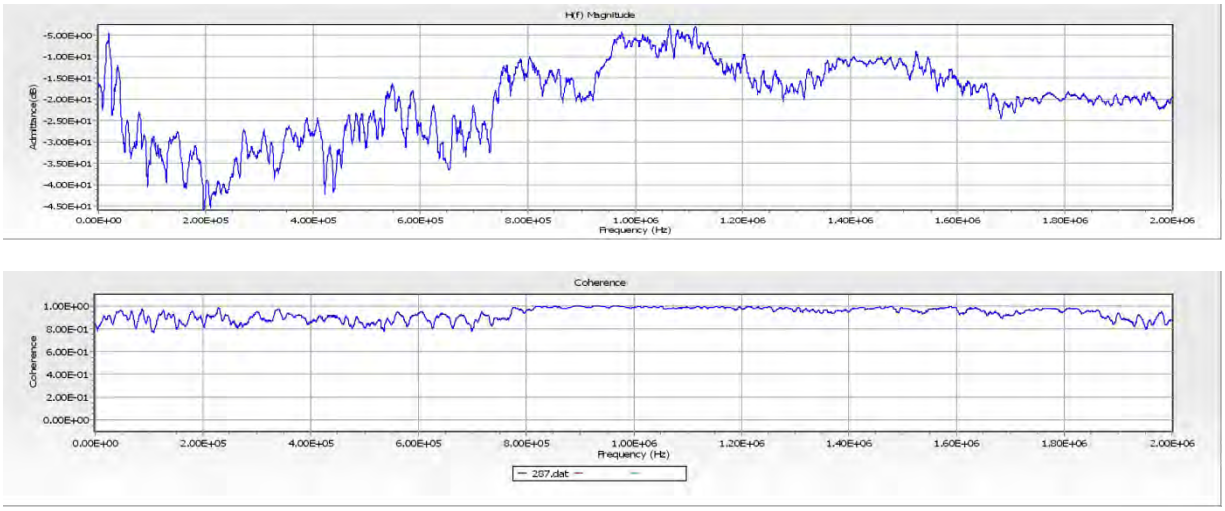

Figure 11–34
X1/H1 On-Line Voltage Ratio for One-Year Period Combining 4L, 5L, and 6L Data

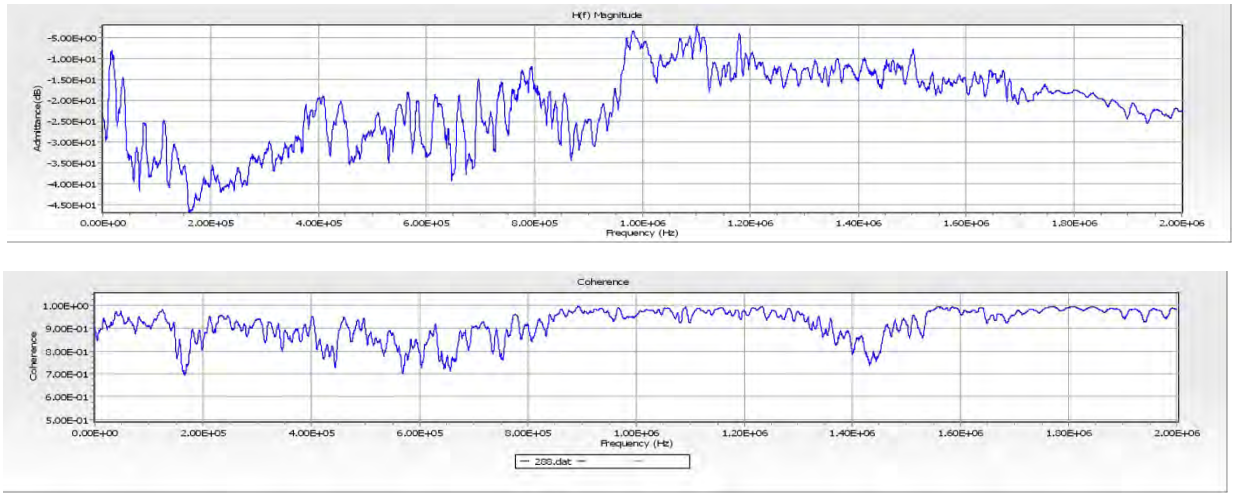

Figure 11–35
X2/H2 On-Line Voltage Ratio for One-Year Period Combining 4L, 5L and 6L Data

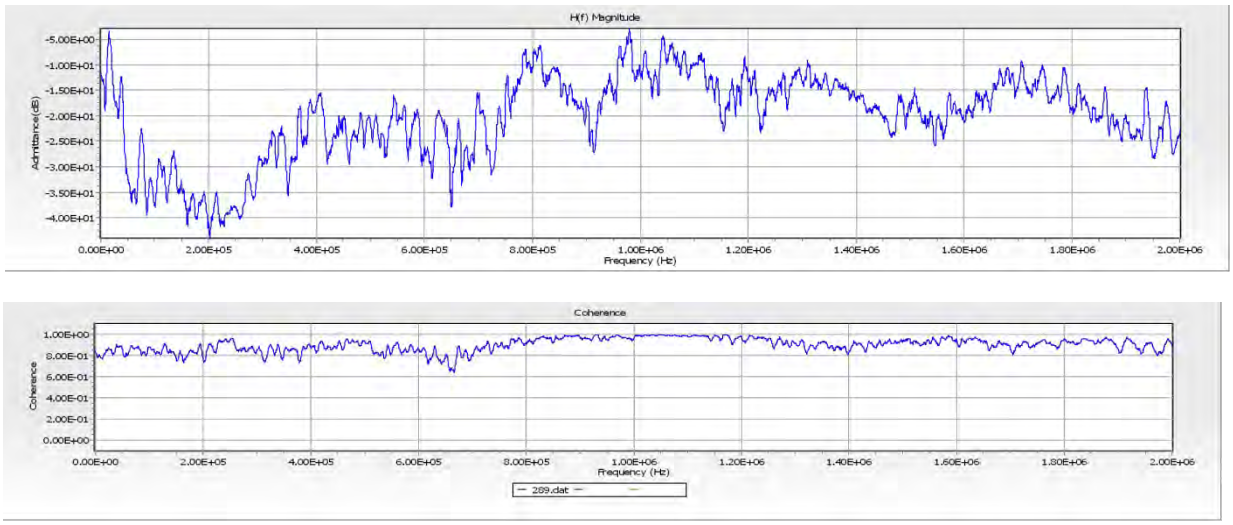

Figure 11–36
X3/H3 On-Line Voltage Ratio for One-Year Period Combining 4L, 5L and 6L Data

Lessons Learned from Transients Produced by the Transformer's Load Tap Changer (LTC)

The transformer's internal transients that are sufficiently high in magnitude to trigger the OLFRA system and that are caused by the tap changing of the LTC are not usable for winding FRA result purposes. This is because FRA requires an output response to a winding input stimulus, not a source from a location inside the winding. Note that the software has an algorithm to determine winding internal transients versus winding external transients and to determine which tap change is the source for the recorded transient.

However, the magnitude and character of the internal transients can potentially reveal previously unknown information about the health of the LTC contacts. For the Oncor LTC, the change-over-selector position change usually produces a high level transient and triggers the OLFRA system. However, the transitions to and from the lower and raise taps, in general, do not produce high level transients to trigger the OLFRA system. Therefore, when the OLFRA is triggered by a raise or lower tap change, these transients are much higher than normal for tap changes.

An example of a normal tap change that is still high enough to trigger the OLFRA system is shown in Figure 11-37. The basis for considering this example as more toward normal is based on the fact that the tap transition triggers in question were of a much higher level. The vertical scale multipliers were determined from initial calibration procedures as part of the equipment install process. The high side and low side voltages use the left vertical scale. The neutral voltage uses the right vertical scale.

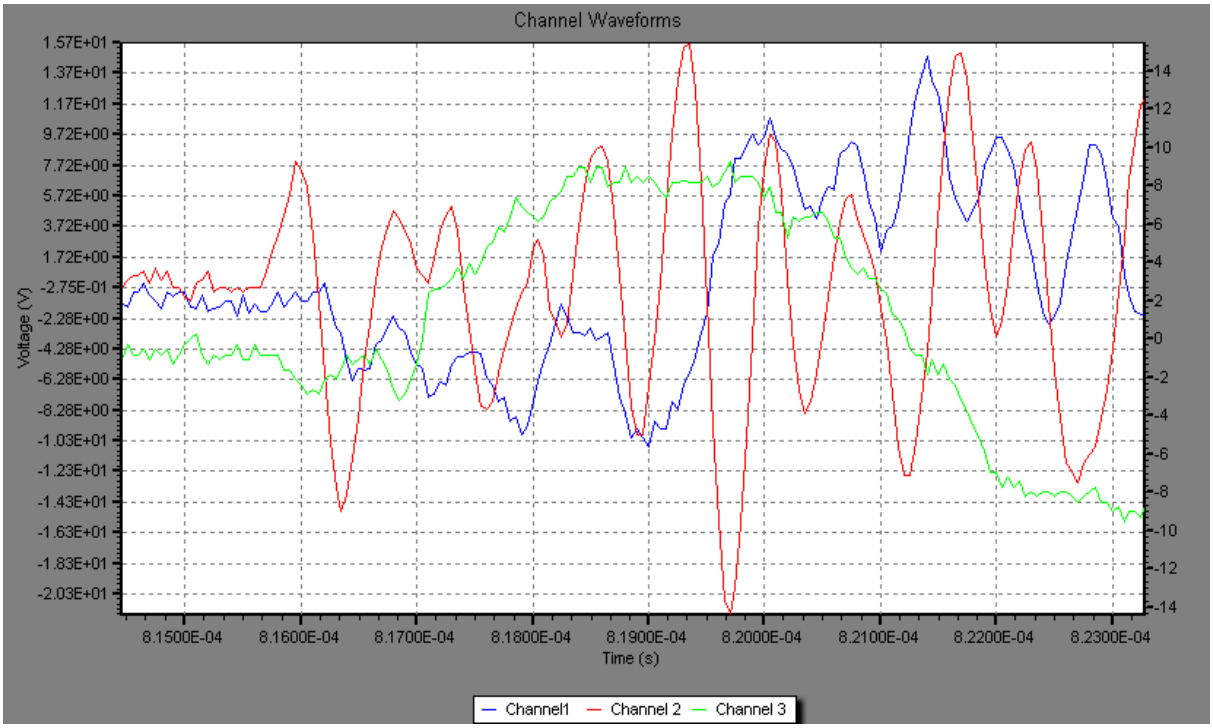

Figure 11–37
Typical Amplitude Tap Change 3L to 4L (5-22-2011). Tap Transition (3L to 4L Shown) for Phase 1. Blue = H1-H3 pk =0.76kV, Red = X1 pk =0.33kV, Green = Neutral pk=0.26kV.

An example of the much higher level tap transition transients is shown in Figure 11-38.

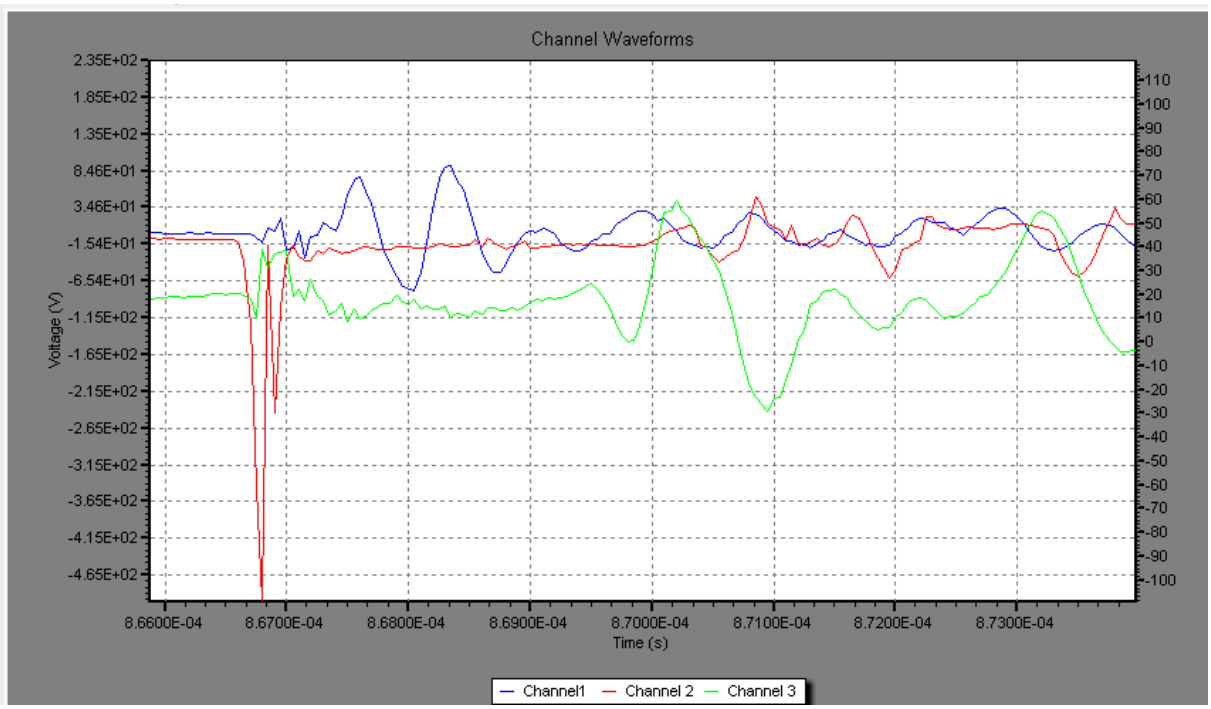

Figure 11–38
Potentially Abnormal Amplitude Tap Change 5L to 6L (11-6-2011). Tap Transition (5L to 6L Shown) for Phase 1. H1-H3 pk =6.6kV, X1 pk =7.5kV, Neutral pk= 2.0kV.

The LTC tap switching transient shown in Figure 11-38 induced a peak voltage of 7.5 kV at the X1 winding input, a peak voltage of 6.6 kV from H1 to H3, and a peak voltage of 2.0 kV at the neutral bushing. This is in contrast to the tap switching transient shown in Figure 11-37 that induced peak voltage of 0.33 kV, 0.76 kV, and 0.26 kV for the X, H, and neutral winding terminals respectively.

There is thus approximately an order of magnitude change in the peak voltage produced by the 5L to 6L tap change compared to any other tap change. The theory is that this high voltage peak relates to an underlying problem with the 5L to 6L tap change. When the LTC is inspected this theory will be tested. If the 5L to 6L tap change is in fact degraded compared to the other taps, it would provide supporting evidence that analysis of these transients may well serve as a helpful diagnosis for emerging tap changer problems.

Bushing OLRPF (On-Line Relative Power Factor) Results

The GridSense OLRPF works simultaneously with the NEETRAC OLFRA using the same bushing taps for signal inputs to both units. The OLRPF results for the H and X bushings for the time period of 5/7/2011 to 10/24/2012 are presented in the following figures.

The plots are expressed in condition value versus time. A condition value ranges from zero to 100 where zero is the best state and a condition value of 100 is a full-alarm state. A yellow alarm state starts at a condition value of 1 and increases in severity to a condition value of 70. Seventy-one starts a red alarm state and can increase in severity to 100 for the most significant alarm state to indicate immediate action needed. The time intervals for a condition value calculation depend on the rate of change of the condition value. The intervals vary from about eight hours before rapid condition value change to about every two hours at rapid change and the

rate of calculation also increases for absolute condition values above 40. The raw data from the bushing sensors is recorded continually at about 30 minute intervals. As with other monitoring technologies, the trend of the output is usually the most important criteria for evaluation of the device under test. See Figure 11-39 to Figure 11-44 for bushing condition value trending. There are three periods of time on the condition value charts where the bushing OLRPF is out of service and the data is replaced by a straight line from last valid data point to next valid data point.

All high side and low side bushings remained below any alarm level (i.e. <70) for the periods of active monitoring for bushing condition value level.

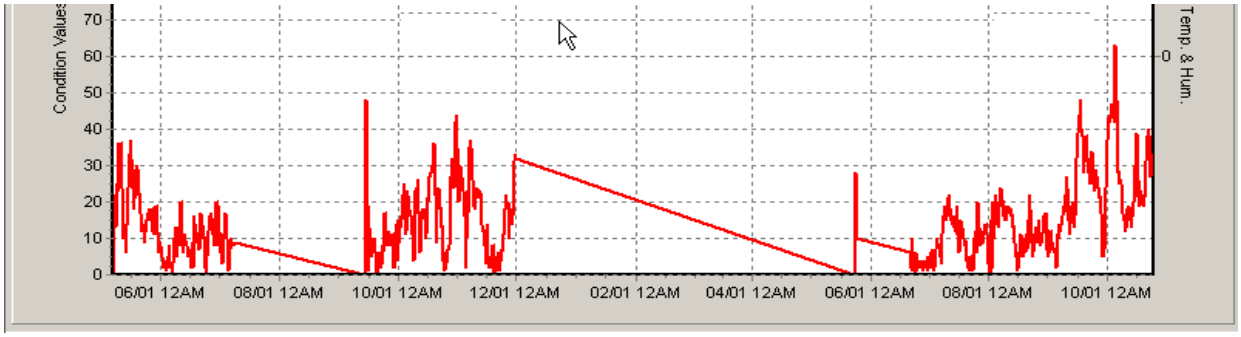

Figure 11–39
H1 Bushing Condition Value

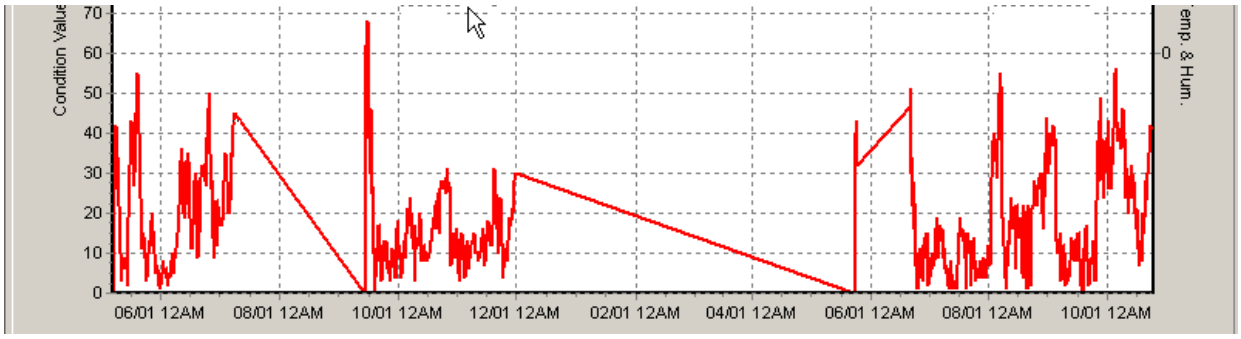

Figure 11–40
H2 Bushing Condition Value

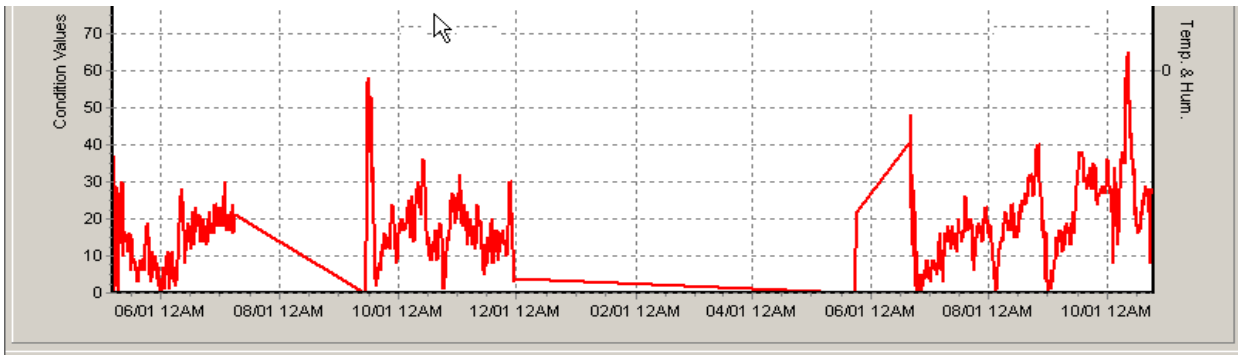

Figure 11–41
H3 Bushing Condition Value

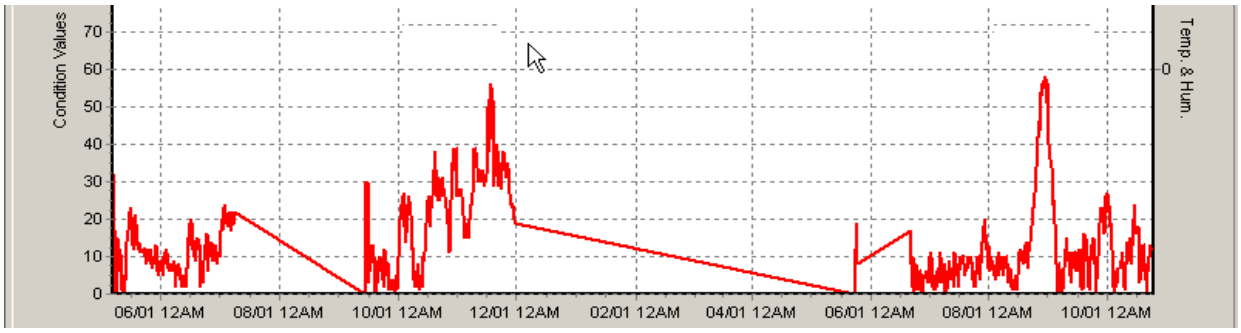

Figure 11–42
X1 Bushing Condition Value

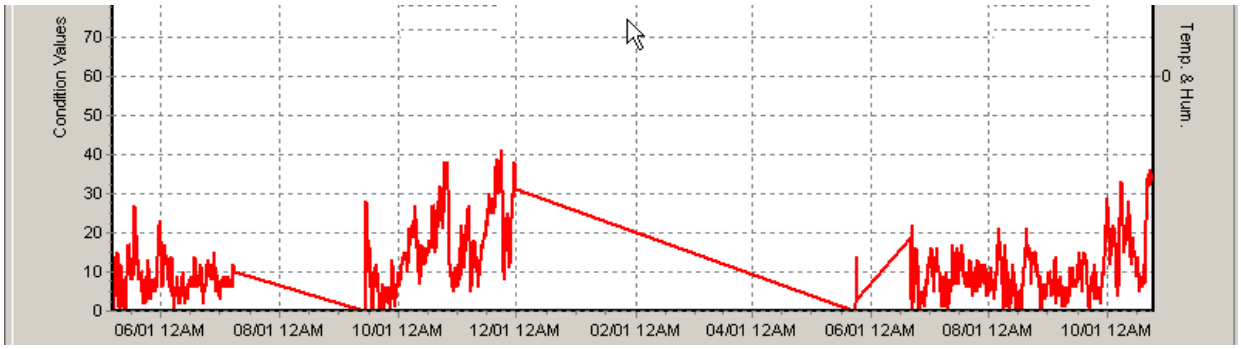

Figure 11–43
X2 Bushing Condition Value

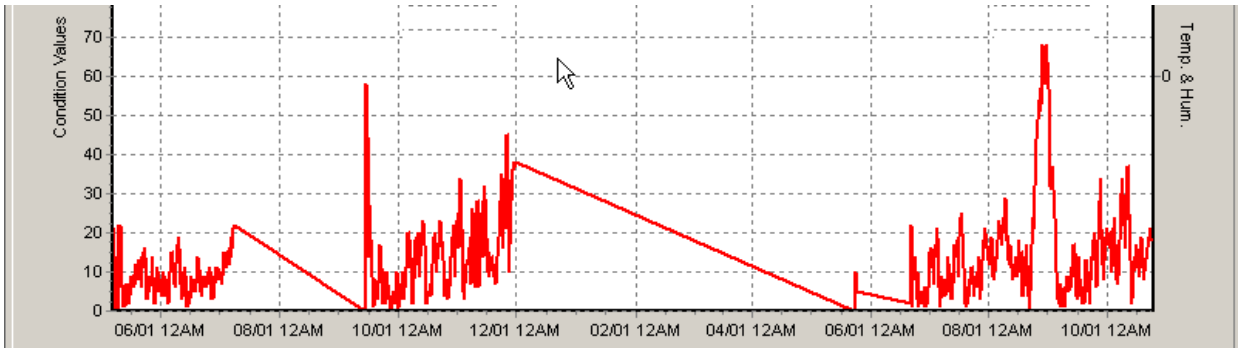

Figure 11–44
X3 Bushing Condition Value

The bushing relative power factor (RPF) trends were also recorded for this Oncor case study. In contrast to the FirstEnergy case study (case study 2), the OLRPF for the Oncor transformer was set up at installation to have separate bushing comparisons between high side and low side voltages. For example, there are three relative comparisons for the high side and three relative separate comparisons for the low side. Each group of three comparisons is in the same voltage group. This is a better approach since it is shown here to minimize the effects of transformer load cycles on the RPF. These load cycle effects were dominant in the FirstEnergy install (case study 2) but eliminated in this case study.

The RFP results for the H bushings are shown in Figure 11-45, Figure 11-46, and Figure 11-47.

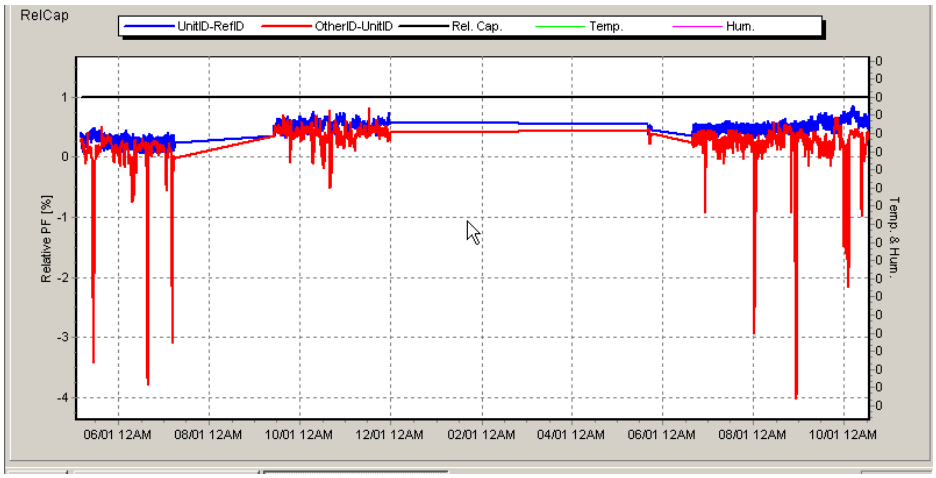

Figure 11–45
Bushing RFP Trend. H1 (Blue Trace) Relative to H2 (Red Trace).

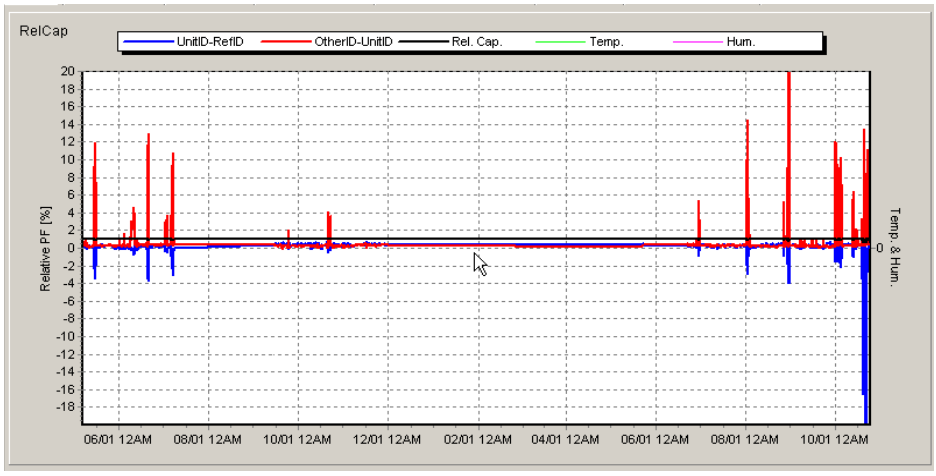

Figure 11–46
Bushing RFP Trend. H2 (Blue Trace) Relative to H3 (Red Trace).

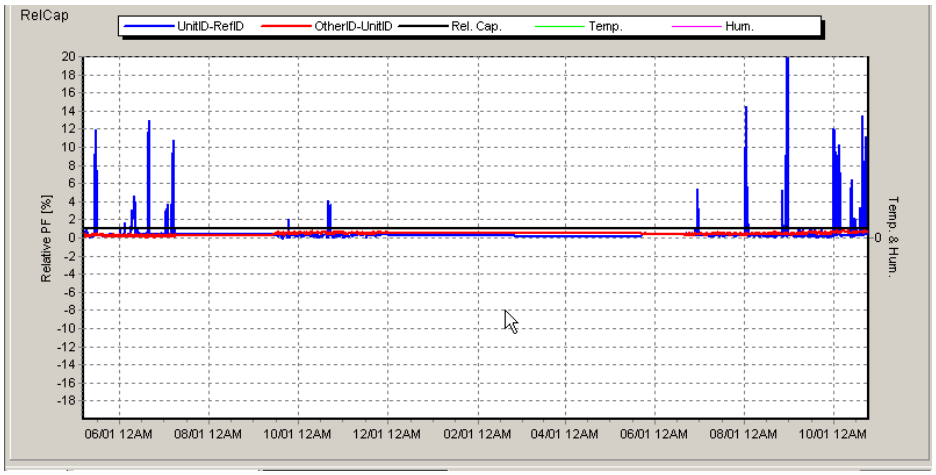

Figure 11–47
Bushing RFP Trend. H3 (Blue Trace) Relative to H1 (Red Trace).

Short term extreme swings in OLRPF still exist for the Oncor installation. As indicated in Figure 11-48, extreme swings can have a time duration of about 12 hours. It is not fully known why the extreme OLRPF swings occur. One possible contributor could be unequal contamination effects on the exterior of the bushings during these short time periods due to changing atmospheric conditions. Better understanding these changes is an area for future research. In the interim, long term trending (days to weeks) would allow for a better assessment of the evolving condition.

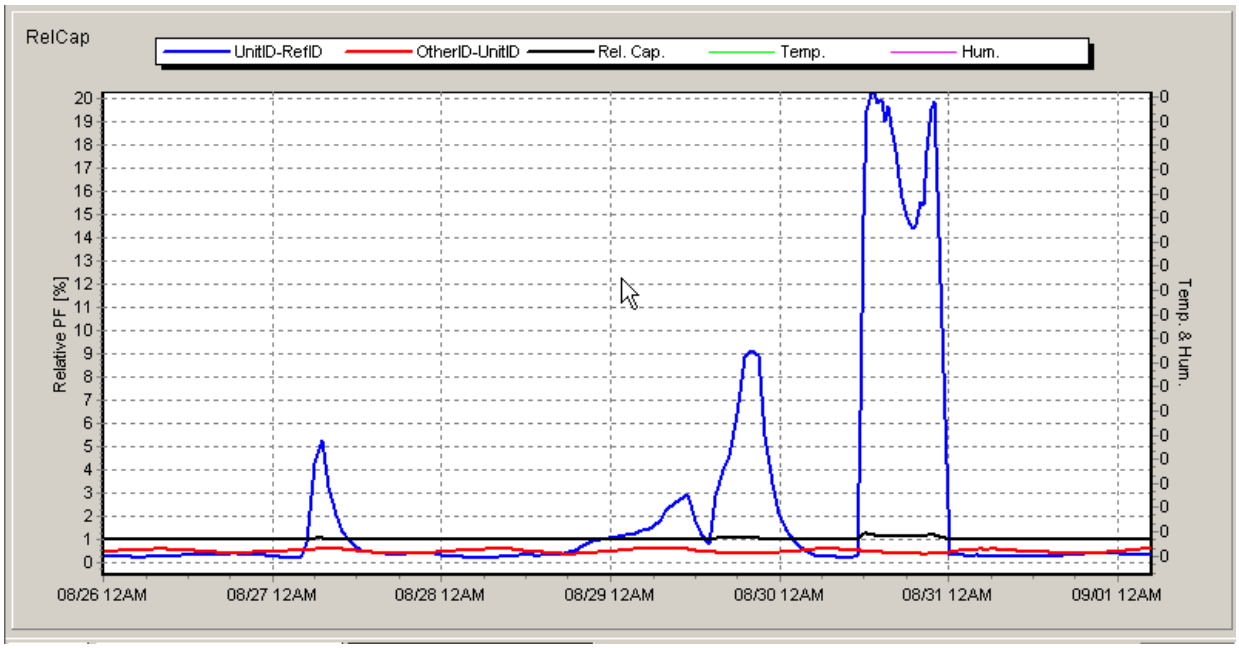

Figure 11–48
H3 (Blue Trace) Relative to H1 (Red Trace), Zoom In on Largest Peak of Figure 11-47

The RFP results for the X bushings are shown in Figures 11-49, Figure 11-50 and Figure 11-51.

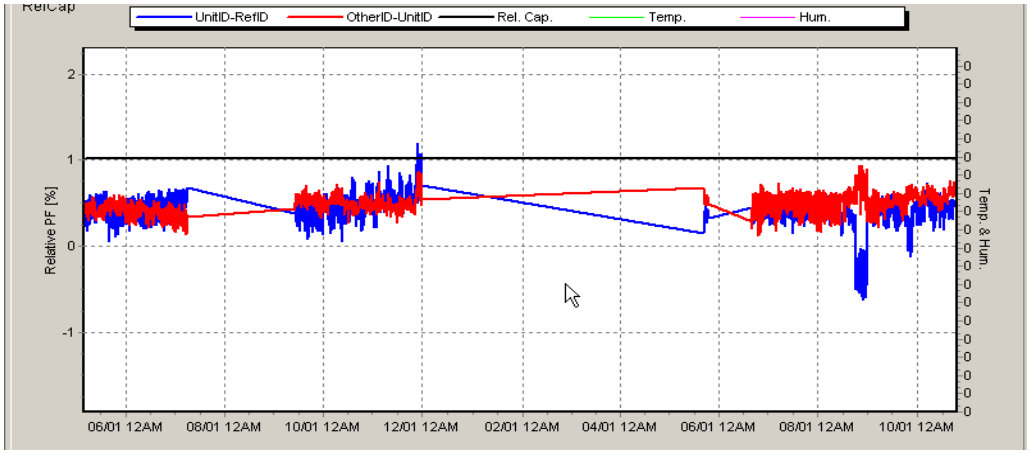

Figure 11–49
Bushing RFP Trend. X1 (Blue Trace) Relative to X2 (Red Trace).

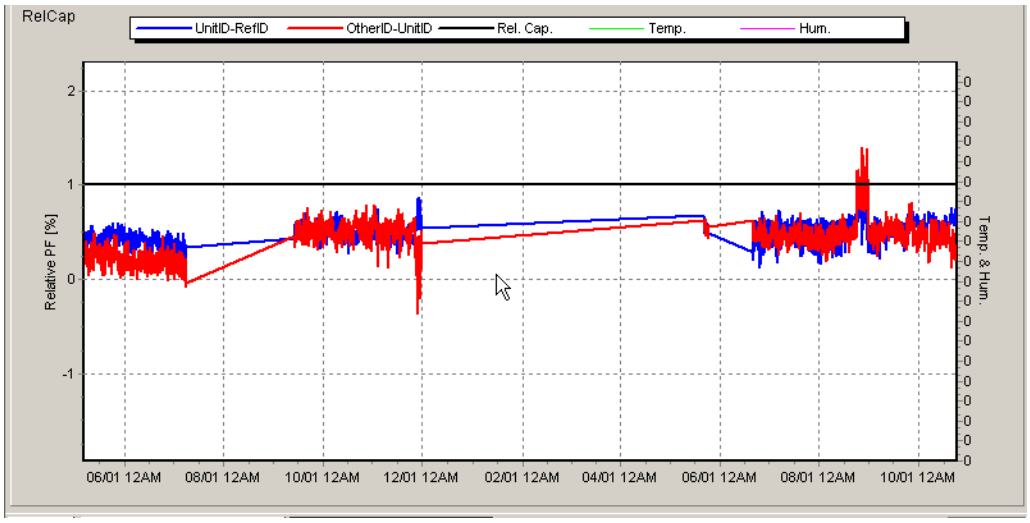

Figure 11–50
Bushing RFP Trend. X2 (Blue Trace) Relative to X3 (Red Trace).

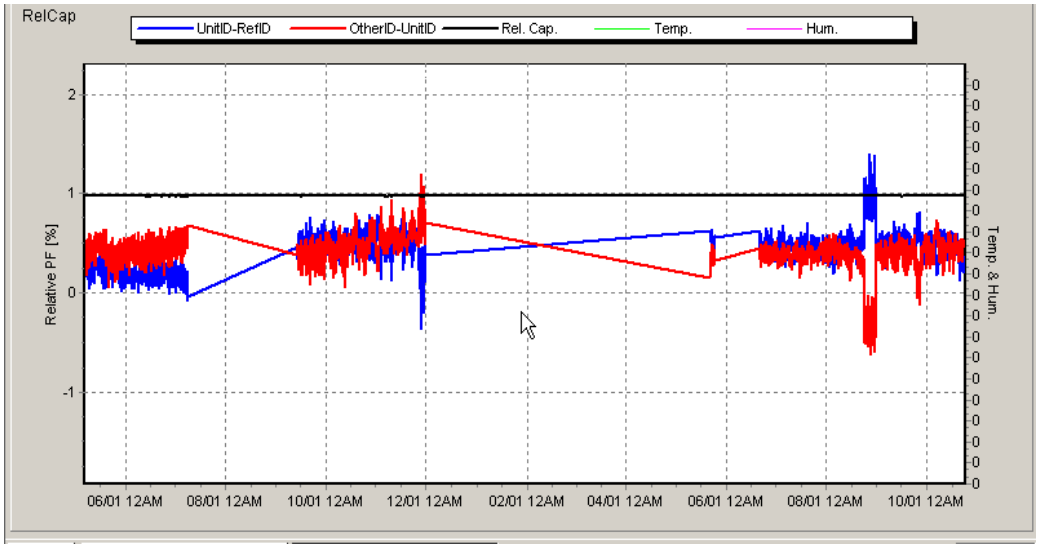

Figure 11–51
Bushing RFP Trend. X3 (Blue Trace) Relative to X1 (Red Trace).

Case Study 4: Three Single-Phase 765/345 KV Auto-Transformers

The OLFRA case study was conducted at AEP on three single-phase 765/345kV, 750 MVA, auto- transformers. The installation was in March 2012. The transformers were manufactured in 2004 and 2005.

This case study was the first installation at the 765 kV voltage level. Sources of electrical interference, such as partial discharge and/or bus corona, generally increase with an increase in voltage which could decrease the signal-to-noise ratio. The transformer and bushing dimensions also increase along with cabling lengths which could decrease output measurement values. Therefore a new equipment challenge was presented to determine OLFRA measurements. The issues were addressed by the vendor (NEETRAC) through an extra level of cable shielding and by combining the input filters and attenuators in a single shielded enclosure.

Off-Line Tests Compared to On-Line Tests Using OLFRA Equipment

A compact high voltage pulse source has been developed by NEETRAC so that off-line and on-line tests could be performed with the same equipment, namely the on-line equipment. Once on-line equipment is installed, there is no need for additional off-line FRA test equipment for future diagnostics. A FRA can thus be more easily performed using the in-place OLFRA equipment with the addition of a single high voltage pulse source. The pulses can be applied to the bushing tops with a hot stick from the pulse source.

The baseline off-line FRA tests are performed with the OLFRA equipment at installation. This baseline test is made using the OLFRA equipment, with grounds attached and the jumpers still attached. The windings can then be condition-assessed when the bank is de-energized without removing jumpers from the transformer bushings and with the safety grounds in place.

The X2-N off-line test results for jumpers and grounds attached are shown in Figure 11-52.

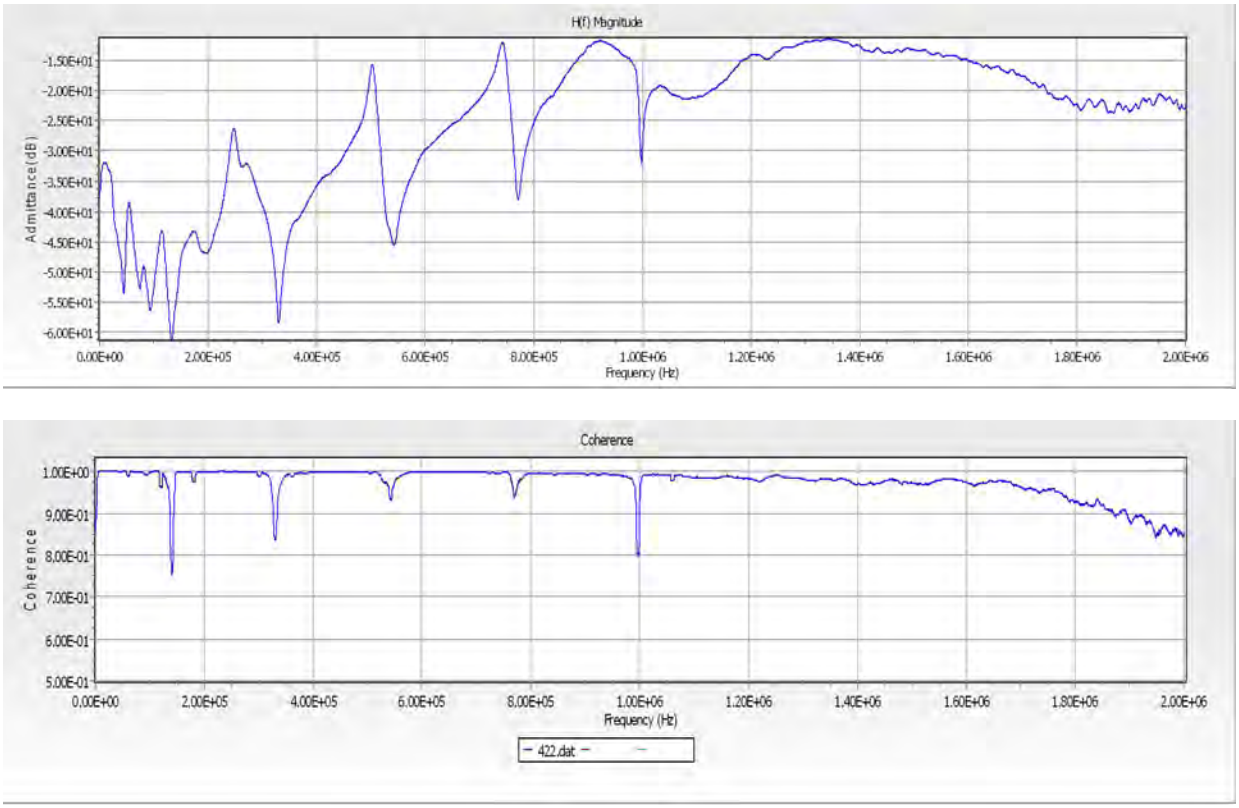

Figure 11–52
X2-N Off-Line for Jumpers and Neutral and Grounds Attached

The top magnitude plot is accurate and repeatable for the frequencies where the coherence is ≥0.9 in the bottom coherence plot of Figure 11-52. If the same or equivalent grounds are placed in approximately the same locations for a future transformer outage, then the future X2-N off-line test should be similar to the original X2-N test at equipment installation and a comparison can be made to the past baseline test. X1-N and X2-N can also be evaluated in the same manner.

In this case study a comparison was also made between the on-line test results and the off-line test results to verify the on-line technique and to gain empirical knowledge and improve the on-line technology. To demonstrate the off-line to on-line test comparisons, the comparisons of the X2-N on-line test results to the off-line tests with different winding terminal impedances are shown in Figure 11-53 from 305 Hz to 2.0 MHz.

Figure 11–53
X2-N Off-Line (Blue Trace), Neutral Attached, H and X Links Open. X2-N On-Line (Red Trace). X2-N Off-Line (Green Trace), Neutral Attached, H and X Links Closed, Safety Grounds On.

The on-line trace (red curve) is similar to the off-line trace with the neutral attached, H and X links open (blue curve) from about 500 kHz to 2 MHz. The high frequencies are similar because the impedance of the jumper/lightning arrester combination is much higher than the transformer winding characteristic for the higher frequencies.

The frequencies less than 500 kHz produce different characteristics because the jumper-arrester-bus connections produce parallel connected impedances that affect the winding measurements at low frequencies, but their effects are generally constant from one test result to the next.

The transfer function with grounds attached (green curve) begins to acquire a more similar characteristic to the others as the frequency is increased above 1.0 MHz as shown in Figure 11-53. The on-line data will have different terminal impedance characteristics on the windings as compared to the off-line tests made with the transformer bushing jumpers removed (H and X test links open and tertiary open) or with the safety grounds applied. But the differences diminish as the frequency of testing increases. The application of safety grounds at a distance from the winding terminals adds additional peaks and valleys to the lower frequencies of the transfer function, but the overall basic characteristic shape remains the same.

It is expected from experience (for example, case study 1 from the off-line FRA tests) that a significant winding deformation will produce a significant difference in the overall basic characteristic, even for the lower frequencies, not just smaller characteristic changes in the transfer function results. So it is expected that a significant winding change can be verified with the off-line test with all jumpers in place and safety grounds connected. For example, a significant change may be detected with two sets of on-line data from a past and a present time period. When the transformer is taken out of service for inspection, a quick off-line test with jumpers and safety grounds in place could thus verify the on-line results by comparison of present off-line test tests to off-line tests at installation using the OLFRA equipment. When comparing the off-line test at installation to a future off-line test, with the same winding terminal connections, the transfer functions should be similar across the frequency test band when no significant winding deformation is present.

Subsequent OLFRA Test Comparisons

This case study has the shortest history for OLFRA data to date. But the available data for the four month period has been high in amplitude and broad in frequency bandwidth. There were many on-line pulses due to induced lightning on the 765kV and 345 kV lines near the transformer. An event date of 5/4/2012 was selected for the OLFRA data. The results calculated before the event date are compared to results calculated after the event date of 5/4/2012. The H-N winding results are shown in Figures 11-54 through 11-59. The curves are the same general shape and magnitude for each plot. An example of curve difference for winding deformation is shown in the first case study for off-line FRA. Therefore, there is no significant change in each H winding condition for before versus after the event date of 5/4/2012. In addition, there is a very good overlay for the low frequencies to 100 kHz.

The horizontal axis is in frequency (hertz) and the vertical axis is in admittance (db). The frequency range is from 305 Hz to 2.0 MHz with a frequency data point at 305 Hz increments. The software automatically determines the most accurate transfer function from about 14 pre-selected and parametrically filtered waveform data sets to determine the curve for each winding.

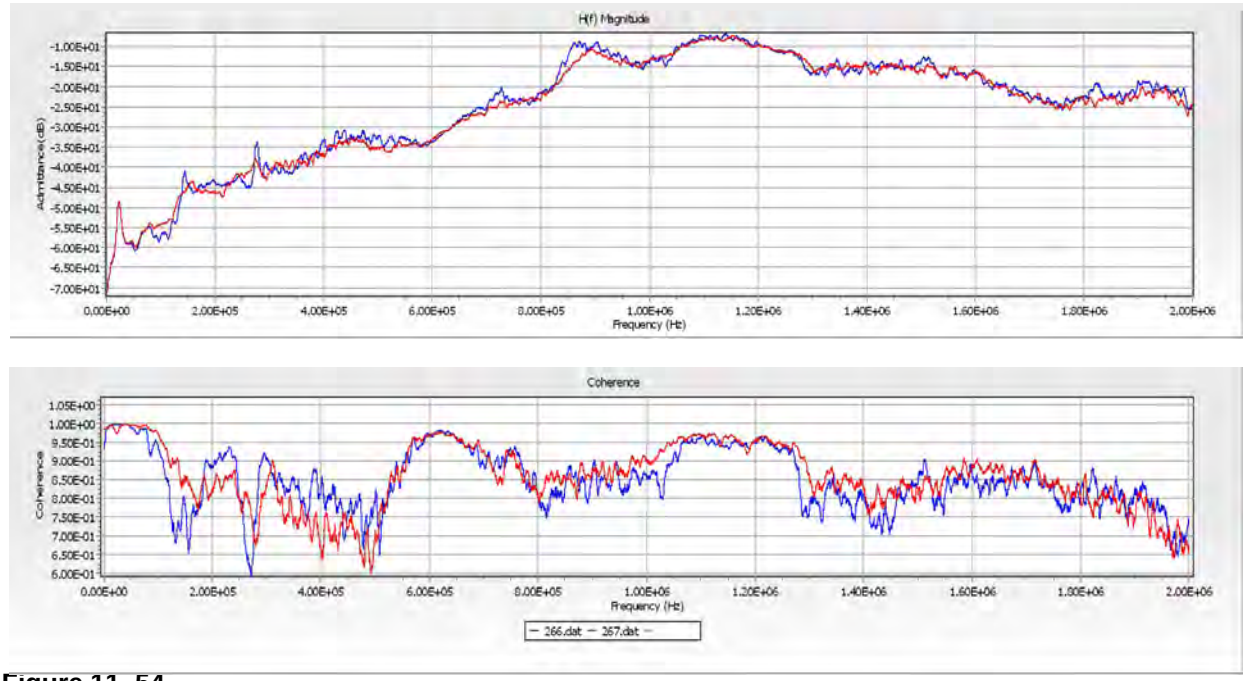

Figure 11–54
H1-N Transfer Function Before Event Date (Blue Trace). H1-N Transfer Function After Event Date (Red Trace).

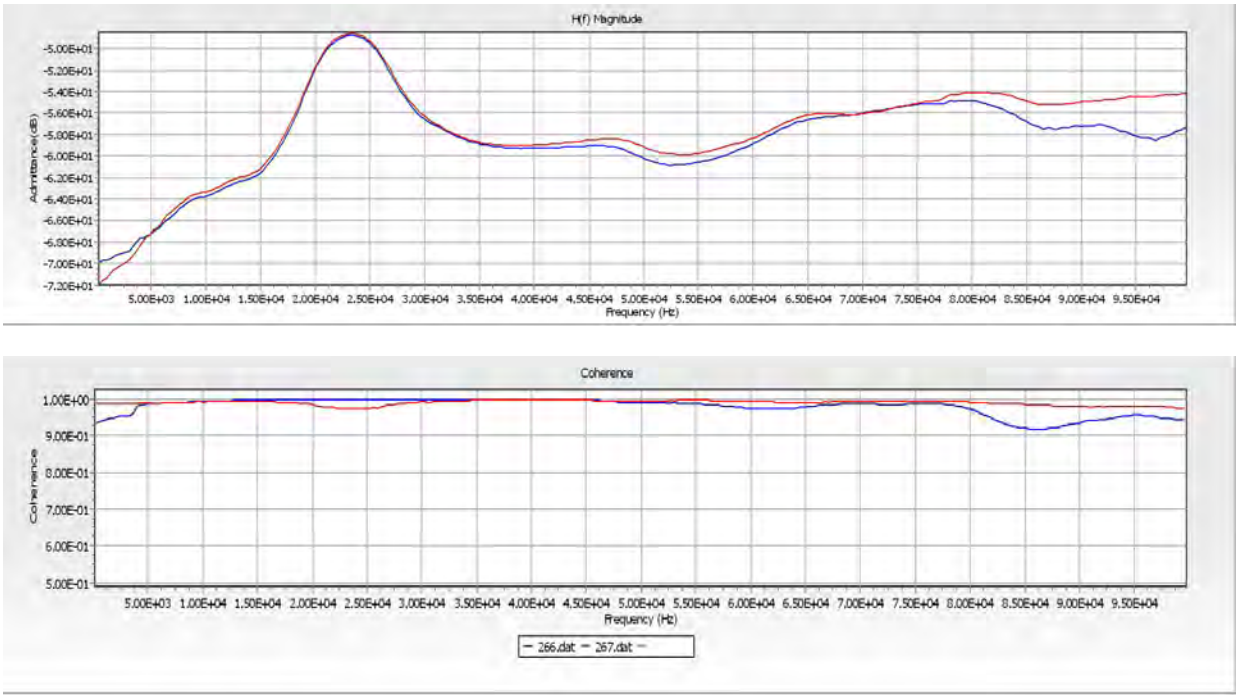

Figure 11–55
Zoom In, 305 Hz to 100 kHz. H1-N Transfer Function Before Event Date (Blue Trace). H1-N Transfer Function After Event Date (Red Trace).

Figure 11–56
H2-N Transfer Function Before Event Date (Blue Trace). H2-N Transfer Function After Event Date (Red Trace).

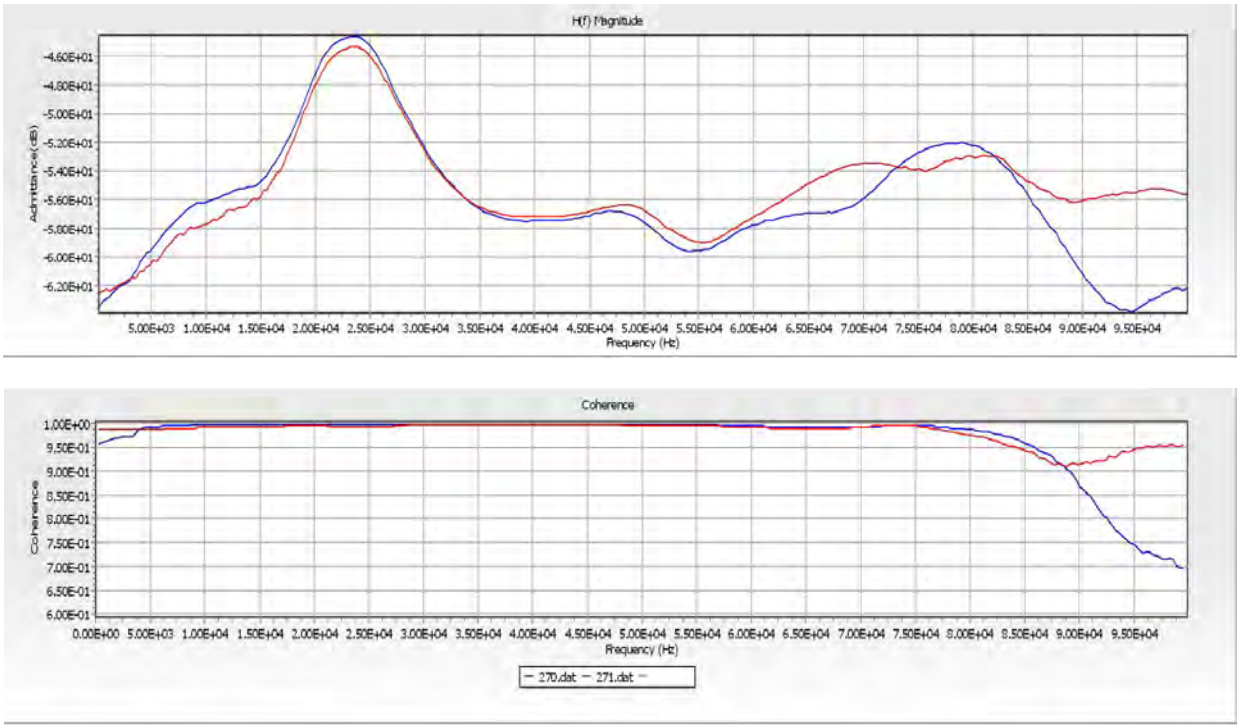

Figure 11–57
Zoom In, 305 Hz to 100 kHz. H2-N Transfer Function Before Event Date (Blue Trace). H2-N Transfer Function After Event Date (Red Trace).

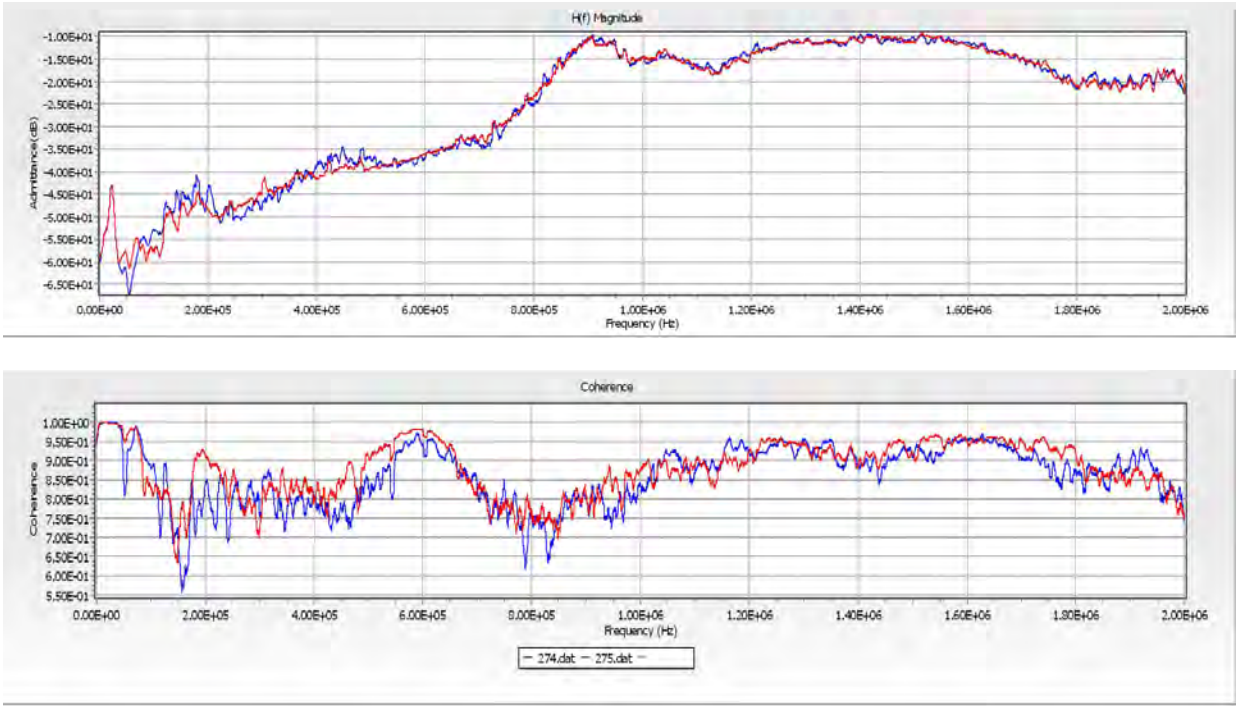

Figure 11–58
H3-N Transfer Function Before Event Date (Blue Trace). H3-N Transfer Function After Event Date (Red Trace).

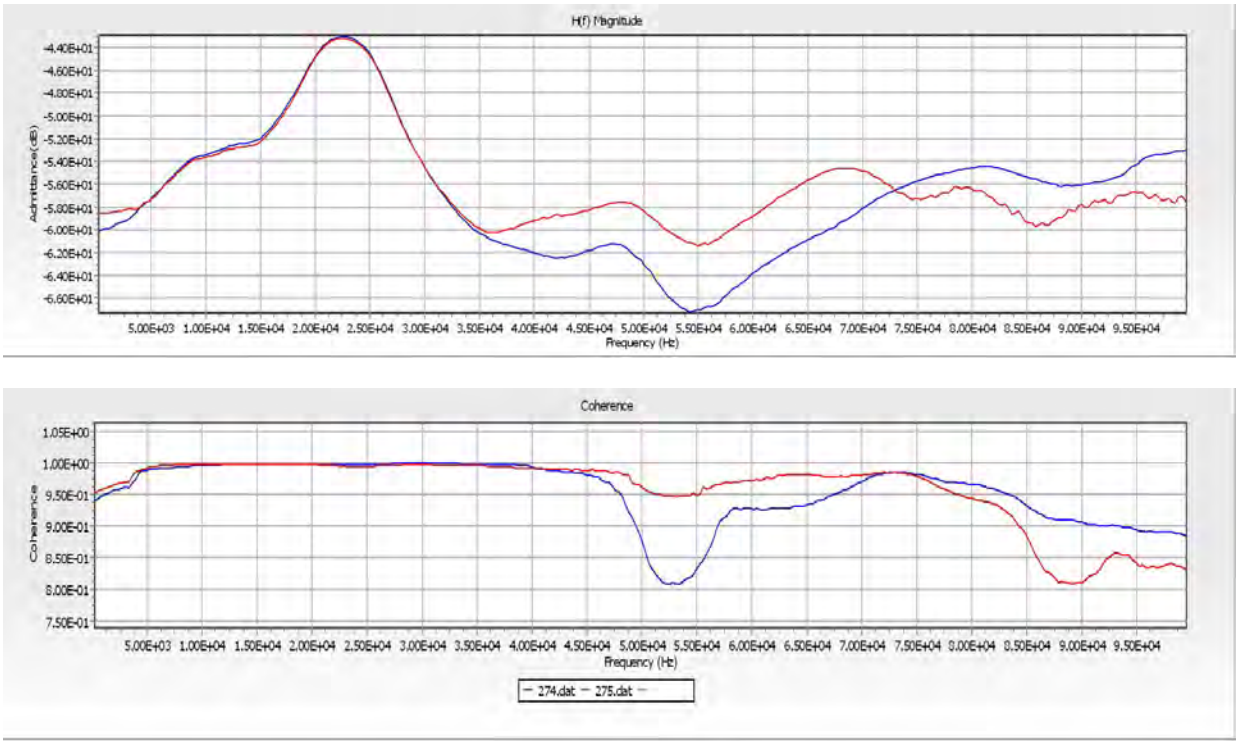

Figure 11–59
Zoom In, 305 Hz to 100 kHz. H3-N Transfer Function Before Event Date (Blue Trace). H3-N Transfer Function After Event Date (Red Trace).

The X-N winding results are shown in Figures 11-60 through Figure 11-64. As with the H windings, the curves are the same general shape and magnitude for each plot. An example of curve difference for winding deformation is given in case study 1. Therefore, there is no significant change in each X winding condition for before versus after the event date of 5/4/2012. In addition, there is a very good overlay for the low frequencies to 100 kHz.

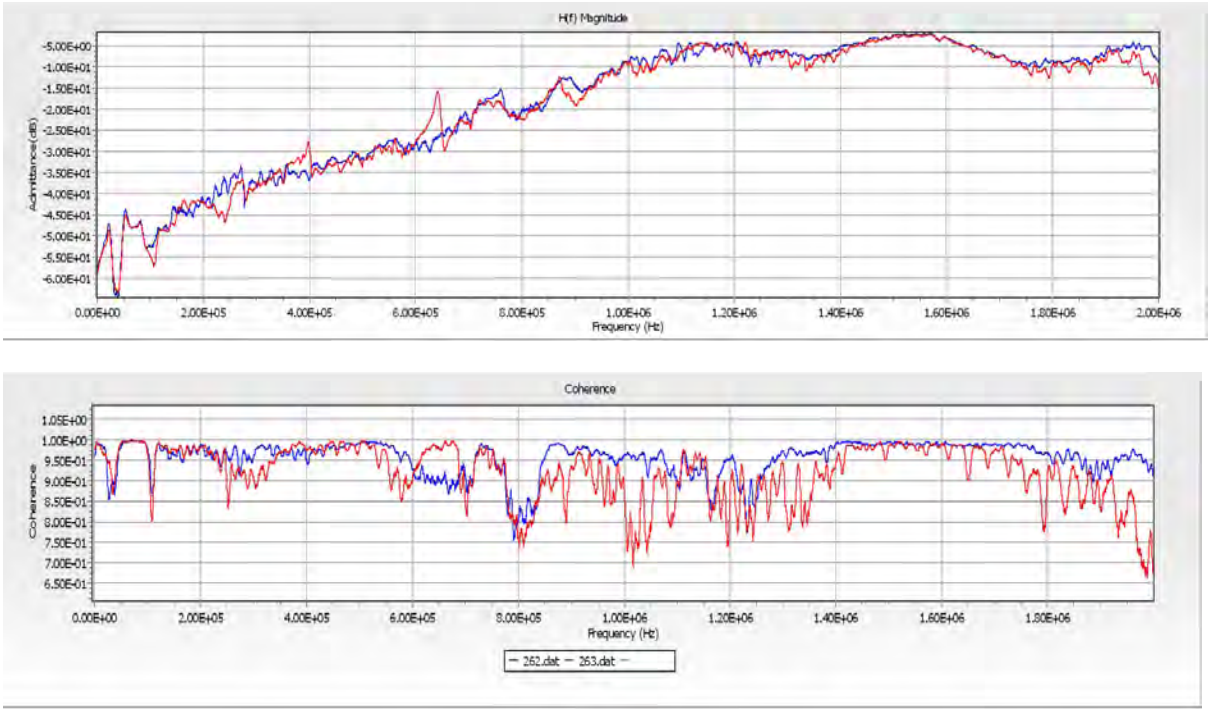

Figure 11–60
X1-N Transfer Function Before Event Date (Blue Trace). X1-N Transfer Function After Event Date (Red Trace).

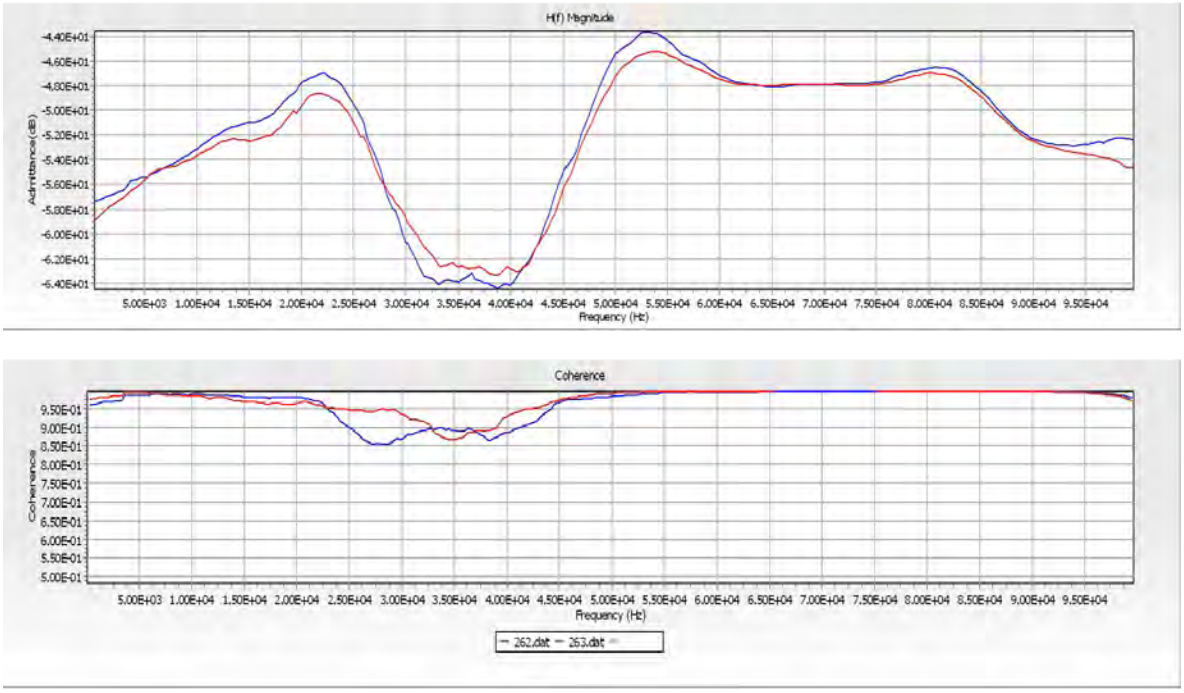

Figure 11–61
Zoom In, 305 Hz to 100 kHz. X1-N Transfer Function Before Event Date (Blue Trace). X1-N Transfer Function After Event Date (Red Trace).

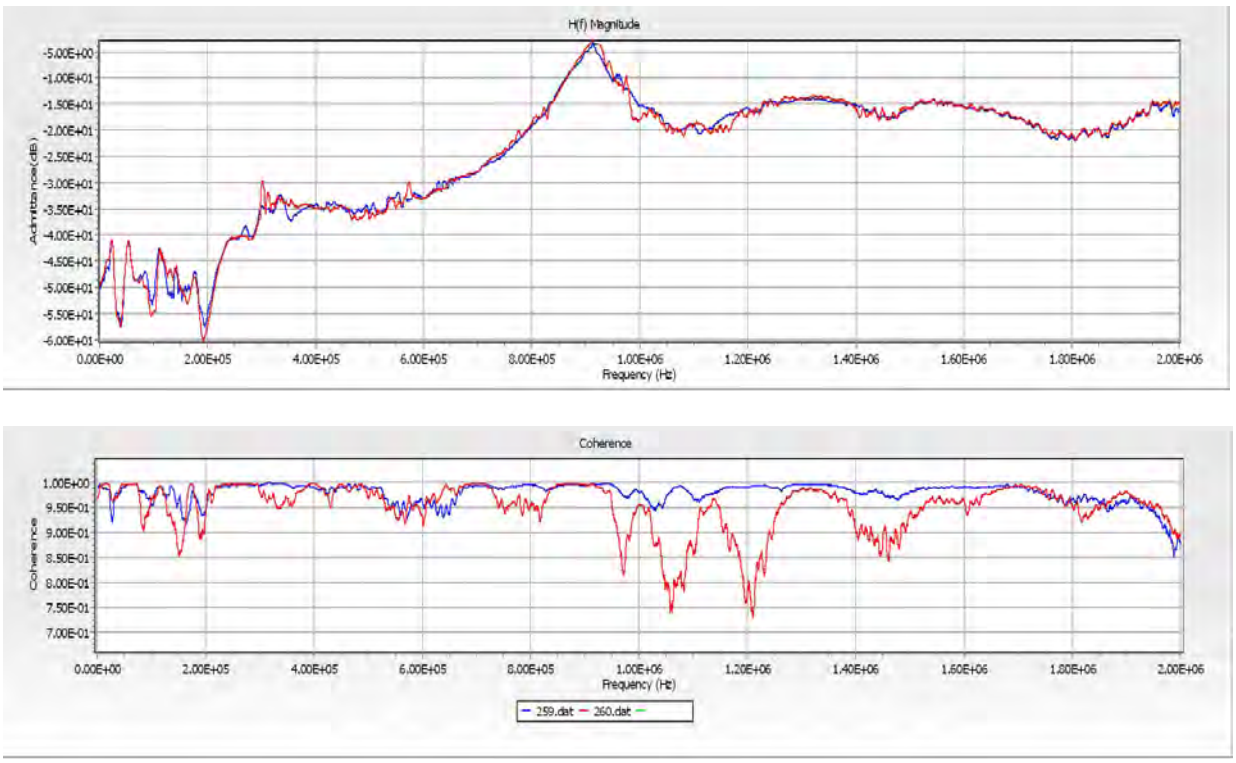

Figure 11–62
X2-N Transfer Function Before Event Date (Blue Trace). X2-N Transfer Function After Event Date (Red Trace).

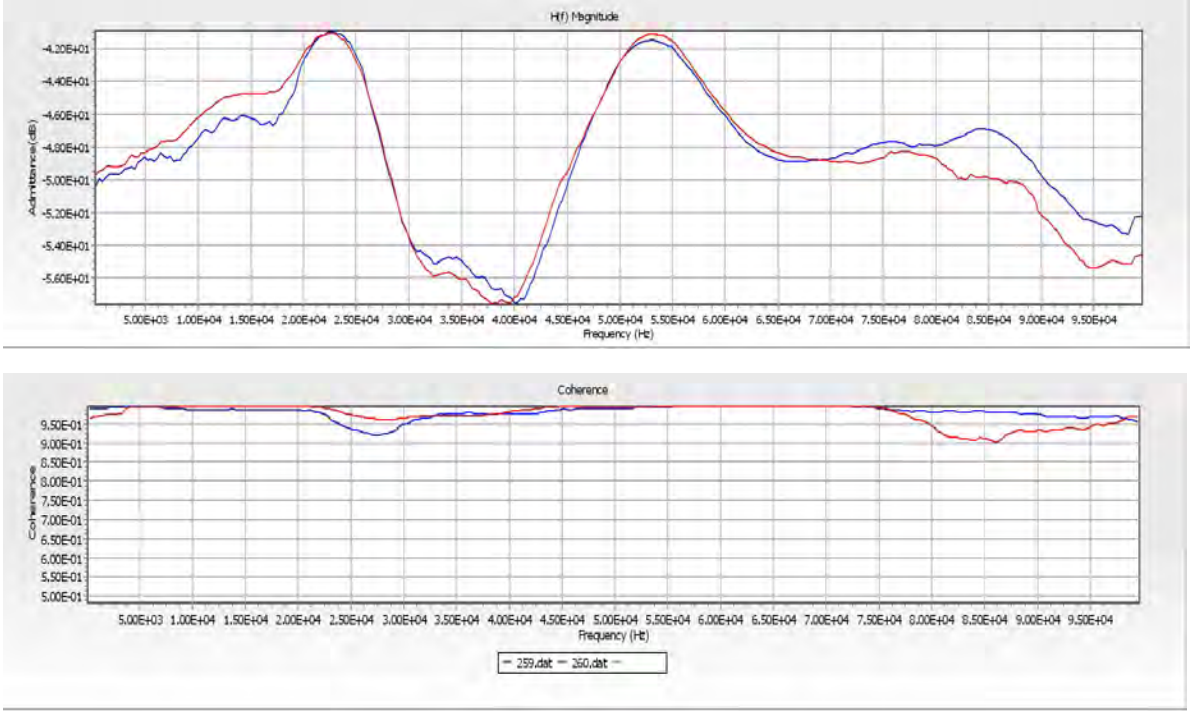

Figure 11–63
Zoom In, 305 Hz to 100 kHz. X2-N Transfer Function Before Event Date (Blue Trace). X2-N Transfer Function After Event Date (Red Trace).

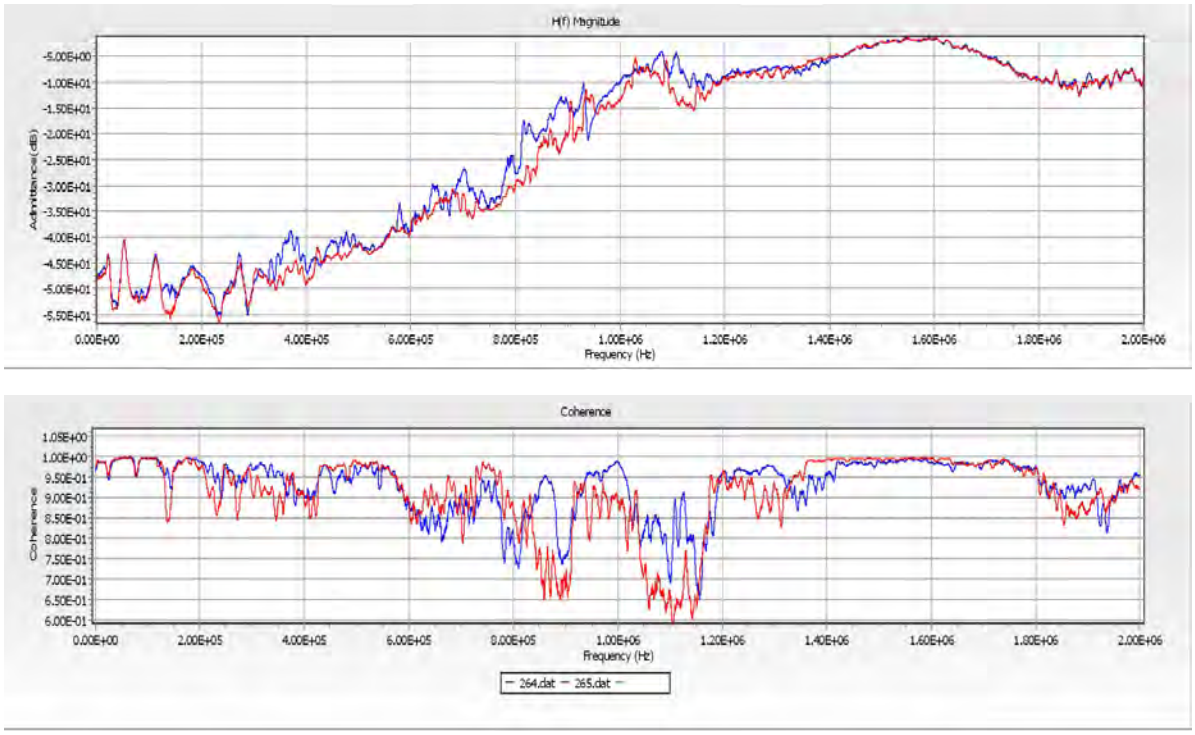

Figure 11–64
X3-N Transfer Function Before Event (Blue Trace). X3-N Transfer Function After Event (Red Trace).

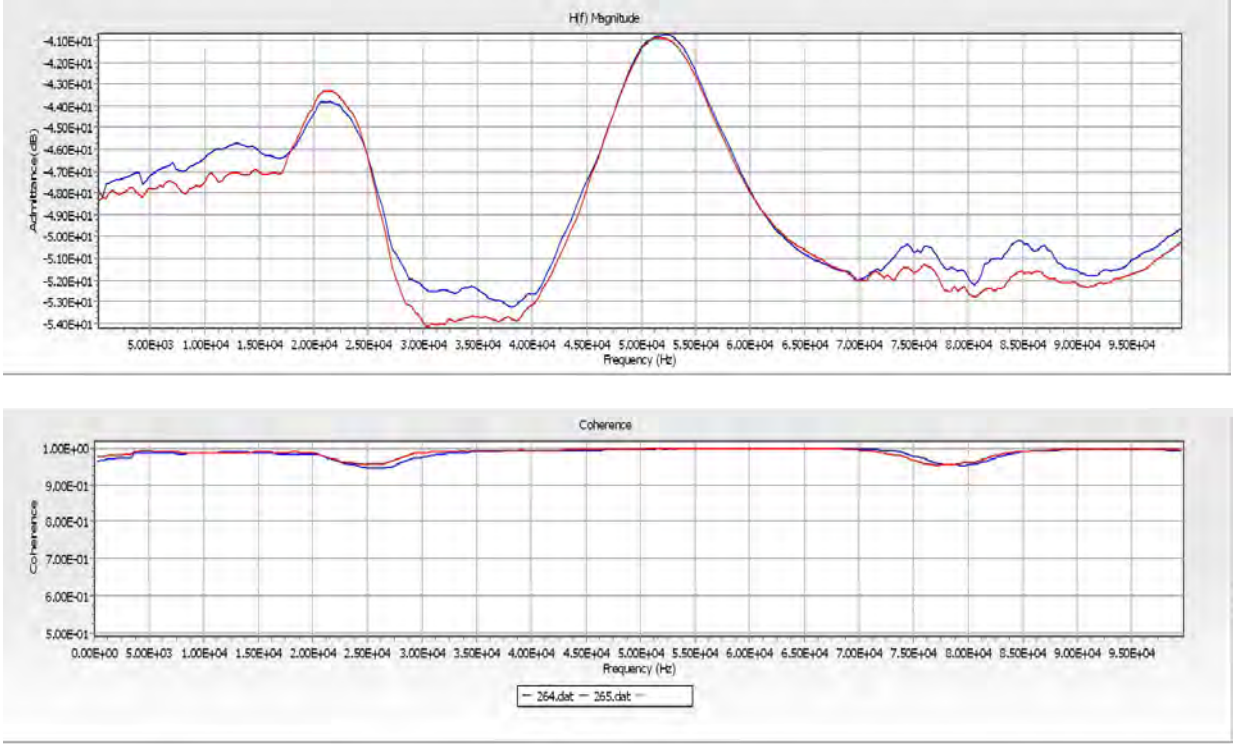

Figure 11–65
Zoom In, 305 Hz to 100 kHz. X3-N Transfer Function Before Event Date (Blue Trace). X3-N Transfer Function After Event Date (Red Trace).

Bushing OLRPF (On-Line Relative Power Factor) Results

The Dynamic Ratings OLRPF works simultaneously with the NEETRAC OLFRA using the same bushing taps for signal inputs to both units. The OLRPF results for the H and X bushings for the time period of 3/22/2012 (equipment installation) to 8/20/2012 are presented in the figures that follow.

Figure 11-66 and Figure 11-67 present the unbalance trend graphs for the H1, H2, and H3 bushings. The blue trend trace is the sum current trend for the three bushings. Values below 1% are normal and there is one data point per hour. The red trend trace represents the top oil temperature of the center transformer (phase 1). The flat portion of the red trace represents a time without temperature data when the main RPF module was not communicating. The OLRPF's 120 volt ac power was reset to re-start the communications. The BHM module was still operational during this time period so the unbalance data is still present. Figure 11-67 is a zoom in on the highest unbalance peak in the unbalance trend of Figure 11-66.

Figure 11-68 is a sum current phasor diagram of all the H1, H2, and H3 bushing unbalance current data points. There is one data point per hour. The phasor diagram dot indicates whether the resultant is more capacitive or resistive and which phase the sum resultant current is corresponding toward. The yellow arc represents phase 1, the green arc represents phase 2, and the red arc represents phase 3. For example, a majority of the data points in Figure 11-68 indicate the most resistive loss for phase 3, all less than 0.6%, and the most capacitive change is for phase 1, all less than 0.65%. All phasor data points are in the low normal range for the H bushings.

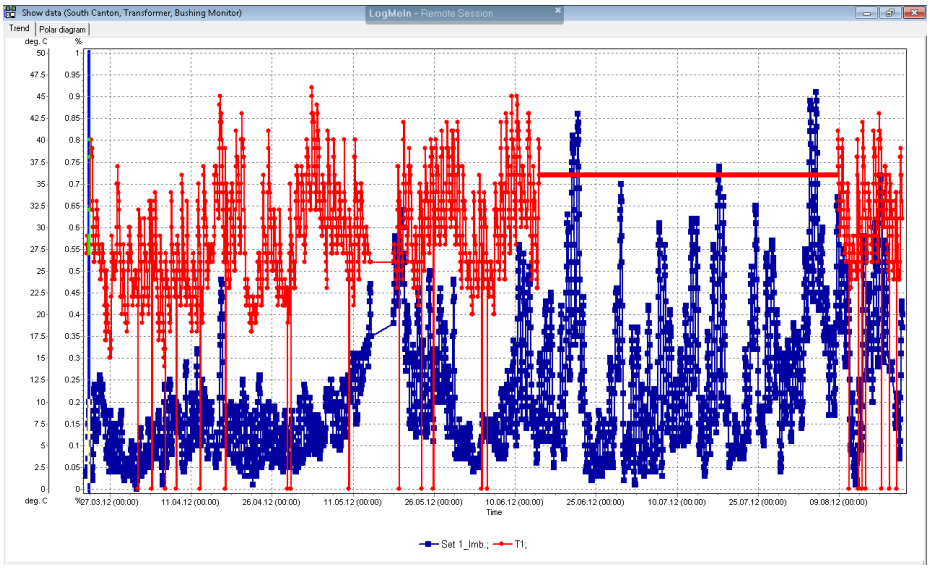

Figure 11–66
H2, H2, H3 Unbalance Sum Current Trend from 3/22/2012 to 8/20/2012

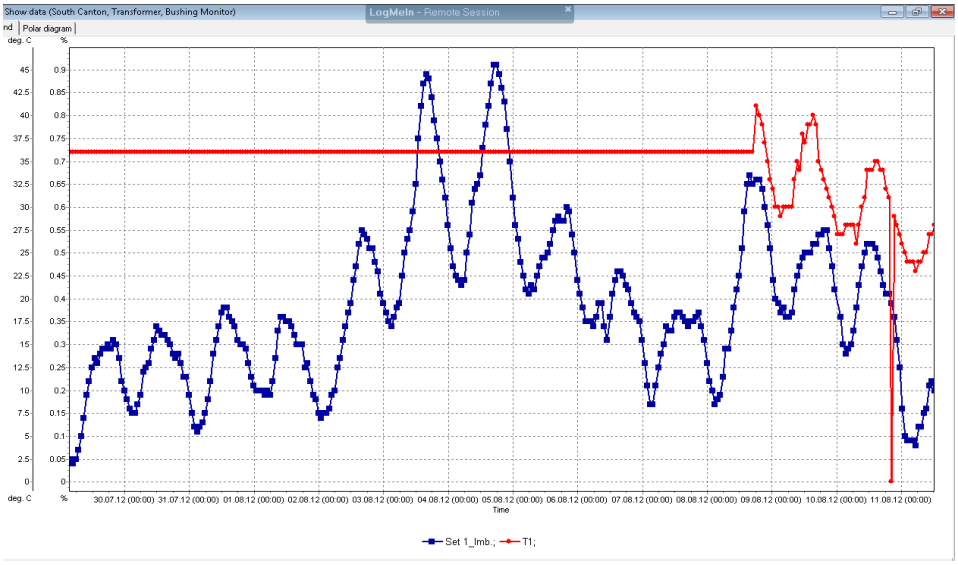

Figure 11–67
H1, H2, H3 Unbalance Sum Current Amplitude Peak (8/4-5/2012)

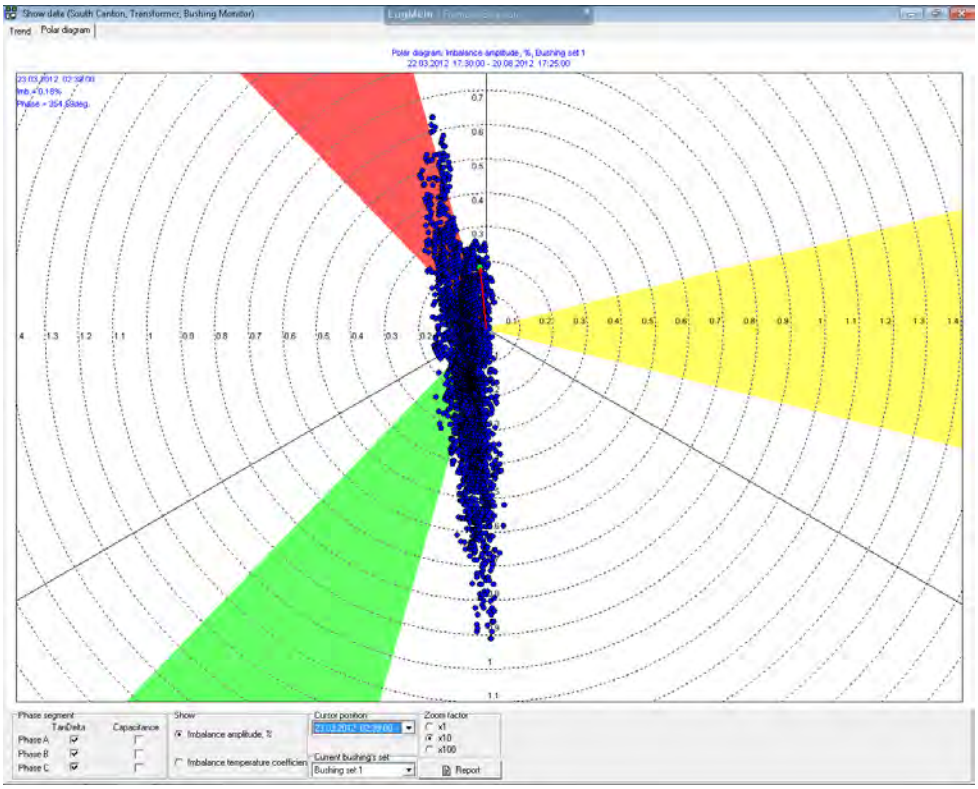

Figure 11–68
H1, H2, H3 Polar Plot. Colored Arcs Represent Tan Delta or Resistive Loss.

See Figure 11-69 and Figure 11-70 for the unbalance trend graphs for the X1, X2, and X3 bushings. The blue trend trace is the sum current trend for the 3 bushings. Values below 1% are normal, and there is one data point per hour. The red trend trace represents the top oil temperature of the center transformer (phase 1). The flat portion of the red trace represents a time without temperature data when the main RPF module was not communicating. The OLRPF's 120 volt ac power was reset to re-start the communications. The BHM module was still operational during this time period so the unbalance data is still present. Figure 11-70 is a zoom in on the highest unbalance peak in the unbalance trend of Figure 11-69.

Figure 11-71 is a sum current phasor diagram of all the X1, X2, and X3 bushing unbalance current data points. There is one data point per hour. The phasor diagram dot indicates whether the resultant is more capacitive or resistive, and which phase the sum resultant current is corresponding toward. The yellow arc represents phase 1, the green arc represents phase 2, and the red arc represents phase 3. For example, the majority of the data points in Figure 11-71 indicate the most resistive loss for phase 3, all less than 1.1%, and the most capacitive change in Figure 11-72 is for phase 2, all less than 0.8%. All phasor data points are in the low normal range for the X bushings.

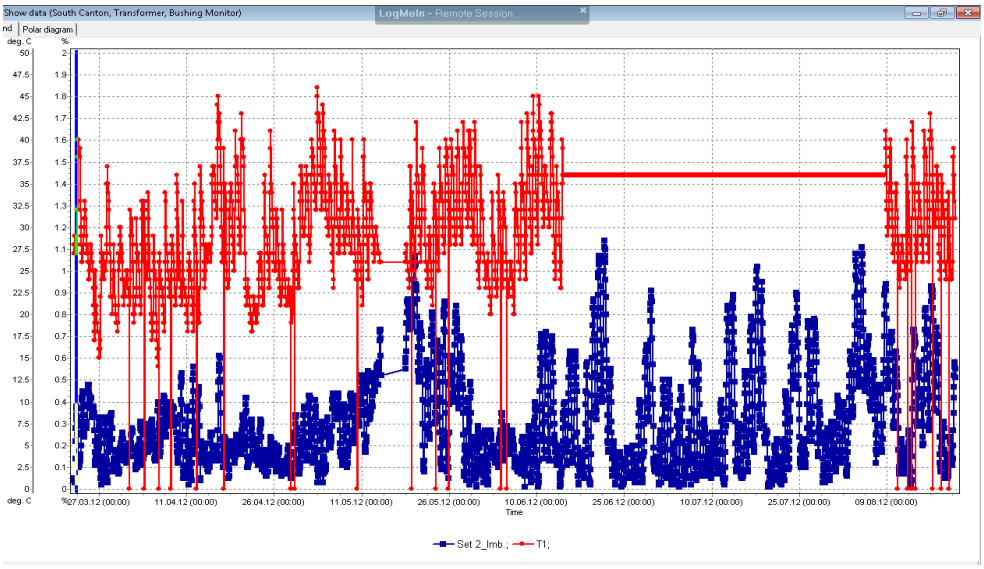

Figure 11–69
X1, X2, X3 Unbalance Sum Current Amplitude Trend

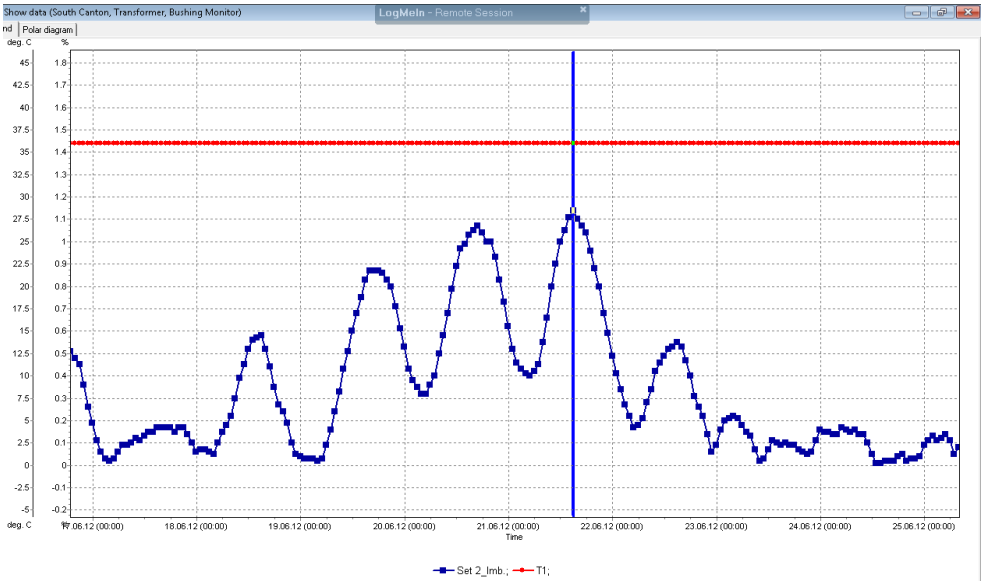

Figure 11–70
X1, X2, X3 Unbalance Amplitude Peak Zoom In (6/21/2012)

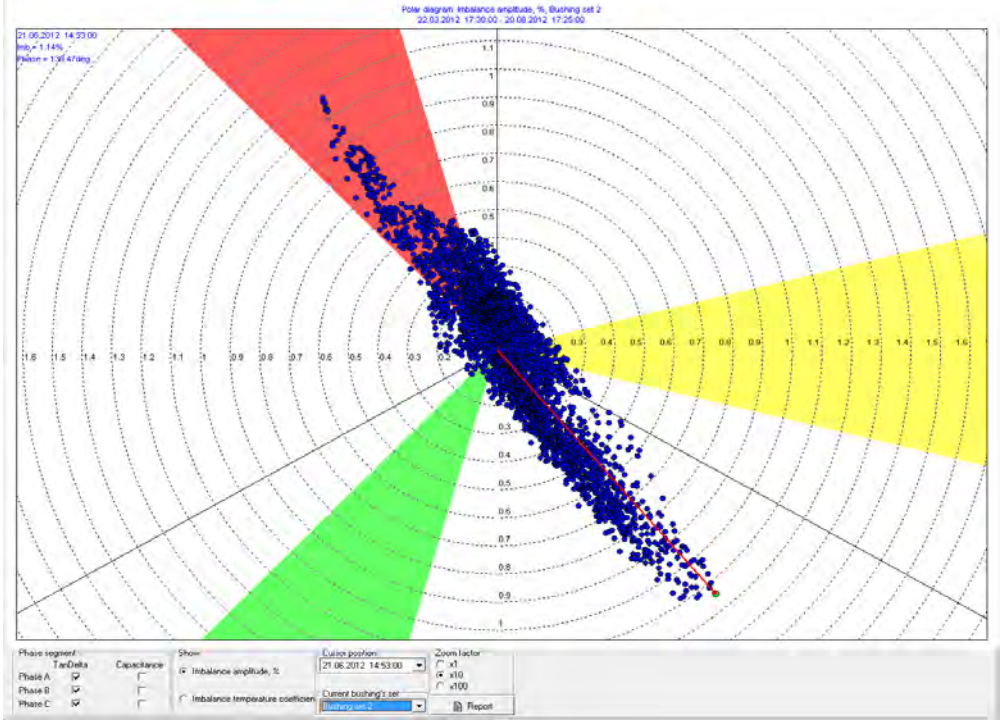

Figure 11–71
X1, X2, X3 Polar Plot

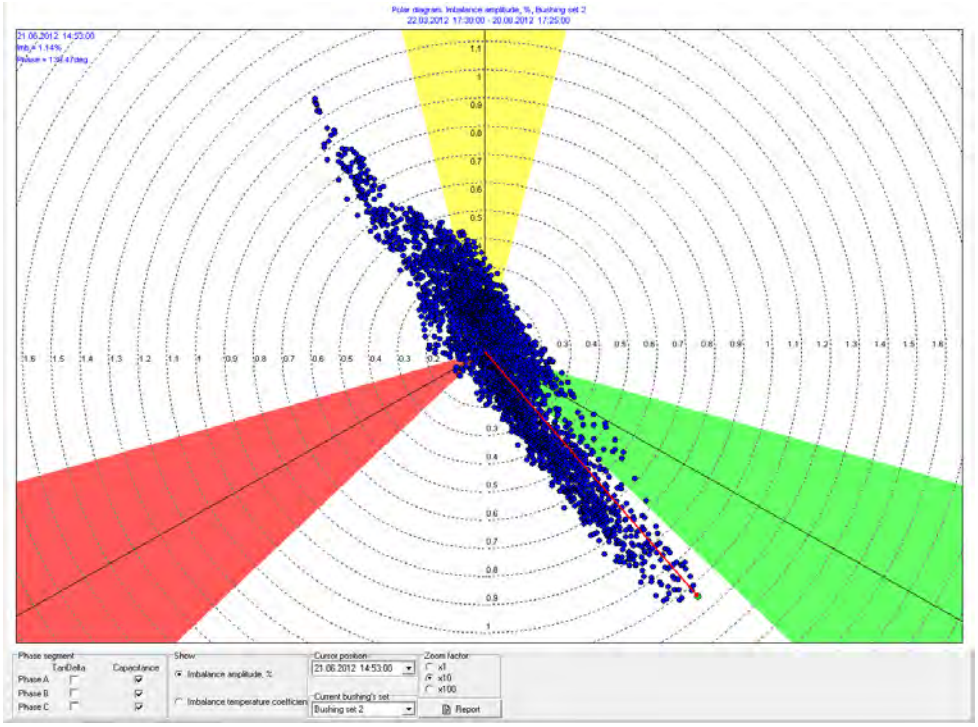

Figure 11–72
X1, X2, X3 Polar Plot. Capacitance Color Zone.

A
REFERENCES

1. *EPRI Power Transformer Guidebook Development*. EPRI, Palo Alto, CA: 2011. 1021892.
2. *Development of a New Acoustic Emissions Technique for the Detection and Location of Gassing Sources in Power Transformers. Phase 1 Results*. EPRI, Palo Alto, CA: 2002. 1007176.
3. "Acoustic Emission R&D – Successes in the Field and Incorporation of the Findings into the R&D," EPRI, Substations Task Force Meeting, San Diego, CA (December 10, 2008).
4. *Guide for the interpretation of dissolved gas analysis (DGA) in bushings where oil is the impregnating medium of the main insulation (generally paper)*. IEC 61464, Ed. 1.0 (1998–08).
5. *IEEE Guide for Acceptance and Maintenance of Insulating Oil in Equipment*, IEEE Std. C57.106-2006 (2006).
6. M.D. Judd, O. Farish, and P.F. Coventry, "UHF Couplers for GIS - Sensitivity and Specification." 10th ISH, Vol. 6 (1997).
7. B. Hampton, "UHF diagnostics for gas insulated substations," paper presented at the Eleventh International Symposium on High Voltage Engineering, Conf. Publ. No. 467 (1999).
8. M.D. Judd, Y. Li, and I.B.B. Hunter, "Partial discharge monitoring of power transformers using UHF sensors. Part 1: sensors and signal interpretation." *Electrical Insulation Magazine*, IEEE. Vol. 21, No. 2, pp. 5–14 (2005). doi: 10.1109/MEI.2005.1412214.

Export Control Restrictions

Access to and use of EPRI Intellectual Property is granted with the specific understanding and requirement that responsibility for ensuring full compliance with all applicable U.S. and foreign export laws and regulations is being undertaken by you and your company. This includes an obligation to ensure that any individual receiving access hereunder who is not a U.S. citizen or permanent U.S. resident is permitted access under applicable U.S. and foreign export laws and regulations. In the event you are uncertain whether you or your company may lawfully obtain access to this EPRI Intellectual Property, you acknowledge that it is your obligation to consult with your company's legal counsel to determine whether this access is lawful. Although EPRI may make available on a case-by-case basis an informal assessment of the applicable U.S. export classification for specific EPRI Intellectual Property, you and your company acknowledge that this assessment is solely for informational purposes and not for reliance purposes. You and your company acknowledge that it is still the obligation of you and your company to make your own assessment of the applicable U.S. export classification and ensure compliance accordingly. You and your company understand and acknowledge your obligations to make a prompt report to EPRI and the appropriate authorities regarding any access to or use of EPRI Intellectual Property hereunder that may be in violation of applicable U.S. or foreign export laws or regulations.

The Electric Power Research Institute, Inc. (EPRI, www.epri.com) conducts research and development relating to the generation, delivery and use of electricity for the benefit of the public. An independent, nonprofit organization, EPRI brings together its scientists and engineers as well as experts from academia and industry to help address challenges in electricity, including reliability, efficiency, health, safety and the environment. EPRI also provides technology, policy and economic analyses to drive long-range research and development planning, and supports research in emerging technologies. EPRI's members represent approximately 90 percent of the electricity generated and delivered in the United States, and international participation extends to more than 30 countries. EPRI's principal offices and laboratories are located in Palo Alto, Calif.; Charlotte, N.C.; Knoxville, Tenn.; and Lenox, Mass.

Together…Shaping the Future of Electricity

1024195

Electric Power Research Institute
3420 Hillview Avenue, Palo Alto, California 94304-1338 • PO Box 10412, Palo Alto, California 94303-0813 • USA
800.313.3774 • 650.855.2121 • askepri@epri.com • www.epri.com